CIVIL ENGINEERING STUDIES

STRUCTURAL RESEARCH SERIES NO. 269

THE EFFECTS OF PATTERN LOADINGS ON REINFORCED CONCRETE FLOOR SLABS

by

JAMES O. JIRSA

METE A. SOZEN

CHESTER P. SIESS

A Report to

THE REINFORCED CONCRETE RESEARCH COUNCIL
OFFICE OF THE CHIEF OF ENGINEERS, U. S. ARMY
GENERAL SERVICES ADMINISTRATION, PUBLIC BUILDINGS SERVICE
HEADQUARTERS, U. S. AIR FORCE, DIRECTORATE OF CIVIL ENGINEERING
U. S. NAVY, ENGINEERING DIVISION, BUREAU OF YARDS AND DOCKS

UNIVERSITY OF ILLINOIS
URBANA, ILLINOIS
JULY, 1963

THE EFFECTS OF PATTERN LOADINGS ON REINFORCED CONCRETE FLOOR SLABS

by

J. O. Jirsa
M. A. Sozen
C. P. Siess

A Report on a Research Project
Conducted by the

CIVIL ENGINEERING DEPARTMENT
UNIVERSITY OF ILLINOIS

in cooperation with the

REINFORCED CONCRETE RESEARCH COUNCIL

OFFICE OF THE CHIEF OF ENGINEERS, U. S. ARMY

GENERAL SERVICES ADMINISTRATION, PUBLIC BUILDINGS SERVICE

HEADQUARTERS, U. S. AIR FORCE

and

U. S. NAVY, ENGINEERING DIVISION, BUREAU OF YARDS AND DOCKS
NBy 37633

UNIVERSITY OF ILLINOIS

URBANA, ILLINOIS

July 1963

TABLE OF CONTENTS

TABLE OF CONTENTS (Cont'd)

LIST OF TABLES

LIST OF FIGURES

LIST OF FIGURES (Cont'd)

LIST OF FIGURES (Cont'd)

1. INTRODUCTION

1.1 General Remarks

The pivotal assumption of working stress design is that if the working stresses in the structure do not exceed certain levels, the structure will behave satisfactorily. In order to proportion the sections to satisfy the limits imposed on the flexural stresses, it is necessary to know the maximum moment at those sections. For example, it is known that the positive moment in a continuous beam on supports which offer no restraint may be doubled if alternate spans are loaded. The negative moments may increase by 25 percent under the pertinent loading. In such a beam the total design moments exceed the static moments considerably.

The use of working stress design for slabs makes it necessary to know the effects of pattern loads on the moments. The analyses of a three-dimensional structure is more difficult and, because of the diverse backgrounds of the design methods for different types of slabs, pattern loads are not treated uniformly. The design moments for two-way slabs are based on checker-board loads giving maximum moments while flat slab design methods largely ignore pattern loads.

With the development and acceptance of limit design methods, the need for designing for more than the static moment has been questioned. Limit design takes advantage of moment redistribution and if the total static moment is provided, the strength of the structure is unimpaired. The moments will be redistributed to the sections until the full capacity of each is utilized. However, accompanying the rotations of the sections necessary for moment redistribution are large deflections and additional cracking. These factors may render the structure unserviceable even though the strength is adequate. It is necessary to consider the effects of pattern loads and it may be advisable to impose certain minimum restrictions on the moment increases in order to satisfy serviceability requirements.

A study of pattern loads is therefore necessary to enable the designer to estimate the effects of such loadings on floor slabs. In this report, the available information is brought together and correlated to provide a unified approach for determining the effects of pattern loadings in slabs.

1.2 Object and Scope

The object of this study is to develop a design procedure to determine the effects of pattern loads on reinforced concrete floor slabs. The procedure is intended to provide a unified approach to the problem of pattern loads in rectangular slabs of all types.

The experimental information used in developing the design procedure was obtained from five test structures: a flat plate, two flat slabs, and two two-way slabs. The strains and deflections measured under pattern loadings are discussed. Moments under pattern loadings are compared with those under uniform loads and also with design moments.

A compilation of existing theoretical solutions in which pattern loads are considered is made for a range of various support conditions. Extensions of these theoretical solutions are made to cover cases not available elsewhere.

The five test structures are described briefly in Chapter 2 which also contains a discussion of their behavior. Chapter 3 is a discussion of the measured moments and a comparison of measured uniform and pattern load moments. The theoretical solutions are compiled in Chapter 4. Chapter 5 is a discussion of current design methods and a comparison of design with measured moments is included. The procedure for estimating the effects of pattern loads is given in Chapter 6. A frame analysis is given in the Appendix for calculating moments in floor slabs. A summary of the study is given in Chapter 7.

1.3 Acknowledgments

This report was prepared as part of an investigation conducted in the Structural Research Laboratory of the Civil Engineering Department at the University of Illinois in cooperation with the following organizations:

Reinforced Concrete Research Council
Directorate of Civil Engineering, Headquarters, U. S. Air Force
General Services Administration, Public Buildings Service
Office of the Chief of Engineers, U. S. Army
Bureau of Yards and Docks, Engineering Division, U. S. Navy

The program of investigation has been guided by an advisory committee on which the following persons have served:

Douglas McHenry, Chairman of the Advisory Committee, Portland Cement Association
L. H. Corning, Past Chairman, Portland Cement Association
G. B. Begg, Jr., Public Buildings Service, General Services Administration
W. J. Bobisch, BuDocks, Department of the Navy
Frank Brown, Wire Reinforcement Institute, Inc.
J. Di Stasio, Sr., Consulting Engineer, Di Stasio and van Buren (Deceased)
A. S. Neiman, Headquarters, U. S. Air Force
N. M. Newmark, University of Illinois
D. H. Pletta, Virginia Polytechnic Institute
J. R. Powers, Headquarters, U. S. Air Force
Paul Rogers, Consulting Engineer, Paul Rogers and Associates
E. J. Ruble, Association of American Railroads
W. E. Schaem, Office of the Chief of Engineers, U. S. Army
M. P. van Buren, Consulting Engineer, Di Stasio and van Buren
C. A. Willson, American Iron and Steel Institute

The project has been under the over-all direction of Dr. C. P. Siess, Professor of Civil Engineering, and the immediate supervision of Dr. M. A. Sozen, Professor of Civil Engineering.

This report was prepared as a thesis under the direction of Professor M. A. Sozen.

1.4 Notation and Definitions

Movable load = the load that can be positioned to create maximum moments

Permanent load = the load that is stationary or, in some cases, the dead load

Total load = sum of movable and permanent loads

Moment ratio = moment in a structure under pattern load divided by the uniform load moment, designated by γ

Load ratio = movable load divided by the total load, designated by β

Pattern ratio = pattern load moment divided by uniform load moment designated by α, generally used for theoretical moments when the load ratio $\beta = 1$

a = span length in direction in which moments are considered

α = pattern ratio

α_{CB}, α_{ST} = pattern ratio for checkerboard and strip loads, respectively

b = span length in direction perpendicular to a

b_1 = the length (the larger dimension) of each rectangular section of the beam.

β = load ratio

a/b = aspect ratio

c = diameter or width of column or capital

c_1 = diameter or width of column or capital in direction of span considered

c_2 = diameter or width of column or capital in direction perpendicular to that of span considered

C = a measure of the torsional rigidity of a beam (See Section A.2 of the Appendix)

C_a, C_b = a measure of torsional rigidity of a beam in the direction of the spans a and b

γ = moment ratio

E = modulus of elasticity

f'_c = compressive strength of concrete

f_r = modulus of rupture of concrete

f_y = yield stress of steel

G = modulus of elasticity in shear, $E/2(1+\mu)$

h = story height

h_i = the height (the larger dimension) of each rectangular section of the beam

H = relative flexural stiffness of beam

H_a = EI_a/bN, $H_b = EI_b/aN$, relative flexural stiffnesses of beams spanning in a and b directions, respectively

I = moment of inertia of gross uncracked section of member

J = relative torsional stiffness of beam

J_a = GC_a/aN, $J_b = GC_b/bN$, relative torsional stiffnesses in a and b directions, respectively

k_c, k_s, k_b = numerical factors reflecting the slope and support conditions of a member

K = $\dfrac{\Sigma\, k_c\, EI_{col}/h}{\Sigma(k_s\, EI_{slab} + k\, EI_{beam})/a}$, ratio of column stiffnesses at a joint to stiffnesses of other members framing into the joint

K_{bc} = stiffness of the beam-to-column combination

L = span length

L_1 = span length in direction considered

L_2 = span length in direction perpendicular to span considered

λ = a constant which is a function of the cross section of a beam

m_1 = a distributed torque applied along the axis of the beam

$\bar{M}$ = average moment across a section

M_o = sum of positive and negative moments in a panel

$\bar{M}_{CB}, \bar{M}_{ST}$ = average moments across a section due to checkerboard and strip loads, respectively

μ = Poisson's ratio

N = $Et^3/12(1-\mu^2)$, a measure of the plate stiffness

q = distributed load per unit of area

Φ = angle of twist per unit of length

t = thickness of a plate

t_1 = minimum thickness of a flat slab

t_2 = thickness of flat slab and drop panel

T = twisting moment

θ_f = total angle of rotation (caused by an arbitrary moment) of the end of a column without translation of either end

θ_t = the average angle of rotation of a beam with respect to the column

W = total load on a panel

W_D, W_L = total dead and live loads on a panel

2. BEHAVIOR OF TEST STRUCTURES UNDER PATTERN LOADINGS

2.1 Introductory Remarks

The effects of pattern loads are most easily studied and observed in terms of deflections and cracking which may be readily visible if excessive. Since deflections and cracking are measures of serviceability, they are studied in order to determine the significance of pattern loads on behavior of structures. Theoretical studies offer little information on deflections and none on cracking since they are concerned with an elastic material. It is necessary to turn to experimental studies to determine the behavior of structures under pattern loads.

A series of structures were built and tested at the University of Illinois. These structures have been fully described in References 1 through 6. Brief descriptions of the structures are given in this chapter. Loading patterns and load levels are also discussed. Deflections and strains under uniform loads are compared with those measured under pattern loads. A general discussion of the serviceability of the structures concludes the chapter.

2.2 Description of the Test Structures

A total of five structures were included in the University of Illinois floor slab test program. They are designated as follows:

F1	Flat Plate
F2	Flat Slab
F3	Flat Slab Reinforced with Welded-Wire Fabric
T1	Typical Two-Way Slab
T2	Two-Way Slab with Shallow Beams

The abbreviated notations will be used in the following discussion, figures and tables.

All the structures were designed according to the controlling criteria in the ACI Building Code Requirements for Reinforced Concrete 318-56 (hereafter referred to as the ACI Code, Ref. 7), except T2 which was modified so that the beams were less stiff than in a typical design. Structures F1, F2 and F3 were designed according to the Empirical Method of Section 1004 of the ACI Code by the firm of Di Stasio and van Buren, Consulting Engineers, New York. Structure T1 was designed following Method I of Section 709 of the ACI Code for "Two-Way Systems with Supports on Four Sides." This design was carried out by the firm of Paul Rogers and Associates, Chicago. Structure T2 was designed on the basis of two fundamental criteria. The first was that the total design moment was taken as the static moment or 0.125 WL. The second was that the behavior and strength were to be intermediate between F1 and T1.

The structures, as designed, had 20-ft square panels. The structures constructed in the laboratory were quarter-scale and had 5-ft square panels. All structures had nine panels arranged three by three.

Layouts of the test structures are shown in Figs. 2.1, 2.2 and 2.3. The data given in the figures include beam and column dimensions. The flat slabs F2 and F3 had the same dimensions, the only difference being the reinforcement. The properties of the materials used in construction of the test structures are given in Table 1. The experimental program consisted of construction, loading and analysis of the structures. Each slab was loaded in a series of tests including both uniform and pattern loads. Deflection and strain data were recorded at the different load levels in each individual load test.

Strains were obtained by placing electrical resistance strain gages on the reinforcement. Gages were placed to take advantage of symmetry of the structures and reduce the number of gages required.

Deflections were measured by means of mechanical deflection dials at 33 locations on the slabs. Readings were taken at the midpoints of the panels and at the midpoints of the column centerlines.

Crack patterns were recorded after selected load levels had been reached. The structures were examined for cracking by means of magnifying glasses and were then marked and photographed.

2.3 Loading Patterns on the Test Structures

All structures were subjected to uniform loading (all panels loaded) and to pattern loading consisting of strips of three panels in structures F1, F2 and F3 and checkerboard patterns in T1 and T2. The patterns are shown in Fig. 2.4. The deflection or moment which is maximized by the loading pattern is also indicated.

Loads were applied to the structure by means of a hydraulic jack system. The load was distributed over each panel by a series of frames which resulted in a 16-point loading. An over-all view of one of the structures is shown in Fig. 2.5.

The loads were measured with ring dynamometers and also with the large H-frames which can be seen in Fig. 2.5. These dynamometers were made up of four-arm bridges and gave accurate readings as well as providing a double check on the loading in each panel.

Each test consisted of the application of load to a given level. The load was applied in predetermined increments. The number of increments depended on the maximum level of loading, the previous loading history, and the expected behavior of the slab. Data were recorded at the initial zero load, at each load increment, and again at zero loads following loading.

The actual dead load of the test structures was less than the design dead load and to compensate for this, the applied load was increased in the uniform load tests. However, in the pattern load tests, the total dead load was not reached by applying additional load. Rather than use dead load and live load terminology, it is more appropriate to use the terms "movable" and "permanent" loads. The ratio of movable load to total load (sum of permanent and movable loads) is especially important in pattern loads since the lower the ratio the less the effect of pattern loads. If the movable to total load ratio is zero or all the load is permanent load, pattern loads are not possible.

The movable and permanent loads on the test structures under pattern loadings are summarized below.

Structure	Movable Load, psf	Permanent Load, psf	Total Load, psf	Movable Load / Total Load
F1	111	44	155	0.72
F2	241	44	285	0.85
F3	300	85	385	0.78
T1	174	41	215	0.81
T2	141	75	215	0.66

2.4 Effect of Pattern Loadings on Strains and Cracking

Strain readings were taken during both uniform load tests and pattern load tests. The strains were read at all the gage locations but of prime interest are those which were maximized as a result of a particular pattern load. The strains measured under the pattern loadings are compared with uniform load strains in Figs. 2.6 and 2.7.

In Fig. 2.6 the strains across the positive moment sections are shown. The increase in strains under checkerboard loading in T1 and T2 were quite small. However, the strains were increased considerably in the remaining structures when strip loads were applied. The strains increased from 17×10^{-5} to 57×10^{-5} in the interior panel of F2. The increases were greater in the interior panel than in the edge panel. The uniform load strains were higher in the edge panel but the change due to pattern loads was less in comparison.

The strains across negative moment sections are shown in Fig. 2.7. The strains in the interior panel were much higher initially and also increased much more. The strains at the edge beams were low and rather insensitive to pattern loads. The comparisons shown in Figs. 2.6 and 2.7 indicate that the changes in strains are greatest in interior panels and also that the positive moment sections are affected more than the negative moment sections.

The crack patterns observed in these tests indicated that there was little change in the over-all crack pattern after pattern load tests had been concluded. However, there is a definite correlation between the extent of cracking under uniform loads and the increase in strains under pattern loads.

Structures T1 and T2 were relatively uncracked at the conclusion of the uniform load tests. The pattern load tests did not increase the strains significantly and they were at low levels during both loadings.

Cracking was most extensive in structure F2 and the strains increased considerably. The crack pattern was not changed after pattern loading concluded, indicating that increases in strains took place largely through the widening of existing cracks.

The moments are increased at the sections where strains increase. In Fig. 3.1, the influence of cracking on the strains is illustrated. If the section has already cracked, any increase in moment must be accommodated by a significant increase in strain. The slope of the uncracked section is much higher and, therefore, the strains increase less for an equal increase in moment. In the sections where cracking had not taken place, as in the positive moment regions of T1, the strain increase was very small; however, the moment may have increased by a larger amount than in some of the sections where large strain increases were recorded. A complete discussion of moments is contained in Chapter 3.

2.5 Effect of Pattern Loadings on Deflections

The deflections were measured at 33 locations on the structures. In Figs. 2.8 through 2.12, the location at which readings were taken are shown by small circles. Since all the structures were partially symmetrical, some of the readings are, in effect, duplicated to provide a check.

The flat plate (F1) deflections are shown in Fig. 2.8. Strip loads increased the edge beam deflections very little and strip load slab deflections could be estimated by increasing the uniform deflections by 10 percent.

The deflections in the flat slabs, F2 and F3, are given in Figs. 2.9 and 2.10. The total loads on these two structures were 285 and 385 psf, respectively, so a direct comparison is not possible. In addition, the concrete strength of structure F2 was lower and cracking was quite extensive before strip loads were applied. The effect of cracking is to reduce the stiffness and thereby increase deflections. This behavior was apparent in structures F2 and F3. Structure F3, having greater loads, did not have correspondingly greater deflections. The strip loads doubled the deflections in F2 at some locations. The increases in F3 were not as great but were as much as 50 percent greater.

The increases in deflections were more significant in the flat slab structures than in the flat plate. The main reason for this difference is that of column stiffnesses. The flat plate had short stiff columns which tended to isolate the strips. The flat slabs had long flexible columns which did not provide the fixity that was present in the flat plate.

The load ratio was also a factor, being 0.72 for F1, 0.85 for F2 and 0.78 for F3. The lower load ratio for the flat plate tended to reduce the effect of strip loads, while the flat slab F2, having the greatest load ratio, also had the greatest increases in deflection.

The deflections measured in T1 and T2 are shown in Figs. 2.11 and 2.12. These structures had the same dimensions, except that the beams in T2 were less stiff. The load ratio was 0.66 for T2 and 0.81 for T1.

The uniform load deflections were less for structure T1 since its beams were stiffer. The beam deflections were nearly twice as large in T2. The effect of the checkerboard loading on these two structures is shown by comparing the uniform with the checkerboard load deflections. The mid-panel deflections in T1 increased about 10 percent while the beam deflections increased about 20-30 percent. The absolute increase in both beam and panel deflections was small. In structure T2, the mid-panel deflections changed very little (less than five percent in most panels). However, the beams, being more flexible than those in T1, deflected considerably under the pertinent checkerboard loads. The edge beam deflections increased from 10-30 percent with the interior span edge beam increasing as much as 50 percent. The interior beam deflections increased 20-30 percent. It can be seen from Figs. 2.11 and 2.12 that the more flexible the beams, the higher the deflections and the less the effect of checkerboard loads on mid-panel deflections. Since the beam deflections are maximized by loading adjacent panels (See Fig. 2.4), it is apparent that the beam deflections would have been about the same had strips been loaded rather than a modified checkerboard pattern.

2.6 Conclusions

The increases in steel strains were greatest across the positive moment sections of the interior panels of all the structures; in panels not supported by beams (F1, F2 and F3), the average increases in steel strains were about 100 percent. The increase was about 75 percent in the edge panels and less in the corner panels. In structures T1 and T2, the checkerboard loads did not produce significant changes in the strain in the positive moment sections.

The negative moment strain increases under pattern loading were less than the increases in positive moment strains in all the structures. At the interior negative moment sections, the strains increased by about one-third in structures F1, F2 and F3. The checkerboard loadings on T1 and

T2 did not change the strains across the negative moment sections. The exterior negative moment regions were virtually unaffected by pattern loads in all the structures.

Since the strains were the greatest in F2 under pattern loading and also increased the greatest amount in comparison with the other structures, it is interesting to examine the stresses in the reinforcement for that structure. The maximum positive moment stress in the interior panel increased from 5 to 18 ksi under strip load. In the edge panel the maximum positive moment stress was 18 ksi under uniform and about 30 ksi under strip load. In the other four structures, the design stress was not exceeded under pattern loads.

The deflections in the flat plate were almost the same under both uniform and strip loads. This can be attributed to the low load ratio and the relatively stiff columns in the structure.

The deflections in structures F2 and F3 were increased under strip loads. However, the extensive cracking in F2 resulted in a lower slab stiffness and the uniform load deflections as well as the increases under strip loads were larger than in F3. The larger increases in F2 resulted, in part, from the difference in the load ratios of the two structures.

The increases in deflections in the two-way slabs T1 and T2 were dependent on the beam stiffness. The pattern loadings resulted in greater increases in mid-panel deflections in T1 than in T2. The beam deflections were increased more in T2 than in T1. The more flexible the beams, the less the increase in slab deflection and the greater the increase in beam deflection under checkerboard loads.

It does not appear that the serviceability, measured in terms of strains and deflections, was impaired in the test structures as a result of pattern loadings.

3. MEASURED MOMENTS UNDER PATTERN LOADINGS

3.1 Introductory Remarks

In this chapter, the moments measured in the structure under pattern loading are compared with uniform load moments. The moments are computed from strain measurements. The analysis is based on the determination of a moment-strain relationship for each structure. The moment-strain relationship depends on concrete strength, reinforcement type and strength, and the percentage of reinforcement at a section.

The moments are computed for each of the five test structures. Comparisons are made between uniform and pattern load moments at the design sections of the structure. The design sections in flat slabs or flat plates are generally referred to as column, middle and wall strips. The moments in the wall strips of F1, F2 and F3 include the edge beam moments even though the beam and slab were designed separately for these cases. The design sections in the two-way slabs T1 and T2 are beams and slabs and the slabs are not divided into strips as in the case of the flat slabs.

In the following discussion, an evaluation of the moments will be given in terms of general trends. Since the conversion of strain to moment may result in larger moment differences in some locations, any abnormal differences can be disregarded if other similar sections yield consistent results.

3.2 Method of Analysis for Computation of Moments

The conversion of measured strains to moments is accomplished by constructing a moment-strain relationship for a particular section. The determination of a moment-strain curve is complicated by the difficulty of an accurate means of estimating the tensile strength of the concrete. The tensile properties of the concrete become extremely important in sections which have low reinforcement ratios since a large portion of the capacity is provided by the tensile strength of the concrete.

A typical moment-strain relationship for a section is shown qualitatively in Fig. 3.1. It is necessary to construct similar curves for each section in which the reinforcement ratio, concrete strength or depth to the steel changed. Each curve is made up of two straight lines. Two points in addition to the origin are needed to describe the curves. The coordinates of the intermediate point are the cracking moment and strain. The coordinates of the end point are the yield moment and strain. In the case of reinforcement having no well defined yield point, the moment at the proportional limit of the steel and the corresponding strain are used.

The cracking moments were computed using the ordinary flexure formula $\sigma=Mc/I$. The transformed section was used in computing the moment of inertia. The strain distribution across a section was assumed to be linear. The cracking stress used in the formula was generally less than the modulus of rupture reported in Table 2.1. However, the control specimens were not reinforced which resulted in higher strengths. The reinforcement in the slab tended to restrain shrinkage and lower the tensile strength. In addition, the assumed tensile strength and cracking strains were chosen to correlate with results of studies of the static moments in the interior panels of the structures which could be computed accurately.

The yield moment of the section was computed using the straight-line formula. It was assumed the tensile strength of the concrete was negligible at yield in the steel and that cracking had developed sufficiently to warrant this assumption.

The moment-strain curves for the beams were developed in the same manner. It was necessary to make an additional assumption about width of the slab that was acting as a flange at the beams. This flange width was assumed to be 4t (four times the slab thickness) in structures F1, F2 and F3 at the deep beam edge and zero at the shallow beam edge. The flange width was 4t in structure T1 for all beams and 3t in structure T2 for all beams.

The assumed cracking strain and stress and the flange widths are summarized in Table 2. The actual concrete properties were given in Table 1 which also includes the properties of the reinforcement.

The proper use of the moment-strain curves depends upon correctly interpreting the strain readings. The strain measurements are affected by electrical drift in the wiring and switch systems. In addition, residual strains are accumulated which must be taken into consideration.

The electrical drift was easily corrected by monitoring a check gage which should have undergone no change in strain during loading. Any changes in the check gages were attributed to electrical drift and a correction was made in the strain measurements for the reinforcement.

The residual strains are determined from the differences between the initial and final zero readings in a given test. These summations of the residuals (ϵ_{res} in Fig. 3.1) are then added to the strains measured in the following test to obtain the total strain for a particular load.

The moment-strain curves gave excellent results if the strains used were higher than any previous strains measured. However, in certain cases the strains were lower than had been measured in a previous test and a slightly different procedure had to be followed. The curve in Fig. 3.1 shows an unloading curve as well as the first-loading curve. If the strains were greater than ϵ_{max}, the first-loading curve could be used $(\epsilon_2 > \epsilon_1)$. If the strains were less than ϵ_{max} or $\epsilon_2 < \epsilon_1$, the slope of the unloading curve was used as indicated in the figure. It is possible for the slope $\bar{K}_1/\epsilon_1$ to change since the value of ϵ_{res} may change while the value of ϵ_{max} remains the same during tests in which ϵ_{max} is not exceeded. However, the slope of the unloading curve does not change greatly between tests and tends to decrease as the strains increase.

3.3 Moments in the Flat Plate

The moments computed from strain measurements in structure F1, the flat plate, are given in Fig. 3.2 as coefficients of qa^3. The uniform load moments shown in the figure were measured at a total load of 155 psf. The strip load moments, shown in red numerals, were based on strains measured under loads of 155 psf on the "loaded" panels and 44 psf on the "unloaded" panels. This loading gives a load ratio of 0.72.

The moments are computed across the critical negative and positive sections used in design. The divisions are made according to column, middle and wall strips. Column and middle strips have a width of one-half the panel width and the wall strip is one-fourth the panel width.

The moments in the middle strips were about 0.02 qa^3 at all sections except the exterior negative. The strip loads did not increase these moments significantly. The column strip negative moments were not changed while the column strip positive moments did increase slightly.

The relatively small changes in slab moments under strip load are explained by the presence of stiff columns. The columns were short and relatively wide, making them flexurally stiff. The stiff columns tended to isolate the strips or, in effect, fix the panels.

The wall strip moments, which include the beam moments, showed much greater increases at some locations. However, the beams were considerably more difficult to analyze and therefore are less accurate. The strain in the beam reinforcement was not measured precisely at the face of the column. Since the moment gradient is quite high at that location, correcting the moment to the face of the column, even if for a short distance, may result in a large absolute moment change.

Several additional factors complicate the beam analysis. Torsional rotations of the beams with respect to the column may induce strains which cannot be gaged. Cracking in the beam at the location of the strain gage is likely to change the distribution of strain along the reinforcement. The loss of bond between the bar and the concrete accompanies the placement of strain gages and also affects the strain distribution. For these reasons, no beam moment corrections were attempted and the moment computed at the gage location was assumed to be the moment at the critical section.

The comparison of strip load moments with uniform load moments is shown in Fig. 3.3. The moments are indicated by the small symbols. Two values of moment ratio ($\gamma = 4/3$, $\gamma = 1$) are indicated by the straight lines. A moment ratio of one indicates no change due to pattern loads. The value of $\gamma = 4/3$ is a precedent that has been frequently given as an allowable increase (See Chapter 5).

Points that lie below the line $\gamma = 1$, indicate that the moment decreased under strip loads. It can be seen that most values lie between the two lines. The only values that lie above $\gamma = 4/3$ are wall strip moments and as was discussed above, these values may not be indicative of the actual moments because of the difficulty with beam analyses. From this figure, it is apparent that the slab moments did not exceed $\bar{\gamma} = 4/3$ and if the beam moments are omitted, $\gamma = 1.2$ for the slab moments.

3.4 Moments in the Flat Slabs

The moments in the two flat slabs were measured at a load level of 285 psf on F2 and 385 psf on F3. The movable loads were 241 psf and 300 psf, respectively, resulting in nearly equal load ratios, 0.85 for F2 and 0.78 for F3.

The critical sections across which the moments are analyzed are the same as those used in the flat plate. The uniform and strip load moments are given in Fig. 3.4 and 3.6.

Since the two structures were identical except for the type of reinforcement, the uniform load moment coefficients should be similar. There was little difference between the moments at most sections. The location of the maximum relative difference is at the interior span positive moment section where the moment is about 0.015 qa^3 in F2 and 0.009 qa^3 in F3 in the middle strips.

It can be seen that the wall strip moments are high, especially at the deep beam edge negative sections. However, for the purpose of this discussion, the relative increases are more important than the absolute moments.

The effects of the strip loadings on F2 and F3 are shown in Figs. 3.5 and 3.7. The lines at $\gamma = 4/3$ and $\gamma = 1$ are drawn and in both structures the moments lie consistently between these lines.

The only values that appear to be greater than $\gamma = 4/3$ are the interior span positive moments in F3. It was pointed out previously that the uniform load appeared to be low across this section and it is evident also in this comparison. The strip load moment coefficients across the interior span positive section are about 0.017 qa^3 in F2 and 0.018 qa^3 in F3. Therefore, the points above the line can be attributed to low uniform load moments.

It is interesting to note that the high absolute moments analyzed in the wall strips are not significant when comparisons are made between strip and uniform load moments. In structure F2, the wall strip moment was very high at the deep beam edge, about 0.06 qa^3, but the moment ratio at this location, shown in Fig. 3.5 is reasonable in view of the general trends.

The moment ratio in F2 was actually not as high as 4/3. Most of the points lie below the moment ratio of 1.2 which indicates that the moments did not undergo serious changes due to strip loads. Although, a few values exceeded $\gamma = 1.2$ in structure F3, it is a more representative value of γ than $\gamma = 4/3$.

3.5 Moments in the Two-Way Slabs

The moments in the two-way slabs were measured at a total load of 215 psf on both T1 and T2. The movable load on T1 was 44 psf and 75 psf on T2 giving load ratios of 0.81 and 0.66, respectively.

The moments are given for slab and beam sections. The slab is not divided as it was in the case of the flat plate and flat slab structures. The uniform and checkerboard load moments are given in Figs. 3.8 and 3.10.

The uniform load moments are as expected in view of the difference in the beam stiffnesses. The interior beam moments are about 50 percent greater in T1 than in T2. However, the slab moments in T1 are less than half of the values in T2.

Checkerboard patterns were used to create maximum loading conditions. The increase in moments in T1 yields moment ratios that lie between $\gamma = 1$ and $\gamma = 4/3$ as shown in Fig. 3.9. The comparisons indicate that the structure behaved well under checkerboard load since no serious deviations occurred in either the slab or the beam moments.

The comparison of checkerboard and uniform load moments for structure T2 are shown in Fig. 3.11. These comparisons indicate that the moment ratio for the structure was about 1.2. However, if only slab moments are considered, γ is about one. It appears that slab moments were not maximized by checkerboard loads. The beam moments which are maximized by modified checkerboard loads account for the value of $\gamma = 1.2$. The beam moments are obtained by loading adjacent panels or what is nearly a strip load and the slab moments may also have been greater if strip loading had been used.

3.6 General Discussion of Measured Moments

The moments measured in the test structures have been discussed in terms of absolute moments and by comparing pattern with uniform load moments. The absolute moment coefficients gave an indication of the magnitude of the moment at a particular location. However, as was pointed out previously, the absolute values may, in some cases, not have been accurate.

Greater accuracy is obtained when the strains are high. In some sections, such as the exterior negative sections, the strains were low under both pattern and uniform loads. Therefore, small changes in strains resulted in large moment changes in moments of rather low magnitude.

In order to determine the relative increases, the pattern load moments were plotted against the uniform load moments. These plots provide a means for determining the effect of pattern loads on the structure as a whole. Locations which have large moment differentials assume less importance if the remaining moment changes are consistent. From these plots (Figs. 3.3, 3.5, 3.7, 3.9 and 3.11) a moment ratio for each of the structures was obtained. For structure F1, the moment ratio γ was 1.2 if the wall strip moments are excluded. The moment ratios for F2 and F3 were also about 1.2. The moment ratio for structure T1 was about 1.2. The slab moment ratio for T2 was about 1.0 and for the total structure about 1.2 since the beam moment ratio was higher. The load ratio on T2 was lower than on T1, 0.66 compared with 0.81, and this has the effect of reducing the moment ratio.

The moment ratios given in the preceding paragraph are average values for the structure as a whole. It can be shown by comparing individual sections that the moment ratios were greater for interior than for exterior panels.

It does not appear that the moments in the test structures were critical under pattern loads. It should be remembered that these are average moments across specific sections and that the local moment at some areas may be higher. However, since reinforced concrete slabs can undergo significant moment redistribution, these effects tend to be minimized and should create no serious problems as indicated by the test results.

4. THEORETICAL SOLUTIONS FOR PATTERN LOADINGS

4.1 Introductory Remarks

A three-dimensional structure composed of several bays and stories generally has a floor slab as one of its structural components. The floor slab is divided arbitrarily into sections referred to as panels which span between the supporting elements of the floor slab. Since such a system has a number of panels, it becomes possible to apply load to individual panels as well as to all panels simultaneously.

The theoretical solutions for the problem of flexure in plates are generally limited to plates of a homogeneous, isotropic, linearly elastic material. The selection of such a material expedites analysis which consists of solving equations based on statics and geometry. The structures analyzed by this process may respond differently from structures studied by direct physical tests. However, the elastic solution does represent a good first approximation to the response of the structure and makes it possible to study the effects of a wide range of variables. The elastic solutions are valuable in making comparisons between structures and establishing continuity between individual physical tests.

A number of elastic solutions are available for study. The range of variables is extensive enough to provide a general understanding of the effect of pattern loadings on slab moments. The major variables which have been considered are the beam flexural stiffness, beam torsional stiffness, column stiffness, aspect ratio of the panels and the loading pattern. These solutions form a framework which may be used to determine the effects of pattern loadings on moments in idealized, elastic structures.

The slab moments discussed in the following sections are average moments, an average moment is expressed in units of load and must be multiplied by the distance across which it acts to obtain the total moment. Beam moments in the idealized structures must, of course, be in terms of total moment. The moments for a given aspect ratio (a/b) are given only for the $\bar{a}$ span, unless otherwise noted. For example, the moment in a panel having an aspect ratio of 0.5 would be in the short span (across the long span edge).

4.2 Definition of Variables

(a) Beam Flexural Stiffness

The relative beam flexural stiffness is defined as follows:

$$H_a = EI_a/bN \text{ or } H_b = EI_b/aN \quad ,$$

where
- I_a = the moment of inertia of the beam in span $\underline{a}$
- b = span perpendicular to span $\underline{a}$
- $N = \dfrac{Et^3}{12(1 - \mu^2)}$, a measure of the plate stiffness per unit width
- t = the plate thickness
- μ = Poisson's ratio, assumed to be zero in these studies.

The beam stiffness parameter relates the stiffness of the beam to the stiffness of the slab in the direction of the beam. The range of beam stiffnesses is from zero to infinity where zero is the case where no beam is present and infinity is a rigid support. The beam has no width in the elastic solutions. In effect, it lies in a vertical plane at the boundary of the panel. The use of such a beam reduces the complexity of the equations needed for a solution.

In the theoretical solutions considered here, the beam flexural stiffness ratios in the two spans of a panel are always related in a definite manner. For a/b = 1.0, $H_a = H_b$; the beams in the two directions are identical. For rectangular panels the EI value of the beam in the long span is always greater than the EI value of the beam in the short span by the ratio of the sides of the panel; $EI_a : EI_b = a:b$. In terms of the relative stiffness parameter, H, this is expressed by $H_a(b/a) = H_b(a/b)$ or $H_a = H_b(a/b)^2$

(b) Beam Torsional Stiffness

The relative beam torsional stiffness is defined as follows:

$$J_a = \frac{G\ C_a}{aN} \quad \text{or} \quad J_b = \frac{G\ C_b}{bN}$$

where G = shear modulus of elasticity

C_a = torsional stiffness in span a

The beam torsional stiffness parameter relates the torsional stiffness of the beam to the flexural stiffness of the slab spanning across the beam. The values of torsional stiffness range from zero to infinity. A value of zero is for the case where no beam is used while an infinite torsional stiffness applies to a clamped edge. As in the case of flexural stiffness, the torsional restraint is applied to the panel through a beam lying in a vertical plane at the boundary of the panel.

(c) Column Flexural Stiffness

The relative column flexural stiffness is given by the expression:

$$K = \frac{\sum k_c\ EI_{col.}/h}{\sum (k_s\ EI_{slab} + k_b\ EI_{beam})/a}$$

where I = moment of inertia of gross, uncracked section of column, slab or beam in direction in which moment is considered

h = story height

a = span length

k = a factor representing the support conditions of the member (e.g., 4 if the far end is fixed and 3 if it is simply supported).

The values of K may range from zero where a slab does not transfer any moment to the column to infinity where heavy columns are used. In the idealized structures, the column stiffness is transmitted to the panel through a vertical line located at the corner of the panel.

(d) The Aspect Ratio (Ratio of Side Lengths)

The aspect ratio a/b may range from zero to infinity. The values of aspect ratio considered in this chapter range from one-half to two. These values cover the range of panel sizes commonly encountered in floor slabs.

(e) Loading Patterns

Three loading patterns were considered in the solutions. Entire panels were loaded uniformly in each case. No studies were made for concentrated loads or loads varying across the panel. In order to determine the effects of the pattern loadings, it was necessary to obtain the moments for all panels loaded uniformly. These moments are referred to as uniform load moments. In addition, the slab systems were loaded by strip (ST) and checkerboard (CB) patterns. These patterns are shown in Fig. 4.1. The patterns may be different when positive or negative moments are being studied. These moments are referred to as maximum moments in the following tables and figures.

The checkerboard loading for maximum negative moment is achieved by placing two checkerboard patterns end to end. The strip pattern for negative moment does not yield the absolute maximum moment since there are always two strips loaded and two under zero load. This loading arrangement resulted from the use of superposition. The maximum moment occurring when two alternate strips are loaded is 0.104 qa^2 while the true maximum moment is 0.11 qa^2. The checkerboard pattern for maximum negative moments was also chosen to allow superposition of available solutions.

The values of moments resulting from pattern loadings were obtained by averaging the uniform load moments and moments in alternately loaded one or two panel strips as shown in Fig. 4.2. The patterns resulting from superposition are also shown in Fig. 4.2.

4.3 Effect of Pattern Loadings on Moments in an Interior Panel

The majority of available solutions in which pattern loadings are considered are concerned with interior panels. The interior panel is defined to be one bounded by an infinite number of identical panels. Interior panels are chosen since they afford the use of symmetry. In the theoretical solutions, the symmetry of the panel reduces the number of equations necessary for a solution. The solutions discussed in this section were obtained from References 8 through 12.

The various theoretical solutions available for an interior panel may be divided into two groups according to the parameters which are varied. The major variable is the beam flexural stiffness in the first group and the beam torsional stiffness in the second group.

In the first group, the beam flexural stiffness varies from zero to infinity. The beam torsional and column flexural stiffnesses are assumed to be zero. Five values of the aspect ratio are considered, 0.5, 0.8, 1.0, 1.25 and 2.0. Table 3 lists average moments at the critical sections for positive moment under uniform, checkerboard, and strip loadings. Table 4 lists negative moments under the same loading conditions.

The strip and checkerboard moments are compared with the uniform load moments in terms of pattern ratios. The pattern ratios, designated as α, are plotted against the parameter $H/(1+H)$ in Figs. 4.4 through 4.8. Since the values of H extend to infinity, the parameter $H/(1+H)$ was used to allow a finite scale for the plots.

Three important trends emerge from a study of the data presented in Table 3 and Figs. 4.4-4.8. These are discussed in the following three paragraphs.

The first trend is one that can be deduced without the necessity of rigorous solutions. As the relative beam stiffness H increases, the slab moments decrease for all types of loading. The decrease may be drastic as in the case of a panel having an aspect ratio of 2.0. The average negative moment across the short edge for strip loading is $0.1042\ qa^2$ for $H = 0$. This value is $0.0079\ qa^2$ for $H = \infty$, a reduction of 92 percent.

As the relative beam stiffness H increases, the checkerboard loading becomes more critical than strip loading. The pattern ratio for a square panel with $H = 0$ is 2 for strip and 0.8 for checkerboard loading (Fig. 4.6). For $H = \infty$, the moment ratio becomes 0.9 for strip and 1.7 for checkerboard loading. It should be emphasized that checkerboard loading does not govern for all finite values of H. The value of H at which the checkerboard loading produces a greater pattern ratio than the strip loading varies with the aspect ratio but in all cases is more than one.

The positive moments are increased more than the negative moments by the pattern loadings in this group of solutions. The negative moment pattern ratios do not exceed 1.25 whereas the positive moments may be as much as twice the uniform load positive moments. This trend can be seen in the curves shown in Figs. 4.4-4.8, where the pattern ratios for positive moment always lie above the negative moment pattern ratios.

The influence of the beam torsional stiffness on the moment can be studied with the help of the second group of solutions given in Table 5. These solutions have been obtained from a moment distribution procedure for slabs supported on rigid beams developed by Siess and Newmark (11)*. The procedure is approximate and all comparisons between uniform load and checkerboard load moments must be made between moments computed by this procedure. Therefore, absolute moment values given in Table 5 may not be the same as those in Tables 3 and 4. The loading patterns used to obtain these moments are shown in Fig. 4.3.

Values given in Table 5 show that as the beam torsional stiffness increases, the checkerboard load has less effect on moments. It is not necessary to consider strip loads in these panels; it was shown previously that checkerboard loadings are critical in the case of flexurally rigid beams. The positive moment increases are generally greater than the negative moment increases in these solutions also. For an aspect ratio of 2.0 where the

---

* Numbers in parentheses refer to entries in the bibliography.

negative moment increases are greater, the absolute values of the moments are quite small and subject to greater errors in the distribution procedure than large absolute moments.

The ratios of checkerboard load moments to uniform load moments are plotted against the beam torsional stiffness represented by the parameter $J/(1+J)$ in Figs. 4.9 and 4.10. The moment is unchanged when J is infinite: the plate becomes clamped at the edges and pattern loadings have no effect.

Very few three-dimensional studies have been made of the variation of slab moments with column stiffness. Morrison (13) obtained solutions for nine-panel structures with square panels and rigid columns and varied the beam flexural and torsional stiffnesses. The moments were for uniform and strip loads. The positive moments for the interior panel are summarized below.

Moments in Interior Panel, $K = \infty$

H	J	Uniform Load Moment, qa^2	Strip Load Moment, qa^2	Pattern Ratio
0	0	0.037	0.046	1.24
0.5	0.5	0.023	0.027	1.17
2.0	0.5	0.017	0.018	1.06
2.0	2.0	0.017	0.017	1.00
5.0	5.0	0.013	0.013	1.00

It is important to note that the pattern ratio for $H = J = 0$ is 1.24 when the columns are rigid and 2.0 when $K = 0$. The moment coefficients shown vary slightly from those shown in Table 4.1, but there are edge effects in the interior panel of a nine-panel structure and the columns have a finite c/L ratio ($c/L = 0.1$).

The effect of increasing column stiffness is similar to increasing beam flexural stiffness. Therefore, as the column stiffness increases, the value of H at which checkerboard loads yield higher moment ratios is decreased; the column imparts additional stiffness to the beams. The increase in moment due to checkerboard loads is not reduced by increasing column stiffness. Only the range over which checkerboard loads are critical is increased. The column stiffness does reduce the increase in moments under strip loading, however.

Westergaard and Slater (14) studied the effects of strip loads on square panels of flat slabs with varying column stiffnesses. Two cases were considered; rigid columns and columns in which the capitals were free to rotate. It was found that for $c/L = 0.15$ and rigid columns the positive moment pattern ratio due to strip loads was 1.20 which compares well with Morrison's value of 1.24 for $c/L = 0.10$.

In order to determine the effects of columns having intermediate stiffnesses, Westergaard proposed a frame analogy enabling interpolation between stiffnesses of zero and infinity. By definition, the column stiffness K is the distribution factor to the column in a two-dimensional frame considering the slab as a beam. For such a frame, it can be shown that the pattern ratio is a function of the equation $K/(1+K)$, the degree of fixity. The degree of freedom is $1 - K/(1+K)$ or $1/(1+K)$. In a frame, the positive moment pattern ratio is 2.0 if the fixity is zero and 1.0 if the fixity is one. However, in a slab with rigid columns there is some "leakage" of moment around the columns since the pattern ratio is 1.20. Therefore, Westergaard interpolated linearly between fixity values of zero and one. The pattern ratio was 1.20 at a fixity of one and 2.0 at a fixity of zero. Therefore, the pattern ratio could be obtained simply by using 1.20 + 0.80 [1/(1+K)].

It is necessary to consider the effects of column stiffness when the aspect ratio is not one. If the aspect ratio is less than one, the columns are not as effective in reducing the influence of strip loads. If the aspect ratio is very small, the columns do not reduce strip load moments. The pattern ratio remains at 2.0. If the aspect ratio is greater than one the columns become more effective. In the case of very large aspect ratios, the pattern ratio becomes 1.0 for rigid columns.

The influences of beam torsional stiffness and column and beam flexural stiffnesses cannot be completely isolated. In order to develop the beam torsional capacity, the column and/or the beam must be able to carry the torsion transmitted to it. In the case of positive moment checkerboard loadings, the column stiffness is not critical since there is a diagonal line of symmetry across the columns. However, for other patterns it is of importance. The general effect of column flexural and beam torsional stiffnesses is to isolate the panel from loadings in adjacent panels. If the values of J and K are increased, the pattern loadings will have less effect.

The first group of solutions (Tables 3 and 4) in which J and K were assumed to be zero are more severe than solutions in which the values of J and K are finite. For a given panel size, the increases in moment would be no greater than those listed in Table 3. The increase in positive moment is greater than the negative moment and the pattern ratio is decreased as the parameters H, J or K are increased.

4.4 Effect of Pattern Loadings on Moments in Panels with One or Two Discontinuous Edges

In most structures, there may be as many panels having discontinuous edges as there are interior panels. Since, these panels behave differently under pattern loads than when all panels are loaded, it is necessary to determine what influence the pattern loads exert on the moments. The solutions discussed here were obtained from References 11 and 12. These solutions make use of the distribution procedure of Reference 11 and the absolute moment values are approximate but they afford the opportunity to make comparisons between uniform and pattern load moments.

Moments in edge and corner panels are given in Tables 6, 7 and 8. In the case of an edge panel, the moments are given for spans parallel and perpendicular to the edge. All moments are in terms of the span $\underline{a}$ which is the span in which moments are considered. The solutions assume flexurally rigid beams and only checkerboard loads are considered.

As in the interior panel, the effect of pattern loads decrease as J is increased. The pattern ratio α for the edge and corner panels is compared with the pattern ratio for a similarly supported interior panel. It can be seen that α is less for a panel with discontinuous edges than for a comparable interior panel. In an edge panel, α is nearly the same as in an interior panel. However, in a corner panel α is considerably less. For example, the positive pattern ratio in an interior panel having an aspect ratio of 0.5 and J = 0 is 1.67. In an edge panel it is 1.55 in the parallel span and 1.47 in the perpendicular span, while in a corner panel it is 1.33. Similar comparisons may be observed for other values of the aspect ratio and torsional stiffness.

In order to discuss the effects of strip loadings in discontinuous panels, the three dimensional structure may be reduced to a two-dimensional frame. In such a frame, it can be shown that the end span is less affected by pattern loadings than the interior spans. Although the uniform load moments are higher in the end span, the moment increase is less. When columns of the frame are made stiffer the spans tend to be isolated further from effects of loading in adjacent spans. Therefore, the solutions for the interior panel strip loadings yield increases in moment which are greater than those in discontinuous panels.

The range of variables for which solutions are available and the frame analogy provide sufficient information to determine the effects of pattern loads on edge and corner panels. The effect of pattern loadings on these panels is dependent on the number of discontinuous edges. There is little difference between moments in an edge panel in the direction parallel to the discontinuous edge and those in an interior panel. However, in all cases the pattern ratios are less in the panels with discontinuous edges than in interior panels. The pattern loadings are less critical in the edge and corner panels than in the interior panels.

4.5 Effect of Pattern Loadings on Moments in Beams

It was shown in Sec. 4.3 that the moment in the panel tends to decrease as the beam flexural stiffness increases. The moment is transferred to the beam. Since these beams may carry large moments, it is important that the effect of pattern loadings on their behavior is discussed.

A limited number of solutions are available for beam moments. Only the effect of strip loads are given since beam moments are greatest when the panels adjoining the beam are loaded. In Table 9, beam moments are listed. As the stiffness of the beam increases the moment carried by the beam increases also. The negative to positive uniform load moment ratio is about 2 to 1, similar to a continuous beam. The values of α for strip load positive moment are between 2 and 3 while the negative moment ratios are about 1.3. These trends are similar to the continuous beam where only certain spans are loaded to create maximum moments. In a continuous simply-supported beam, the positive moment may be twice as large by loading alternate spans and the negative maximum moment 1.25 times the moment when all spans are loaded.

The values of α for strip loads are plotted against the beam stiffness in Fig. 4.11. These curves show quite definitely that the negative moment is not altered as substantially by the strip loads as is the positive moment. The negative moment increases fall within a narrow band. However, the positive moment ratios are quite scattered. As the aspect ratio increases, the positive moment increases less with greater beam stiffness. It will approach the ratio of 2 as the aspect ratio becomes large. In effect, the continuous beam case is approached.

The increase in beam moments in the beams supporting a slab are quite similar to those in a continuous beam. The trends exhibited by these beams as far as negative to positive moment distribution and increases in moment due to pattern loads can be closely predicted by examining a continuous beam.

4.6 Conclusions

In the preceding sections, the available theoretical solutions for pattern loadings were compiled. The effects of strip and checkerboard patterns on continuous and discontinuous panels were studied. Certain conclusions based on the theoretical solutions are presented here. The trends in moment changes in the slab and the beams are summarized separately.

Three distinct conclusions can be drawn from a study of the effects of pattern loads on slab moments. First, it was shown in Tables 6, 7 and 8 and in the frame analogy that the pattern ratios are less for both strip and checkerboard loads in a discontinuous panel than in an interior or continuous panel. Therefore, the effects of pattern loads are more critical in the interior panel and it is sufficient to concentrate on such panels.

Secondly, checkerboard loads do not control for all values of finite beam stiffness. As H increases, pattern ratios for checkerboard loads increase, however, may not be critical until the beam stiffness reaches a value considerably above zero.

Thirdly, the positive moments are affected more than the negative moments by pattern loadings as illustrated by the curves in Figs. 4.4-4.10.

The effects of pattern loads on the beams in slab structures are very similar to the effects on continuous beams. The positive moment increases are greater and slightly larger than those occurring in a continuous beam. This is due to the moment being attracted from the slab to the beam and resulting in a proportionally greater moment under pattern loads.

5. COMPARISON OF DESIGN AND MEASURED MOMENTS

5.1 Introductory Remarks

In the preceding chapter, solutions were presented for the effects of pattern loads on moments. Various values of the stiffness parameters were considered. It was shown that the transition between slabs with no beams and slabs supported on beams is a gradual and continuous transition. However, in the various design procedures currently in use, a distinction is made between slabs with or without beams; two-way slabs or flat slabs.

In this chapter, the development of the design procedures is discussed. The important features of the methods are pointed out and special emphasis is given to the provisions included for pattern loadings.

The typical design resulting from use of these methods is given. The design moments used in the test structures were obtained using ACI Code provisions. Finally, a comparison is made between the design and measured moments in the test structures. Both pattern and uniform load moments are compared with the design moments. In this way, an evaluation of the design procedures as to their ability to provide for the actual moments is possible.

5.2 Design Methods

Design of reinforced concrete slabs has been divided into two classes; the flat slab and the two-way system with supports on all sides which is usually called a two-way slab. Basically, the flat slab is supported directly on columns and may have capitals and drop panels. If there are no capitals or drop panels it is commonly referred to as a flat plate. The two-way slab is supported along its edges by walls or beams.

However, the two types are often combined, the flat slab having beams and the two-way slab having none in some spans, but the design procedure is quite different depending upon the basic type of slab chosen.

The reason for the difference is mainly one of development of design methods. The development of each method is briefly discussed in Sec. 5.3 and 5.4. Particular emphasis is given to the provisions for pattern loading.

5.3 Design Methods for Flat Slabs

The actual construction of flat slabs preceded any formal design procedure and resulted in a wealth of differing opinion as to their adequacy and analysis. Engineers who had successfully built and tested their designs could defend them on principles of pragmatism. In Reference 15, the various procedures are discussed.

Most of the engineering public considered flat slabs to have properties which precluded rigorous analysis and until J. R. Nichols (16) wrote his paper presenting a relatively simple solution, no one ventured into the area of analysis. He developed an equation which, for the total moment in an interior panel of a pin supported slab, would be

$$M^+ + M^- = M_o = \frac{WL}{8} \tag{5.1}$$

where M^+ and M^- are moments across the positive and negative sections and M_o is the total moment. This equation did not give the distribution to negative and positive moment sections but specified the sum. For a slab supported on finite columns, Nichols derived an approximate expression:

$$M_o = \frac{WL}{8}\left(1 - \frac{2c}{3L}\right)^2 \tag{5.2}$$

However, the First Joint Committee (17) in 1916 gave the design static moment as $M_o = 0.107\ WL\ (1 - \frac{2c}{3L})^2$ or 85 percent of that computed by Eq. 5.2. This was subsequently (1920) reduced even further to $M_o = 0.09\ WL\ (1 - \frac{2}{3}\frac{c}{L})^2$. The Second Joint Committee (18) recommended the same equation with explicit recognition of the fact that they were designing for 72 percent of the moment resulting from a consideration of statics. The 1956 ACI Building Code (7) added a factor F ($F = 1.15 - c/L$, but $F \bar{>} 1$) which was to prevent the possibility of low design moments in slabs with low c/L ratios, $M_o = 0.09\ WL\ F(1 - \frac{2}{3}\frac{c}{L})^2$.

Up to this time, no explicit consideration had been given to pattern load conditions. All moment coefficients were based on uniform loads over all panels. Studies made for the 1941 ACI Building Code (19) showed that various arrangements of the movable load gave significantly higher moments at some locations. Rather than alter the moment coefficients since they had been in long satisfactory use, the flexibility of the columns was limited in order to minimize the effects of live load differentials between panels.

It was considered satisfactory for the maximum moments to exceed the uniform load moments by not more than 33 percent. It was found that this could be accomplished by establishing a minimum average moment of inertia for the columns above and below the floor (See Ref. 20). This was given by the formula which is found in Sec. 1004(b) in ACI 318-56.

$$I_c = \frac{t^3 h}{0.5 + \frac{W_D}{W_L}} \tag{5.3}$$

where I_c = minimum moment of inertia of column but $I_c > 1000$ in^4

t = the minimum required slab thickness in inches as given in Sec. 1004(d)

h = story height

W_D and W_L = total dead load and live loads on panel

The formula was derived by analyzing a number of frames with varying column stiffnesses and load ratios W_D/W_L and limiting the increase of the sum of the maximum negative and positive moments to 33 percent.

It was recognized that the maximum negative and positive moments would not occur simultaneously and that redistribution of moment would have a beneficial effect in reducing the severity of the loading imbalance. Therefore an increase of 33 percent was allowed.

Since the maximum positive and negative moments cannot occur simultaneously, the equation limits either the positive or negative moment increases under strip loads to 33 percent. The effectiveness of this equation may be estimated by considering the moment of inertia of a typical column and comparing the moment increases that are known to result from certain column stiffnesses.

The efficiency of columns in reducing the effects of strip loads was discussed in Sec. 4.3. The increase in moments in a square panel could be computed by the equation $1.20 + 0.80\,[1/(1+K^*)]$. It is interesting to compare the increase in positive moment that would occur if minimum values of column stiffness prescribed by the ACI Code are used. For typical value

---

* $$K = \frac{\sum k_c\, EI_{col.}/h}{\sum (k_s\, EI_{slab} + k_b\, EI_{beam})/a}$$ (See Sec. 4.2c)

of t, H, L, and $W_D/W_L = 0$, the value of K is usually greater than 1.0 so the moment ratio may be about 1.60 which is more than the prediced value of 1.33. The values of K must be about 5 in order to keep the moment ratio less than 1.33. Although the dead to live load ratio will usually be less severe than used here, it does not appear that the limiting column stiffness (Eq. 5.3) is sufficient to reduce the effects of strip loads, within the allowable range. In addition, for aspect ratios less than one, the efficiency of columns is further reduced.

The need for a more rational method for the design of flat slabs arose from the inability of the empirical method to account for the effects of pattern loadings on moments in slabs and columns. Out of this concern the frame or elastic analysis was developed which essentially reduces the three-dimensional structure to a two-dimensional frame.

The Elastic Analysis appeared in the 1941 ACI Code but was modified to yield answers comparable to the empirical method so it did little to alleviate the problem of pattern loads. The moments were obtained in the frame by using either the known load conditions or by positioning the full live load on the spans to obtain maximum moments. (The 1963 ACI Code, Ref. 21, uses 3/4 of the live load in pattern load configurations to take advantage of the probability of a greater dead load-live load ratio and moment redistribution effects.) The moments in the frame were based on conditions of equilibrium and therefore were higher than those of the empirical design. To eliminate this discrepancy, the negative moments at a distance from the column center line could be used in design. The consequences of this recommendation were moments that were nearly the same as the empirical design moments. The benefit of a solution based on equilibrium was lost. The method did serve to alert the designer to pattern loads and provided a method of design when the aspect ratio was beyond the limits imposed by the empirical method ($0.75 \leq a/b \leq 1.33$).

The design of flat slabs largely ignores the effects of pattern loads. The empirical method limits column stiffness but is not adequate to reduce pattern load effects to a predetermined level. The elastic analysis considers pattern loads in determining design moments then reduces the negative moments to a level which gives total moments nearly equal to the total moment in the empirical method.

5.4 Design Methods for Two-Way Slabs

The recommended design of two-way slabs is currently by use of any one of three methods given in the 1963 ACI Code. Method 1 has appeared in the ACI Code since 1936, Method 2 since 1947 and Method 3 in 1963. The development and essential aspects of each method will be discussed in this section. Detailed discussions of these methods appear in Reference 22.

(a) Method 1

Unlike the flat slab which was attributed extraordinary strength, the two-way slab was analyzed by routine flexural computations. The two-way action of the slab was not fully recognized or utilized. The beams on which the slab rested spanned between the columns and seemed to indicate that the one-directional action that had been used for floors comprised of joists and girders carrying the load to the columns was applicable.

This led to an analysis similar to the elastic analysis in flat slabs. The three-dimensional problem was reduced to a two-dimensional approximation of a plate on rigid supports. The method is explained in References 23 and 24.

In developing the procedure, two basic simplifications were made. First the load was divided to the two slab spans by a formula which was modified to make results conform with available theoretical analyses. Secondly, the distribution of load along the span was assumed. To account for the end restraints of the slab, the points of contraflexure in the slab were determined from a frame analysis and used to obtain the effective span in the slab.

Since part of the load was assigned to each span in the slab, the remainder of the load was carried by the beams so that all the load was carried in each direction.

The slab moments were based on loading patterns to create maximum moment conditions. In addition beams were designed by the continuous beam moment coefficients which also consider pattern load. Therefore, Method 1 resulted in design moments that were in excess of those given by a solution considering equilibrium of the slab. It was apparent that pattern loads were provided for.

(b) Method 2

Method 2 had its foundation in the 1921 paper of Westergaard and Slater (14), in which they gave moment coefficients for slabs and the supporting beams. The solutions used to obtain the moments were for continuous plates supported on rigid beams which provided no torsional restraint. Since flat slabs were designed for 72 percent of the static moment the maximum moment coefficients (based on pattern loadings) were reduced by 28 percent.

The moment coefficients were incorporated into the 1947 ACI Code with some modifications made by the 1940 Joint Committee (25). The coefficients were given for single panels having different boundary conditions. Any unbalanced moment at the boundaries was assumed to be resisted partly (1/3 of the unbalanced moment) by the torsional restraint of the beams which was specified by requiring beams and slabs to be cast monolithically.

In addition, the load to the beams was specified by assigning a certain area of the slab to be transferring load to the beam. The beams were then designed by use of the coefficients specified for continuous beams in which pattern loads were considered.

(c) Method 3

The basis for Method 3 is found in a procedure recommended by Marcus (26). Marcus divided the slab which was supported on rigid beams into strips and determined the moment coefficient for the strips. Since this did not account for the torsional restraint between the strips, the moments were corrected to conform to elastic solutions.

Checkerboard loads were used to obtain positive moments and uniform loads for negative moments since Marcus concluded that the pattern loads did not affect negative moments materially.

The coefficients obtained by the Marcus method were only slightly modified and given for isolated panels with various boundary conditions in the 1963 ACI Building Code (21). The coefficients for positive moment are different for live load and dead load in keeping with the original solutions Marcus obtained. Since the positive dead load moments are for uniform loading, no increase in moment is necessary, whereas the live load may cause an increase in moment, the coefficients for checkerboard load are given.

As in the other methods, a portion of the panel load is assigned to be uniformly distributed along the beam and the beam moments are computed using the coefficients for beams given in the ACI Code.

(d) Summary

The design of two-way slabs is basically the same for all the methods. The moment coefficients are determined for continuous slabs supported on rigid beams. These coefficients are obtained for pattern loadings to yield maximum moments. In each case a portion of the load is assigned to the beam which is then designed using beam moment coefficients based on pattern loadings on continuous beams.

Therefore each method results in coefficients which give total moments that are in excess of the static moment in a panel. This is in sharp contrast to flat slabs which do not effectively account for pattern loads and are not even designed for the total static moment in a panel.

5.5 Design Moments in the Test Structures

Four of the test structures were designed according to provisions of the ACI Code. The flat plate F1 and the flat slabs F2 and F3 were designed according to the Empirical Method. The typical two-way slab T1 was designed by Method 1 for slabs supported on all sides. The two-way slab with shallow beams was designed to provide a beam stiffness that was about midway between F1 and T1. It was designed using a total design moment based on the static moment 0.125 WL.

The design moment coefficients are shown in Figs. 5.1-5.4. The beam and the slab moment are combined in the wall strip in F1, F2 and F3 even though in design these elements are considered separately.

5.6 Comparison of Measured with Design Moments

Ideally, a design procedure should provide for the moment at a given section. Further, for an economical design, it is equally important that certain sections are not over-designed while others are under-designed. A balance should be maintained if possible. In view of the background regarding the design methods, the design moments are compared with the uniform and pattern load measured moments.

In Figs. 5.5-5.9, the measured moments are plotted against the design moments. The measured moments are taken from Figs. 3.2, 3.4, 3.6, 3.8 and 3.10. The moments are shown by different symbols for the column or middle strip and the wall strip. Open symbols represent uniform load moments and solid symbols designate pattern load moments. A line has been drawn from the origin at 45 degrees which is the ideal case of measured moments and design moments being equal.

In Fig. 5.5 the moments in structure F1 are considered. It can be seen that the points are scattered and lie both above and below the 45 degree line. The wall strip moments (including the beams) lie well below the line. However, the beams which constitute the major portion of the moment are not typical cases. First, the beams tend to be conservatively designed and secondly, the measured beam moments are not as reliable as the measured slab moments.

The solid symbols should lie above the open symbols since the loads were applied to create maximum moment conditions. However, no definite trend is evident in that respect. The concentration of points at the lower left of Fig. 5.5 are the only values that are above the equality line. These points represent interior negative middle strip moments and positive moments in the middle and column strips. These sections appear to be under-designed even for uniform loads. However, with the preponderance of points below the line, it appears that the flat plate has been adequately designed as a whole structure despite the under-designed interior panel sections.

The design and measured moments for the flat slabs, F2 and F3, are considered in Fig. 5.6 and 5.7. In these two structures, the measured moments exceeded the design moments at almost all sections. This is in contrast with the flat plate in which the design moments were in excess of measured moments in a majority of the sections. The pattern load moments are slightly higher than the uniform load moments. However, it is significant that the uniform load moments exceeded the design moments. Had the design moments been sufficient to provide for the uniform load, it is unlikely that the pattern load moments would have exceeded the design moments.

Since the flat plate and the flat slabs are designed according to the empirical method, it is important to consider the three structures as a group in any comparison with design moments. In the previous discussion it was shown that beam moments are designed as separate elements of the structure. In doing this an additional strength is imparted to edge panels. Therefore, the moments in the interior panel are of greatest importance.

In the three structures the measured positive moments in the column and middle strips and the middle strip negative moments exceeded the design moments. These sections constitute a major portion of the moment capacity in an interior panel. If the design moments are not adequate at these sections, the beneficial effects of moment redistribution are lost.

The comparison of moments in structure T1 is shown in Fig. 5.8. The points for uniform load moments lie consistently below the equality line. Even the pattern load moments are generally below the line. This comparison indicates that the structure was over-designed. It is desirable to have the uniform load moments be about equal to the design moments with the pattern load moments exceeding the design moments by a small percentage. However, in structure T1 which was designed by Method 1 of the ACI Code, the measured moments were almost all below the design moments. This result is consistent with the fundamental aspects of the Method 1 in which the beams and slab are both designed for maximum moments. In doing this the design moments are quite large and over-designing results.

The comparison of moments in structure T2, shown in Fig. 5.9, results in several interesting conclusions. The design moments appear to adequately provide for uniform load. The design moments are low at some sections and high at others but over-all the design seems to be sufficient. The pattern load moments generally were greater than the design moments but were not excessively high. It appears that the main criticism of the method is that it does not distribute the moment to the sections very well. However, pattern loads did not seem to exceed design moments sufficiently to be given particular considerations.

In summary, the empirical design method did not provide for the uniform load and therefore did not provide for the pattern load. The mitigating condition is that the pattern load moments were not substantially greater than the uniform load moments in structures F1, F2 and F3. Method 1 for two-way slabs resulted in a design that provided more moment capacity than was needed under uniform or pattern loads. The method used for structure T2 appeared to have provided sufficient capacity for the moments in the structure as a whole, however, the moment was not well distributed between the sections.

6. A PROCEDURE FOR DETERMINING THE EFFECT OF BEAM AND COLUMN STIFFNESSES

6.1 Introductory Remarks

In the preceding chapter, design procedures for slabs were discussed. It was shown that the treatment of pattern loads is not consistent for the different methods. From that discussion it is apparent that considerably disagreement exists as to the importance of pattern loads. If pattern loads are important, the design methods do not satisfactorily stipulate how they shall be included in the design.

A method is presented in this chapter to estimate the effects of pattern load in a given slab. The procedure is not intended to provide absolute values of pattern load moment, but rather to indicate when pattern loads should be given further attention in a particular case.

The procedure consists of developing domains of stiffness parameter combinations which satisfy a given pattern ratio. The establishment of the domains was accomplished by using the available theoretical solutions and extending them to cover additional cases where H, J, and K are varied. The influence of the load ratio on the effects of pattern loads is included. A discussion of pattern load effects on beams is also given.

Finally, the procedure is compared with the results of pattern load tests on the five test structures.

6.2 Development of a Procedure to Estimate the Effect of Beam and Column Stiffnesses

The combinations of the stiffness parameters that have been studied were discussed in Chapter 4. The available solutions include the effects of beam stiffness H on moments under both strip and checkerboard loads with $J = K = 0$. There are also solutions for varying values of J and $H = \infty$, $K = 0$. The aspect ratios varied from 0.5 to 2.0 in these solutions.

In addition, the effect of strip loads were studied for square panels having rigid columns with $H = J = 0$. By a method of interpolation, flexible columns could be included in this solution.

The pattern ratios for strip loadings in panels having combinations of finite values of both H and K were not available. There were no solutions for varying values of K and J in panels under strip loads. The effect of checkerboard loads had not been studied for panels in which J and K were varied along with a varying value of H. However, most of these cases had been studied at some extreme values of the stiffness parameters such as rigid beams or no beams.

In order to approximate the pattern ratios for the cases which were not studied previously, a means of establishing these ratios was devised. The construction for these solutions is shown in Fig. 6.1. Pattern ratios for a panel having an aspect ratio of one are shown and only positive moments are included since these were shown in the preceding discussions to be critical. The basic curves, uppermost in Fig. 6.1, are identical to those shown in Fig. 4.6. These top lines give the pattern ratios for cases of strip loading with $K = 0$, H varying and checkerboard loading with $J = 0$, H varying.

The remaining curves for the condition of strip loads were determined in the following manner. For $a/b = 1.0$, it was known that for $H = 0$, $K = \infty$, the pattern ratio α was approximately 1.20. In addition a linear interpolation for the pattern ratio between values of $K = 0$ and $K = \infty$ could be used.

Therefore, a vertical linear scale was established on the $H/(1+H) = 0$ axis. A straight line was drawn connecting $\alpha = 1.20$, $H/(1+H) = 0$ and $\alpha = 1.0$, $H/(1+H) = 1.0$. The exact shape of this curve may not be a straight line, but may decrease very rapidly for low values of H and approach an asymptote at $H/(1+H) = 1.0$, however the straight line is a conservative approximation. The curves for values of $K/(1+K)$ between zero and one were drawn using a linear vertical interpolation.

This construction completed the pattern ratios for strip loads for varying values of H and K, $J = 0$. By examining the curves for strip loads, it can be seen that the effect of finite values of J is to further decrease the curves so that $\alpha = 1.0$ is approached. However, the effectiveness of J in reducing moments depends on the capacity of the column and beam to withstand the torsion transmitted to them. No accurate estimation of the parameter J in reducing effects of strip loads was available, therefore, it was considered conservative to assume that increasing J did not reduce strip load pattern ratios.

The curves which completed the combinations of stiffness parameters for checkerboard load pattern ratios were constructed by using the following procedure. From the available solutions, the pattern ratios were known for cases of $J = 0$ and H being varied. Solutions for the influence of J in checkerboard loadings with $H = \infty$ were shown in Fig. 4.9. It can be seen that the variation of the pattern ratio is almost linear with increasing values of J. This is conservative since a small increase in J is more efficient in reducing the pattern ratio at low values of J than at higher values. This led to a vertical linear scale of $J/(1+J)$ along the $H/(1+H) = 1.0$

axis between values of $J/(1+J)$ of zero and one. A further assumption was made that the values of α would be 1.0 for $J/(1+J) = 1.0$ regardless of the value of H and that the origin of all the curves was at the point where the curves for $J = 0$ crossed the line for $\alpha = 1.0$. All the curves may not cross at this point, however, the variation should not be too great. The curves for intermediate values of $J/(1+J)$ were constructed using a linear vertical interpolation between the limiting curves.

The influence of K on checkerboard load pattern ratios was not needed since only positive moments are critical and K has no influence on these ratios; there is a diagonal line of symmetry across the panels.

This method of extending the available solutions to other values of the aspect ratio was accomplished with only one additional assumption. The checkerboard load curves for any values of the aspect ratio can be constructed just as for $a/b = 1.0$. However, for strip loads the efficiency of the stiffness of the columns in reducing the pattern ratio decreases as the aspect ratio decreases. In order to complete the curves for strip loads, it was assumed that for $a/b = 0.5$ finite column stiffness did not reduce the moments while for $a/b = 2.0$, rigid columns were completely effective in isolating the panels from strip loads. By fitting a curve through the known points, the pattern ratios were determined to be approximately 2.0 for $a/b = 0.5$, 1.4 for $a/b = 0.8$, 1.2 for $a/b = 1.0$ (this value was previously known), 1.1 for $a/b = 1.25$ and 1.0 for $a/b = 2.0$.

It can be seen that the effects of pattern loads are divided into strip load effects in which H and K are the major variables and checkerboard load effects in which H and J are the major variables. This division made it possible to chart domains in which combinations of the stiffness parameters satisfy a particular pattern ratio.

These domains are indicated in Figs. 6.2-6.6. Three values of the pattern ratio (4/3, 3/2, 5/3) are used and the domains are given for five aspect ratios. The domains were obtained using the curve shown in Fig. 6.1 for a/b = 1.0 and similar curves were constructed to establish the domains for the remaining aspect ratios.

The shaded areas in Figs. 6.2-6.6 indicate the combinations of the stiffness parameters which result in the moment ratio being exceeded. Therefore, if a particular combination of H and J or H and K falls within this "danger" area, the patterns ratio may be surpassed. It should be pointed out that the areas are not sharply delineated since the curves from which the values were obtained are not exact in all cases. These domains give an indication when further attention to the effects of pattern loads is needed. The use of these domains in practical problems is discussed in the following section.

6.3 Application of the Proposed Procedure

The development of the procedure discussed in Sec. 6.3 was based on theoretical solutions in which the permanent load was assumed to be zero. In an actual structure, there will be some permanent load on the floor slab. Since the procedure is to be applied to slabs having varying values of permanent and movable loads it is necessary to adjust the pattern ratio to obtain the moment ratio.

The pattern ratio α was previously defined as the ratio of pattern to the uniform load moment where the entire load was a movable load. The moment ratio γ was the ratio of pattern to uniform load moment in a structure having a load ratio β. The load ratio β is the ratio of movable to total load.

In a structure having a value of β less than one, the effects of pattern loads are less severe than when $\beta = 1.0$ (the case of pattern ratios). Equation 6.1 relates α, β, and γ.

$$\alpha = 1 + \frac{\gamma - 1}{\beta} \qquad (6.1)$$

The equation is derived by considering the moment in a structure to be the sum of the permanent load multiplied by the uniform load moment coefficient and the movable load multiplied by the pattern load moment coefficient.

The use of this equation in conjunction with the domains of Fig. 6.2-6.6 for a given structure consists of the following five steps.

1. Determination of the load ratio, β.
2. Selection of the allowable moment ratio γ.
3. Determination of the pattern ratio α using Eq. 6.1.
4. Computation of relative stiffnesses H, J and K.
5. Using Fig. 6.2-6.6, determine whether pattern loads may result in greater increases in moment than were allowed in Step 2.

The first three steps are self-explanatory. However, the fourth and fifth steps need further explanation. The method of computing H, J and K are given in Sec. 6.5. In the case of a rectangular slab having different beams in the two spans, a check is made for the effects of pattern loads in each direction. In making these checks, the effects of different beam flexural stiffness (H_b) in the perpendicular span are covered automatically.

If the torsional stiffnesses of the beams in the two spans are different, it is conservative to use the lower value of J for both spans.

Step 5 involves making two checks for a particular panel: one for the effects of strip load and one for checkerboard load. The check for strip load is made by computing the values of $H/(1+H)$ and $K/(1+K)$ and this point is located on the coordinates of Figs. 6.2-6.6. Similarly the value of $J/(1+J)$ is computed and the point $J/(1+J)$, $H/(1+H)$ is located. If these two points do not lie in the shaded areas, the pattern loads should not increase the average moments more than the prescribed amount.

For example, if the pattern ratio is determined to be 3/2 for a panel having an aspect ratio of one and stiffness parameters of $H/(1+H) = 0.5$, $J/(1+J) = 0$, $K/(1+K) = 0.2$ it can be seen in Fig. 6.4 that checkerboard load moments will not exceed the allowable α but strip load moments may exceed the value of $\alpha = 1.50$. However if $K/(1+K)$ is 0.3 strip loads should not yield pattern ratios exceeding 1.50.

The steps outlined in the preceding paragraphs are for the effects of pattern loads on the slab positive moments in an interior panel. In Chapter 4 it was pointed out that these moments are the most critical with respect to pattern loads. This is confirmed by the measured moments given in Fig. 3.2, 3.4, 3.6, 3.8, and 3.10. Therefore, any combinations of the stiffness parameter satisfying the requirements for positive slab moment in the interior panel should also be sufficient for edge or corner panels.

It is important to remember that as the values of the beam flexural stiffness increase the distribution of moment to the beam also increases. For large values of H, the major portion of the moment is carried by the beam.

It is necessary to determine the effect of pattern loads on the beams since these may be the critical sections. The beam moments are maximized by strip loadings in most cases and strip loadings will produce increases equal to modified checkerboard loadings in the remaining cases. A frame analysis is given in the Appendix for computing the moment ratios in slab structures approximated by a two-dimensional frame and loaded uniformly or by strip patterns.

6.4 Comparison of Test Results With the Proposed Procedure

The procedure outlined in this chapter has been based strictly upon theoretical considerations. It is desirable to determine how well it correlates with the results of the five test structures. The procedure is intended for use in estimating the effects of pattern loads on a given structure. However, for the purposes of this comparison the procedure is altered slightly. Rather than assume a value for the allowable moment ratio γ, the moment ratios measured in the test structures are used and for the values of the load ratio β on the structures, the measured values of α are determined. The measured values of α are compared with the estimated values of α according to the suggested procedure. The comparison is made in terms of the positive moment ratio in the interior panels of the structures.

In any comparison, the similarities and differences between the stiffness parameters of the test structures and idealized stiffness parameters must be examined. The greatest difference is in the supporting elements. In the test structures the beams and columns have finite widths and thicknesses. In the theoretical solutions, these elements are dimensionless. The neutral axis of the beams and slabs are the same in the theoretical solutions eliminating T-beam action of the slab.

The values of K are determined routinely with the stiffness of the column capitals considered as outlined in the Appendix.

The values of the stiffnesses and stiffness parameters are given below for the interior panels of the test structures. A range rather than a single value is given for beam stiffnesses of structures T1 and T2. The lower bound of the range corresponds to a rectangular beam while the upper bound corresponds to a T-beam as described above.

Structure	H	J	K	$\frac{H}{1+H}$	$\frac{J}{1+J}$	$\frac{K}{1+K}$
F1	0	0	11	0	0	0.9
F2, F3	0	0	1	0	0	0.5
T1	2-3	1	4	0.67-0.75	0.5	0.8
T2	0.4-0.6	0.3	9	0.28-0.38	0.23	0.9

To estimate the effects of pattern loads on the test structures, Fig. 6.7 is used. This figure was constructed in the same manner as were Figs. 6.2-6.6 in which "safe" domains were shown. In Fig. 6.7 contours approximate the values of the pattern ratios.

Using the values of H, J and K given in the table above, points are located on Fig. 6.7 for the pertinent combinations of the stiffness parameters for each structure.

It can be seen that checkerboard loads should be of no concern in structures F1, F2 and F3. Since these structures have no beams, the important consideration is the strip load effect. Structure F1 should not be seriously affected by strip loads. The value of K/(1+K) is large and the value of α is about 1.2. However, the value of α for F2 and F3 is about 1.6. The columns were relatively flexible as indicated by the value of K/(1+K) = 0.5 and strip loads must be given consideration.

The points plotted for structures T1 and T2 are shown as lines as a result of the range of beam flexural stiffnesses that were computed. The location of the lines for T1 indicates that the value of α for either checkerboard or strip loads is less than 1.2. This pattern ratio is quite low and pattern loads should be of no consequence in T1.

The location of the line relating J/(1+J) and H/(1+H) for T2 shows that the effects of checkerboard loads should be negligible. Figure 6.7 indicates that the effect of strip loads will be greater than the effect of checkerboard loads. However, the strip load pattern ratio should be about 1.2 which is quite low.

The values of α measured in the tests are summarized below. The value of β was known, γ was measured in the tests and α was obtained by use of Eq. 6.1.

Structure	β	$\gamma_{meas.}$	$\alpha_{meas.}$
F1	0.72	1.09	1.13
F2	0.85	1.14	1.17
F3	0.78	1.64	1.82
T1	0.81	1.21	1.26
T2	0.66	1.03	1.05

It can be seen that the estimated values of α compare favorably with the measured values. Strip loads resulted in a pattern ratio slightly greater than 1.1 in F1 and this is nearly the value that was estimated. The measured value of α is quite low in F2 and high in F3. It is felt that these are extreme values and the actual pattern ratio lies between. The estimated pattern ratio was 1.6 which seems reasonable. The value of α estimated for T1 was about equal to that measured. It was predicted that checkerboard loads would be of no consequence in T2 and this was confirmed by the tests.

It must be remembered that the values of measured moment used to compute the pattern ratio are across the interior panel positive moment section and therefore are subject to localized irregularities which cannot be eliminated as easily as when the average moment ratio is taken for the entire structure. However, the estimated values are sufficiently accurate for design purposes.

7. SUMMARY

7.1 Object and Scope

The object of this study is to evaluate the effects of pattern loadings on reinforced concrete floor slabs. This report brings together and correlates the available analytical and experimental information on the effects of pattern loadings in floor slabs in order to develop a unified approach to the problem.

The experimental studies consist of load tests on a series of five multiple-panel reinforced concrete floor slabs. The test structures included two flat slabs, a flat plate and two two-way slabs. Layouts of these slabs are shown in Figs. 2.1-2.3.

The available theoretical solutions for plates under pattern loadings are listed in Tables 3-9. Panels having aspect ratios from 0.5 to 2.0 are considered. The variables are the beam torsional and flexural stiffnesses and the column flexural stiffness.

7.2 Behavior of Test Structures Under Pattern Loads

Two types of pattern loads were applied to the structures. Checkerboard patterns were used in the two-way slabs and strip patterns in the flat slabs. The loading patterns are shown in Fig. 2.4.

Representative strain distributions across critical sections for uniform and pattern loadings are shown in Figs. 2.6 and 2.7. Deflections are compared in Figs. 2.8-2.12. The pattern loadings increased strains across all the sections. However, in some cases this increase was negligible. The increases in deflection ranged from 10 percent in F1 to 100 percent in F3 but the absolute increases in deflection were small in all the structures. The crack patterns were nearly unaffected by the pattern loads. No new cracks were formed but a slight widening and lengthening of the existing cracks was observed. On the basis of the deflection, strain and crack observations, it can be said that the serviceability of the test structures was unimpaired by pattern loads.

The moments in the test structures were calculated from strain measurements for both pattern and uniform loads and are compared in Figs. 3.2-3.11.

The strip load moments in the flat plate and slabs were about 20 percent greater than uniform load moments. Under checkerboard loads, the moments increased by about 30 percent in the typical two-way slab, but were unchanged in the two-way slab with shallow beams.

7.3 Theoretical Solutions for Pattern Load Moments

The available solutions for the effects of pattern load on moments are given in Tables 3-9. The trends evinced by these solutions are shown in Figs. 4.4-4.11.

The theoretical solutions indicate that the effects of pattern loads on the slab moments in edge or corner panels are less than on an interior panel and positive moments are affected more than negative moments. In addition, it is shown that checkerboard loads result in greater moment increases than strip loads only if beams having very large flexural stiffness support the slab.

7.4 <u>Procedure for Estimating the Effects of Pattern Loads</u>

The discussion of development of current design methods in Chapter 5 indicates that pattern loads are not treated consistently in the various methods. They are included in determining two-way slab design moments and largely ignored in flat slab design.

A method is developed in Chapter 6 for predicting the effects of pattern loads on a slab supported by beams or columns of any stiffness. The method is based on the available theoretical solutions and plausible extensions of these solutions for a wider range of variables. The method consists of determining whether the given combinations of the stiffness parameters are sufficient to limit the moment increases to a prescribed level (See Figs. 6.2-6.6). The beam flexural and torsional stiffnesses must provide for checkerboard loads; columns cannot limit the effects of checkerboard loads on positive moments. The beam and column flexural stiffnesses must provide for the effects of strip loads. It is assumed that the beam torsional stiffnesses do not decrease the effects of strip loads.

The suggested procedure for estimating the effects of pattern loads shows that checkerboard loads are not critical unless very stiff beams are used. It is also shown that in most structures, strip loads are of prime concern and significant moment increases result if relatively flexible beams or columns are employed.

A frame analysis is presented in the Appendix for determining the uniform or strip load moments in any type of slab. The frame analysis enables computation of absolute moment values at design sections.

BIBLIOGRAPHY

1. Mayes, G. T., M. A. Sozen, and C. P. Siess, "Tests on a Quarter-Scale Model of Multiple-Panel Reinforced Concrete Flat Plate Floor," Structural Research Series No. 181, Department of Civil Engineering, University of Illinois, September 1959.

2. Hatcher, D. S., M. A. Sozen, and C. P. Siess, "An Experimental Study of a Reinforced Concrete Flat Slab Floor," Structural Research Series No. 200, Department of Civil Engineering, University of Illinois, June 1960.

3. Hatcher, D. S., M. A. Sozen, and C. P. Siess, " A Study of Tests on a Flat Plate and a Flat Slab," Structural Research Series No. 217, Department of Civil Engineering, University of Illinois, July 1961.

4. Gamble, W. L., M. A. Sozen, and C. P. Siess, "An Experimental Study of a Two-Way Floor Slab," Structural Research Series No. 211, Department of Civil Engineering, University of Illinois, June 1961.

5. Vanderbilt, M. D., M. A. Sozen, and C. P. Siess, "An Experimental Study of a Reinforced Concrete Two-Way Floor Slab with Flexible Beams," Structural Research Series No. 228, Department of Civil Engineering, University of Illinois, November 1961.

6. Jirsa, J. O., M. A. Sozen, and C. P. Siess, "An Experimental Study of a Flat Slab Floor Reinforced with Welded Wire Fabric," Structural Research Series No. 249, University of Illinois, June 1962.

7. American Concrete Institute, Building Code Requirements for Reinforced Concrete (ACI 318-56).

8. Sutherland, J. G., L. E. Goodman, and N. M. Newmark, "Analysis of Plates Continuous over Flexible Beams," Structural Research Series No. 42, Department of Civil Engineering, University of Illinois, January 1953.

9. Timoshenko, S., and S. Woinowsky Krieger, "Theory of Plates and Shells," Second Edition, McGraw-Hill Book Co., New York, 1959.

10. Newmark, N. M., "A Distribution Procedure for the Analysis of Slabs Continuous over Flexible Beams," Bulletin 304, Engineering Experiment Station, University of Illinois, 1938.

11. Siess, C. P., and N. M. Newmark, "Moments on Two-Way Concrete Floor Slabs," Bulletin 385, Engineering Experiment Station, University of Illinois, 1950.

12. Gamble, W. L., M. A. Sozen, and C. P. Siess, "Measured and Theoretical Bending Moments in Reinforced Concrete Floor Slabs," Structural Research Series No. 246, Department of Civil Engineering, University of Illinois, June 1962.

13. Morrison, G. D., "Solutions for Nine-Panel Continuous Plates with Stiffening Beams," M.S. Thesis, Department of Civil Engineering, University of Illinois, 1961.

14. Westergaard, H. M., and W. A. Slater, "Moments and Stresses in Slabs," Proceedings ACI, Vol. 17, 1921, pp. 415-538.

15. Sozen, M. A., and C. P. Siess, "Investigation of Multiple-Panel Reinforced Concrete Floor Slabs, Design Methods, Their Evolution and Comparison," ACI Journal, August 1963.

16. Nichols, J. R., "Statical Limitations Upon the Steel Requirements in Reinforced Concrete Flat Slab Floors," Trans. ASCE, Vol. 77, 1914, pp. 1670-1681.

17. [First] Joint Committee Report on Concrete and Reinforced Concrete, "Final Report" 1 July 1916.

18. [Second] Joint Committee on Standard Specifications for Concrete and Reinforced Concrete, "Standard Specifications for Concrete and Reinforced Concrete," ACI Proceedings, V. 21, 1925.

19. American Concrete Institute, Standard Building Regulations for Reinforced Concrete (ACI 318-41).

20. DiStasio, J. and M. P. van Buren, "Background of Chapter 10, 1956 Regulations for Flat Slabs," Unpublished report prepared for ACI Committee 318.

21. American Concrete Institute Building Code Requirements for Reinforced Concrete (ACI 318-63).

22. Casillas, Juan G. de L., and C. P. Siess, "Comparative Studies of Design Procedures for Two-Way Reinforced Concrete Slabs," Structural Research Series No. 215, Department of Civil Engineering, University of Illinois, May 1961.

23. DiStasio, J. and M. P. van Buren, "Slabs Supported on Four Sides," ACI Proceedings, Vol. 32, 1936, pp. 350-364.

24. Bertin, R. L., J. DiStasio and M. P. van Buren, "Slabs Supported on Four Sides," ACI Proceedings, Vol. 41, 1945, pp. 537-556.

25. [Third] Joint Committee on Standard Specifications for Concrete and Reinforced Concrete, "Recommended Practice and Standard Specifications for Concrete and Reinforced Concrete," American Concrete Institute, Detroit, 1940.

26. Marcus, H., "Die vereinfachte Berechnung beegsamer Platten," Julius Springer, Berlin, 1929.

27. Corley, W. G., M. A. Sozen, and C. P. Siess, "The Equivalent Frame Analysis for Reinforced Concrete Slabs," Structural Research Series No. 218, Department of Civil Engineering, University of Illinois, June 1961.

28. Seely, F. B., and J. O. Smith, "Advanced Strength of Materials," Wiley, New York, Second Edition, 1952, p. 271.

TABLE 1 PROPERTIES OF MATERIALS IN TEST STRUCTURES

Structure	f'_c psi	E_c ksi	f_r psi	Age days	Reinforcement	f_y ksi	Design Loads Live Load psf	Design Loads Dead Load psf
F1	2510	2400	700	76	1/8 in. sq. bars	36.7	70	85
F2	2760	3100	600	78	1/8 in. sq. bars	42.0	200	85
F3	3760	3700	750	55	*	70**	200	85
T1	2830	3000	590	76	1/8 in. sq. bars	42.0	70	75
T2	3550	3300	940	50	1/8 in. sq. bars	47.6	70	75

* Wires with diameters ranging from 0.142 to 0.0625 in.

** Based on average of wires at 0.2% offset.
Proportional limits of wires 50-55 ksi.

Concrete properties are based on tests of 2 by 4-in. cylinders.

TABLE 2 ASSUMED PROPERTIES USED IN MOMENT-STRAIN RELATIONSHIPS

Structure	Cracking Strain	Cracking Stress, psi	Beam Flange Widths	
			Edge Beams	Interior Beams
F1	0.00015	310	4t, deep beam 0, shallow beam	- -
F2	0.00015	360	4t, deep beam 0, shallow beam	- -
F3	0.00019	600	4t, deep beam 0, shallow beam	- -
T1	0.00015	400, slab 350, beams	4t	4t
T2	0.00020	550, slab 500, beams	3t	3t

TABLE 3 COMPARISON OF PATTERN WITH UNIFORM LOAD POSITIVE MOMENTS IN AN INTERIOR PANEL

$J = K = 0$

Aspect	Beam Flexural Stiffness*		Average Slab Positive Moments, M/ca^2			
			Checkerboard		Strip	
a/b	H_a	M_{UL}	M_{CB}	$\frac{M_{CB}}{M_{UL}} = \alpha_{CB}$	M_{ST}	$\frac{M_{ST}}{M_{UL}} = \alpha_{ST}$
0.5	0	0.0417	0.0533	1.28	0.0833	2.00
	0.25	0.0304	0.0477	1.57	0.0601	1.98
	0.5	0.0278	0.0464	1.67	0.0521	1.87
	1.0	0.0263	0.0456	1.73	0.0456	1.73
	2.5	0.0255	0.0452	1.77	0.0401	1.57
	∞	0.0251	0.0450	1.79	0.0352	1.40
0.8	0	0.0417	0.0384	0.92	0.0833	2.00
	0.4	0.0277	0.0314	1.13	0.0521	1.88
	0.8	0.0232	0.0291	1.25	0.0398	1.72
	1.6	0.0197	0.0280	1.42	0.0313	1.59
	4.0	0.0172	0.0261	1.52	0.0230	1.34
	∞	0.0152	0.0251	1.65	0.0161	1.06
1.0	0	0.0417	0.0327	0.78	0.0833	2.00
	0.5	0.0263	0.0250	0.95	0.0454	1.73
	1.0	0.0208	0.0222	1.07	0.0331	1.59
	2.0	0.0164	0.0200	1.22	0.0234	1.43
	5.0	0.0127	0.0182	1.43	0.0155	1.22
	∞	0.0096	0.0166	1.73	0.0090	0.94
1.25	0	0.0417	0.0313	0.75	0.0833	2.00
	0.63	0.0248	0.0228	0.92	0.0408	1.65
	1.25	0.0185	0.0197	1.06	0.0279	1.51
	2.50	0.0133	0.0172	1.29	0.0182	1.37
	6.25	0.0088	0.0148	1.68	0.0105	1.19
	∞	0.0049	0.0128	2.61	0.0042	0.86
2.0	0	0.0417	0.0256	0.61	0.0833	2.00
	1.0	0.0208	0.0158	0.76	0.0313	1.50
	2.0	0.0139	0.0124	0.89	0.0195	1.40
	4.0	0.0085	0.0097	1.14	0.0113	1.33
	10.0	0.0041	0.0075	1.83	0.0051	1.24
	∞	0.0005	0.0033	6.60	0.0004	0.80

* $H_b = H_a(b/a)^2$.

TABLE 4 COMPARISON OF PATTERN WITH UNIFORM LOAD NEGATIVE MOMENTS IN AN INTERIOR PANEL

$J = K = 0$

Aspect Ratio a/b	Beam Flexural Stiffness* H_a	Average Slab Negative Moments, M/qa^2				
			Checkerboard		Strip	
		M_{UL}	M_{CB}	$\frac{M_{CB}}{M_{UL}} = \alpha_{CB}$	M_{ST}	$\frac{M_{ST}}{M_{UL}} = \alpha_{ST}$
0.5	0	0.0833	-	-	0.1042	1.25
	0.25	0.0581	-	-	0.072	1.24
	0.5	0.0556	-	-	0.069	1.24
	1.0	0.0548	-	-	0.067	1.22
	2.5	0.0550	0.0472	0.86	0.065	1.18
	∞	0.0558	0.0732	1.31	0.0642	1.15
0.8	0	0.0833	-	-	0.1042	1.25
	0.4	0.0519	-	-	0.064	1.23
	0.8	0.0463	-	-	0.056	1.21
	1.6	0.0428	0.0338	0.79	0.051	1.19
	4.0	0.0405	0.0436	1.08	0.045	1.11
	∞	0.0390	0.0532	1.37	0.0415	1.06
1.0	0	0.0833	-	-	0.1042	1.25
	0.5	0.0488	-	-	0.060	1.23
	1.0	0.0417	-	-	0.050	1.20
	2.0	0.0364	0.0333	0.92	0.043	1.18
	5.0	0.0324	0.0373	1.15	0.035	1.08
	∞	0.0291	0.0428	1.47	0.0299	1.03
1.25	0	0.0833	-	-	0.1042	1.25
	0.63	0.0458	-	-	0.056	1.22
	1.25	0.0370	-	-	0.044	1.19
	2.5	0.0303	0.0276	0.91	0.035	1.16
	6.25	0.0248	0.0297	1.20	0.026	1.05
	∞	0.0201	0.0317	1.58	0.0200	1.00
2.0	0	0.0833	-	-	0.1042	1.25
	1.0	0.0385	-	-	0.047	1.22
	2.0	0.0278	-	-	0.033	1.19
	4.0	0.0197	0.0160	0.81	0.023	1.17
	10.0	0.0133	0.0150	1.13	0.014	1.05
	∞	0.0079	0.0133	1.68	0.0079	1.00

* $H_b = H_a(b/a)^2$.

TABLE 5 COMPARISON OF CHECKERBOARD WITH UNIFORM LOAD MOMENTS IN AN INTERIOR PANEL

$H = \infty,\ K = 0$

Aspect Ratio	Beam Torsional Stiffness		Average Slab Moments, M/qa^2					
			Positive Moment			Negative Moment		
a/b	J_a	J_b	M_{UL}	M_{CB}	α_{CB}	M_{UL}	M_{CB}	α_{CB}
0.5	0	0	0.0279	0.0467	1.67	0.0556	0.0728	1.31
	0.78	1	0.0279	0.0360	1.29	0.0556	0.0676	1.22
	1.54	2	0.0279	0.0330	1.18	0.0556	0.0633	1.14
	∞	∞	0.0279	0.0279	1.00	0.0556	0.0556	1.00
0.8	0	0	0.0168	0.0262	1.56	0.0389	0.0523	1.36
	0.79	0.83	0.0168	0.0213	1.27	0.0389	0.0473	1.22
	1.58	1.66	0.0168	0.0196	1.17	0.0389	0.0449	1.15
	∞	∞	0.0168	0.0168	1.00	0.0389	0.0389	1.00
1.0	0	0	0.0119	0.0178	1.50	0.0290	0.0434	1.50
	0.81	0.81	0.0119	0.0146	1.22	0.0290	0.0371	1.28
	1.62	1.62	0.0119	0.0136	1.14	0.0290	0.0342	1.18
	∞	∞	0.0119	0.0119	1.00	0.0290	0.0290	1.00
1.25	0	0	0.0065	0.0099	1.52	0.0199	0.0322	1.62
	0.83	0.79	0.0065	0.0083	1.28	0.0199	0.0261	1.31
	1.66	1.66	0.0065	0.0077	1.18	0.0199	0.0245	1.23
	∞	∞	0.0065	0.0065	1.00	0.0199	0.0199	1.00
2.0	0	0	0.0023	0.0032	1.39	0.0079	0.0156	1.98
	1	0.78	0.0023	0.0027	1.17	0.0079	0.0128	1.62
	2	1.54	0.0023	0.0026	1.13	0.0079	0.0105	1.33
	∞	∞	0.0023	0.0023	1.00	0.0079	0.0079	1.00

TABLE 6 COMPARISON OF CHECKERBOARD WITH UNIFORM LOAD MOMENTS IN AN EDGE PANEL - PARALLEL TO EDGE

$H = \infty,\ K = 0$

Aspect Ratio	Beam Torsional Stiffness		Average Slab Moments, M/qa^2							
				Positive Moment				Negative Moment		
a/b	J_a	J_b	M_{UL}	M_{CB}	α_{CB}	Int.* Panel α_{CB}	M_{UL}	M_{CB}	α_{CB}	Int.* Panel α_{CB}
0.5	0	0	0.0310	0.0480	1.55	1.67	0.0586	0.0794	1.36	1.31
	0.78	1	0.0292	0.0362	1.24	1.29	0.0577	0.0678	1.19	1.22
	1.54	2	0.0286	0.0330	1.15	1.18	0.0572	0.0628	1.10	1.14
0.8	0	0	0.0194	0.0271	1.40	1.56	0.0465	0.0556	1.20	1.36
	0.79	0.83	0.0181	0.0214	1.18	1.27	0.0426	0.0483	1.13	1.22
	1.58	1.66	0.0177	0.0196	1.11	1.17	0.0414	0.0450	1.09	1.15
1.0	0	0	0.0109	0.0173	1.59	1.50	0.0376	0.0479	1.27	1.50
	0.81	0.81	0.0113	0.0142	1.26	1.23	0.0337	0.0379	1.13	1.28
	1.62	1.62	0.0115	0.0135	1.17	1.14	0.0319	0.0348	1.09	1.18
1.25	0	0	0.0084	0.0109	1.30	1.52	0.0287	0.0366	1.28	1.62
	0.83	0.79	0.0075	0.0085	1.13	1.28	0.0238	0.0273	1.15	1.31
	1.66	1.58	0.0072	0.0077	1.07	1.18	0.0224	0.0244	1.09	1.23
2.00	0	0	0.0027	0.0034	1.26	1.39	0.0129	0.0180	1.39	1.97
	1	0.78	0.0025	0.0027	1.08	1.17	0.0102	0.0124	1.22	1.62
	2	1.54	0.0024	0.0026	1.13	1.13	0.0094	0.0107	1.14	1.33

* Interior panel α_{CB} is M_{CB}/M_{UL} for an interior panel supported similarly.

TABLE 7 COMPARISON OF CHECKERBOARD WITH UNIFORM LOAD MOMENTS IN AN EDGE PANEL - PERPENDICULAR TO EDGE

$H = \infty,\ K = 0$

Aspect Ratio a/b	Beam Torsional Stiffness J_a	J_b	Average Slab Moments, M/qa^2: Positive Moment M_{UL}	M_{CB}	α_{CB}	Int.* Panel α_{CB}	Interior Negative Moment M_{UL}	M_{CB}	α_{CB}	Int.* Panel α_{CB}	Exterior Negative Moment M_{UL}	M_{CB}	α_{CB}	Int.* Panel α_{CB}
0.5	0	0	0.0336	0.0493	1.47	1.67	0.0640	0.0810	1.27	1.31	0	0	-	1.31
	0.78	1	0.0305	0.0363	1.19	1.29	0.0612	0.0683	1.12	1.22	0.0282	0.0352	1.25	1.22
	1.54	2	0.0295	0.0331	1.12	1.18	0.0598	0.0639	1.07	1.14	0.0374	0.0433	1.16	1.14
0.8	0	0	0.0173	0.0263	1.52	1.56	0.0415	0.0539	1.30	1.36	0	0	-	1.36
	0.79	0.83	0.0172	0.0211	1.23	1.27	0.0404	0.0475	1.18	1.22	0.0195	0.0242	1.24	1.22
	1.58	1.66	0.0171	0.0195	1.14	1.17	0.0401	0.0449	1.12	1.15	0.0259	0.0305	1.18	1.15
1.0	0	0	0.0154	0.0195	1.27	1.50	0.0290	0.0431	1.49	1.50	0	0	-	1.50
	0.81	0.81	0.0137	0.0150	1.10	1.23	0.0290	0.0364	1.26	1.28	0.0145	0.0191	1.32	1.28
	1.62	1.62	0.0131	0.0138	1.05	1.14	0.0291	0.0342	1.18	1.18	0.0194	0.0233	1.20	1.18
1.25	0	0	0.0063	0.0099	1.57	1.52	0.0202	0.0320	1.58	1.62	0	0	-	1.62
	0.83	0.79	0.0064	0.0082	1.28	1.28	0.0199	0.0264	1.32	1.31	0.0100	0.0134	1.34	1.31
	1.66	1.58	0.0065	0.0076	1.17	1.18	0.0199	0.0243	1.22	1.23	0.0132	0.0164	1.24	1.23
2.0	0	0	0.0025	0.0033	1.32	1.39	0.0082	0.0156	1.90	1.97	0	0	-	1.98
	1	0.78	0.0024	0.0027	1.13	1.17	0.0080	0.0118	1.48	1.62	0.0040	0.0061	1.53	1.62
	2	1.54	0.0024	0.0026	1.08	1.13	0.0079	0.0103	1.30	1.33	0.0053	0.0071	1.34	1.33

* Interior panel α_{CB} is M_{CB}/M_{UL} for an interior panel supported similarly.

TABLE 8 COMPARISON OF CHECKERBOARD WITH UNIFORM LOAD MOMENTS IN A CORNER PANEL

$H = \infty,\ K = 0$

Aspect Ratio a/b	Beam Torsional Stiffness J_a	J_b	Positive Moment M_{UL}	M_{CB}	α_{CB}	Int.* Panel α_{CB}	Interior Negative Moment M_{UL}	M_{CB}	α_{CB}	Int.* Panel α_{CB}	Exterior Negative Moment M_{UL}	M_{CB}	α_{CB}	Int.* Panel α_{CB}
0.5	0	0	0.0393	0.0522	1.33	1.67	0.0716	0.0846	1.18	1.31	0	0	-	1.31
	0.78	1	0.0324	0.0368	1.14	1.29	0.0644	0.0692	1.08	1.22	0.0298	0.0354	1.29	1.22
	1.54	2	0.0306	0.0333	1.09	1.18	0.0617	0.0644	1.04	1.14	0.0386	0.0435	1.13	1.14
0.8	0	0	0.0234	0.0291	1.24	1.56	0.0520	0.0603	1.16	1.36	0	0	-	1.36
	0.79	0.83	0.0190	0.0214	1.13	1.27	0.0449	0.0490	1.09	1.22	0.0218	0.0247	1.13	1.22
	1.58	1.66	0.0182	0.0199	1.09	1.17	0.0429	0.0459	1.07	1.15	0.0279	0.0308	1.10	1.15
1.0	0	0	0.0156	0.0196	1.26	1.50	0.0401	0.0488	1.22	1.50	0	0	-	1.50
	0.81	0.81	0.0134	0.0148	1.10	1.23	0.0339	0.0378	1.11	1.28	0.0170	0.0197	1.16	1.28
	1.62	1.62	0.0128	0.0137	1.07	1.14	0.0321	0.0348	1.08	1.18	0.0217	0.0239	1.10	1.18
1.25	0	0	0.0088	0.0112	1.27	1.52	0.0298	0.0370	1.24	1.62	0	0	-	1.62
	0.83	0.79	0.0075	0.0084	1.12	1.28	0.0241	0.0270	1.12	1.31	0.0125	0.0146	1.17	1.31
	1.66	1.58	0.0071	0.0077	1.04	1.18	0.0226	0.0250	1.11	1.23	0.0151	0.0168	1.11	1.23
2.0	0	0	0.0029	0.0035	1.21	1.39	0.0134	0.0181	1.35	1.97	0	0	-	1.97
	1	0.78	0.0026	0.0028	1.08	1.17	0.0103	0.0123	1.19	1.62	0.0052	0.0064	1.23	1.62
	2	1.54	0.0025	0.0026	1.04	1.13	0.0094	0.0105	1.12	1.33	0.0063	0.0073	1.16	1.33

Average Slab Moments, M/qa^2

* Interior panel α_{CB} is M_{CB}/M_{UL} for an interior panel supported similarly.

TABLE 9 COMPARISON OF STRIP WITH UNIFORM LOAD MOMENTS IN BEAMS

$J = K = 0$

Aspect Ratio a/b	Beam Flexural Stiffness* H_a	Beam Moments, M/ca^2b: Positive Moment M_{UL}	Positive Moment M_{ST}	Positive Moment $\frac{M_{ST}}{M_{UL}} = \alpha_{ST}$	Negative Moment M_{UL}	Negative Moment M_{ST}	Negative Moment $\frac{M_{ST}}{M_{UL}} = \alpha_{ST}$
0.5	0	.0	0	∞	0	0	∞
	0.25	0.0113	0.0232	2.05	0.0252	0.032	1.27
	0.5	0.0139	0.0313	2.25	0.0278	0.036	1.28
	1.0	0.0155	0.0378	2.45	0.0285	0.038	1.31
	2.5	0.0162	0.0433	2.67	0.0284	0.039	1.39
	∞	0.0166	0.0482	2.91	0.0275	0.0400	1.45
0.8	0	0	0	∞	0	0	∞
	0.4	0.0140	0.0314	2.24	0.0315	0.040	1.27
	0.8	0.0185	0.0435	2.35	0.0371	0.048	1.29
	1.6	0.0219	0.0527	2.41	0.0406	0.054	1.33
	4.0	0.0246	0.0604	2.45	0.0428	0.059	1.38
	∞	0.0266	0.0673	2.53	0.0442	0.0626	1.42
1.0	0	0	0	∞	0	0	∞
	0.5	0.0154	0.0380	2.47	0.0345	0.048	1.39
	1.0	0.0208	0.0503	2.42	0.0417	0.054	1.29
	2.0	0.0253	0.0600	2.37	0.0469	0.062	1.[illegible]
	5.0	0.0290	0.0679	2.34	0.0510	0.069	[illegible]
	∞	0.0321	0.0744	2.32	0.0542	0.0743	
1.25	0	0	0	∞	0	0	[illegible].30
	0.63	0.0169	0.0426	2.52	0.0376	0.049	1.30
	1.25	0.0231	0.0554	2.40	0.0462	0.06[illegible]	1.30
	2.50	0.0284	0.0651	2.29	0.0530	0.[illegible]	1.32
	6.25	0.0329	0.0729	2.21	0.0586	0[illegible]	1.32
	∞	0.0367	0.0792	2.16	0.0633		∞
2.0	0	0	0	∞	0		1.30
	1.0	0.0210	0.0522	2.49	0.04[illegible]2		1.26
	2.0	0.0278	0.0640	2.30	0.[illegible]90		1.29
	4.0	0.0332	0.0722	2.18	0[illegible]0964		1.29
	10.0	0.0376	0.0784	2.09			1.29
	∞	0.0412	0.0830	2.01			

* $H_b = H_a(b/a)^2$.

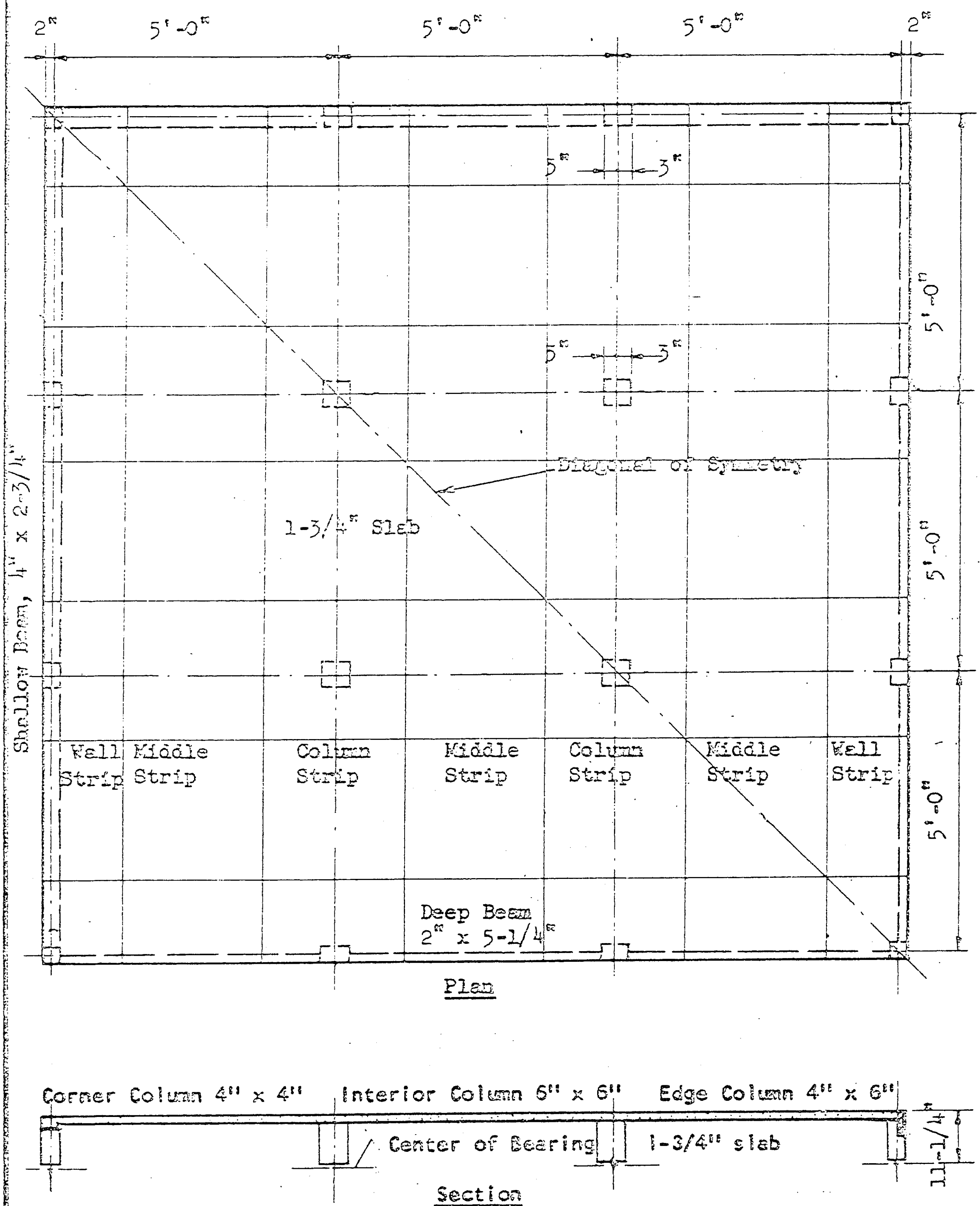

FIG. 2.1 LAYOUT OF FLAT PLATE TEST STRUCTURE (F1)

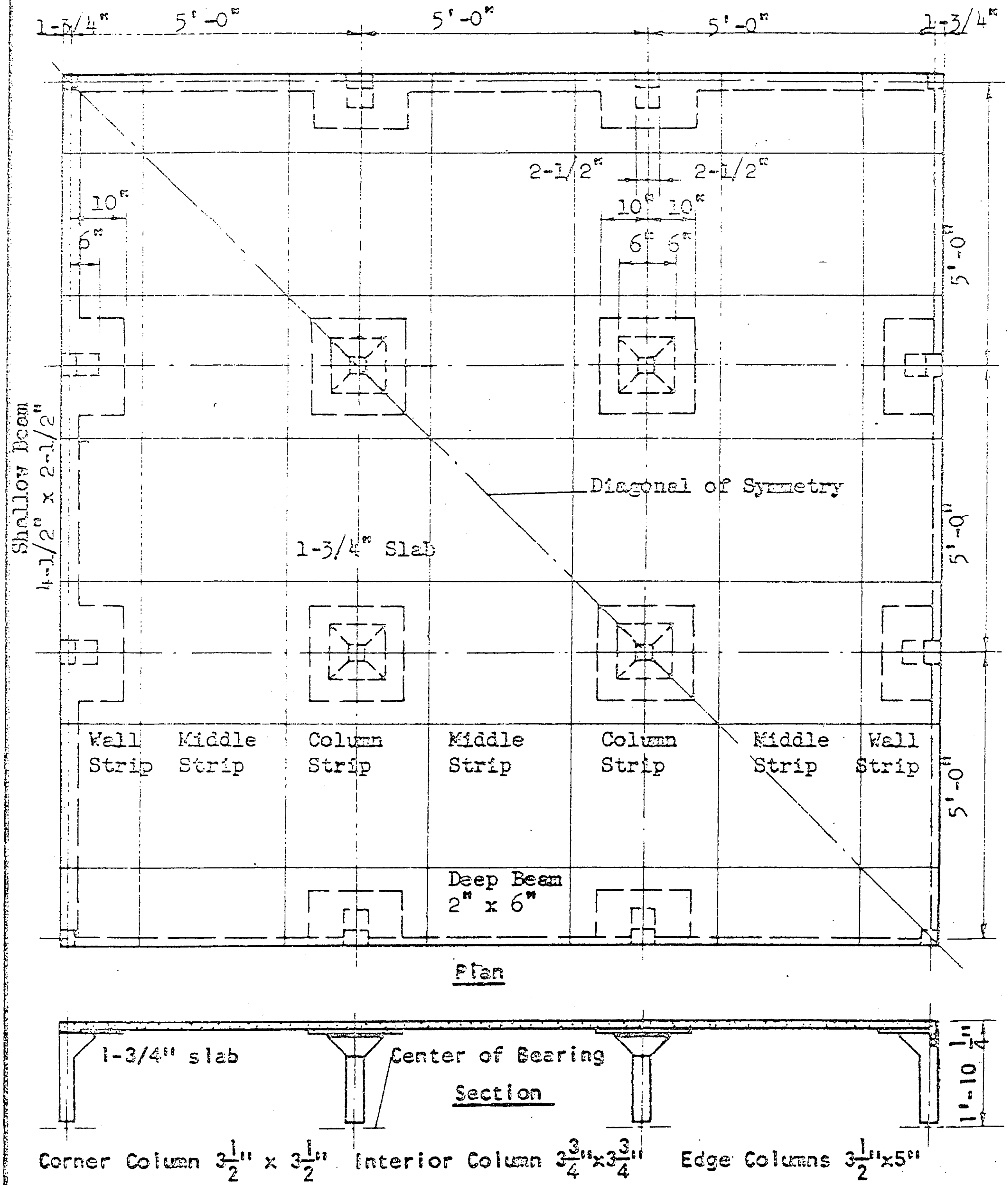

FIG. 2.2 LAYOUT OF FLAT SLAB TEST STRUCTURES (F2, F3)

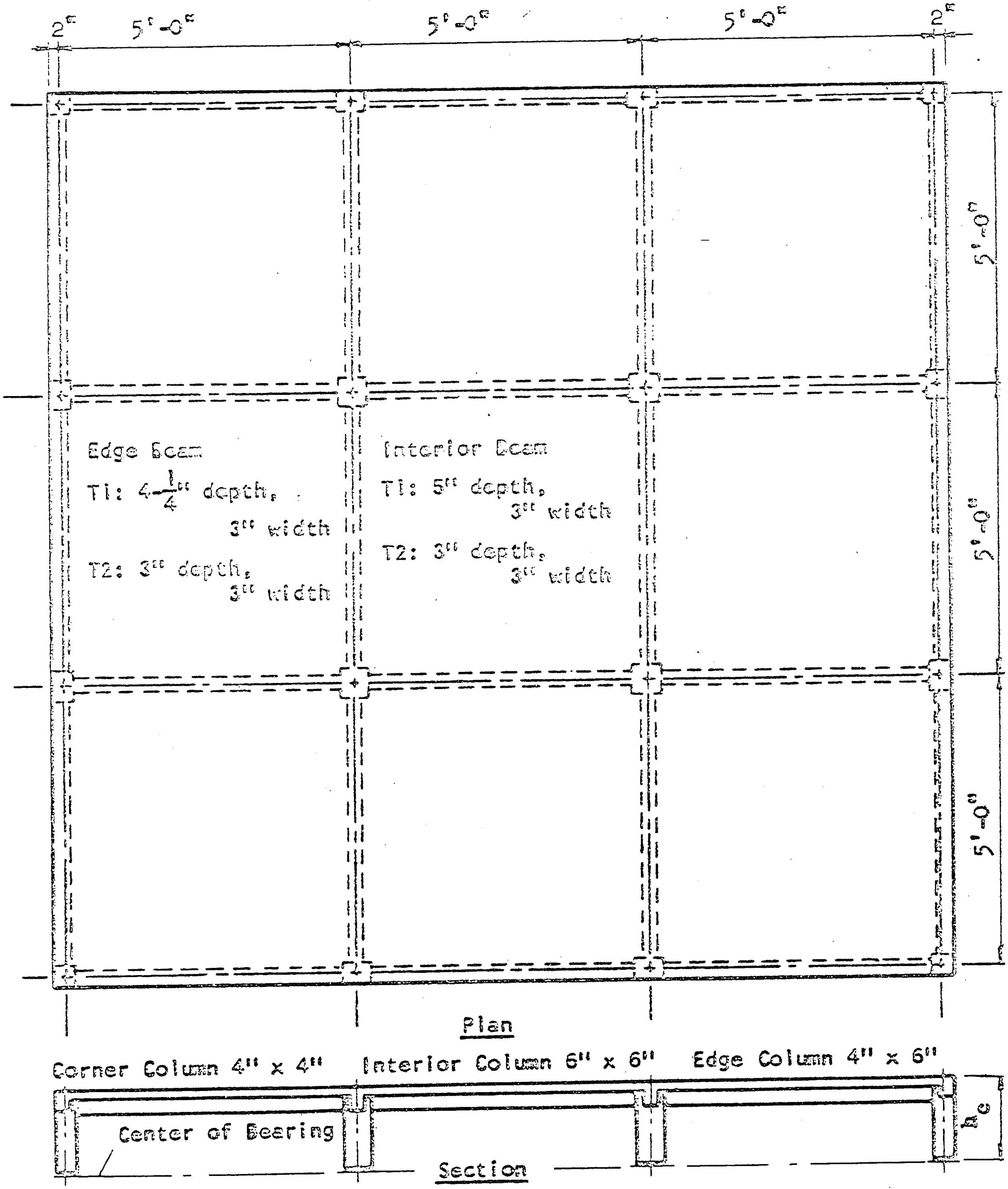

Note: Dimension h_c = 16-5/8" in Typical Two-Way Slab (T1) and
h_c = 13-7/8" in Two-Way Slab with Shallow Beams (T2)

FIG. 2.3 LAYOUT OF TWO-WAY SLAB TEST STRUCTURES (T1, T2)

Maximum Positive and
Exterior Negative Moment

Maximum Midspan Deflection

F1, F2, F3

Maximum Negative Moment

F1, F2, F3

Maximum Positive Moments
Maximum Midpanel Deflections

T1, T2

Maximum Negative Moments
Maximum Beam Deflections

T1, T2

Maximum Negative Beam Moments

T1, T2

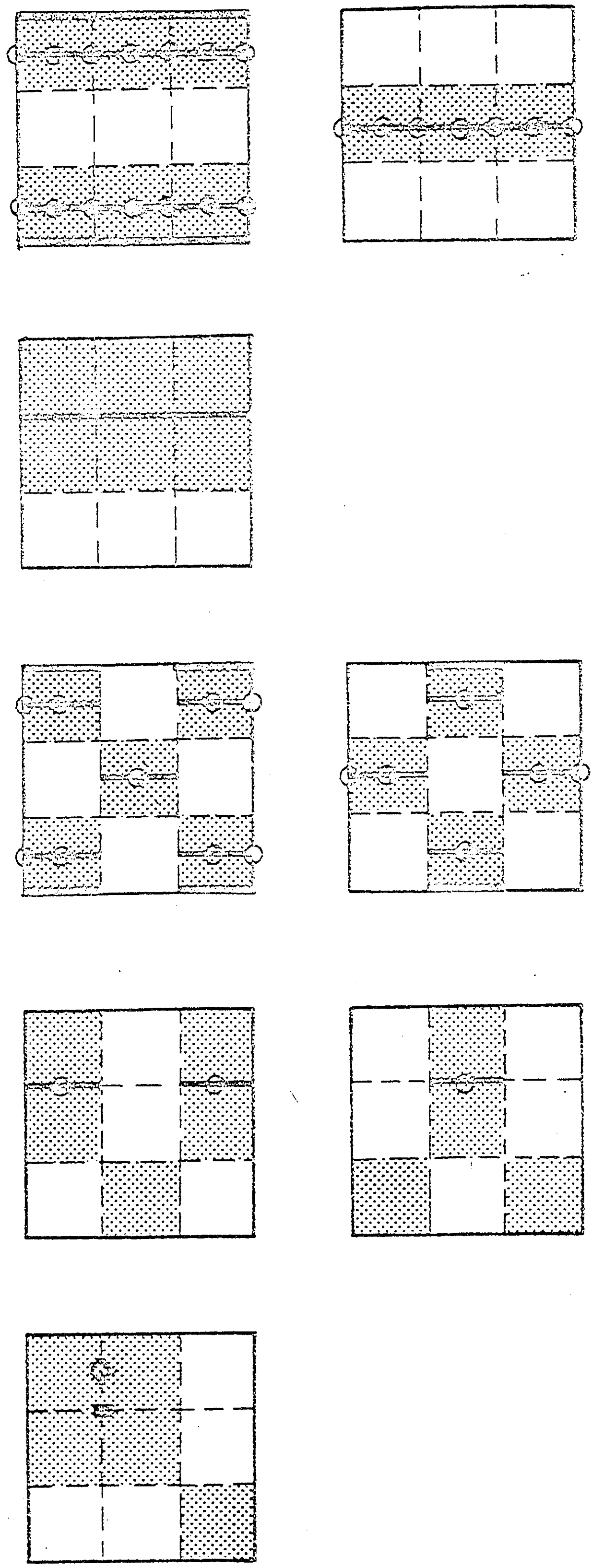

Note: Heavy lines indicate sections of maximized moment
Circles indicate locations of maximized deflection

FIG. 2.4 LOADING PATTERNS

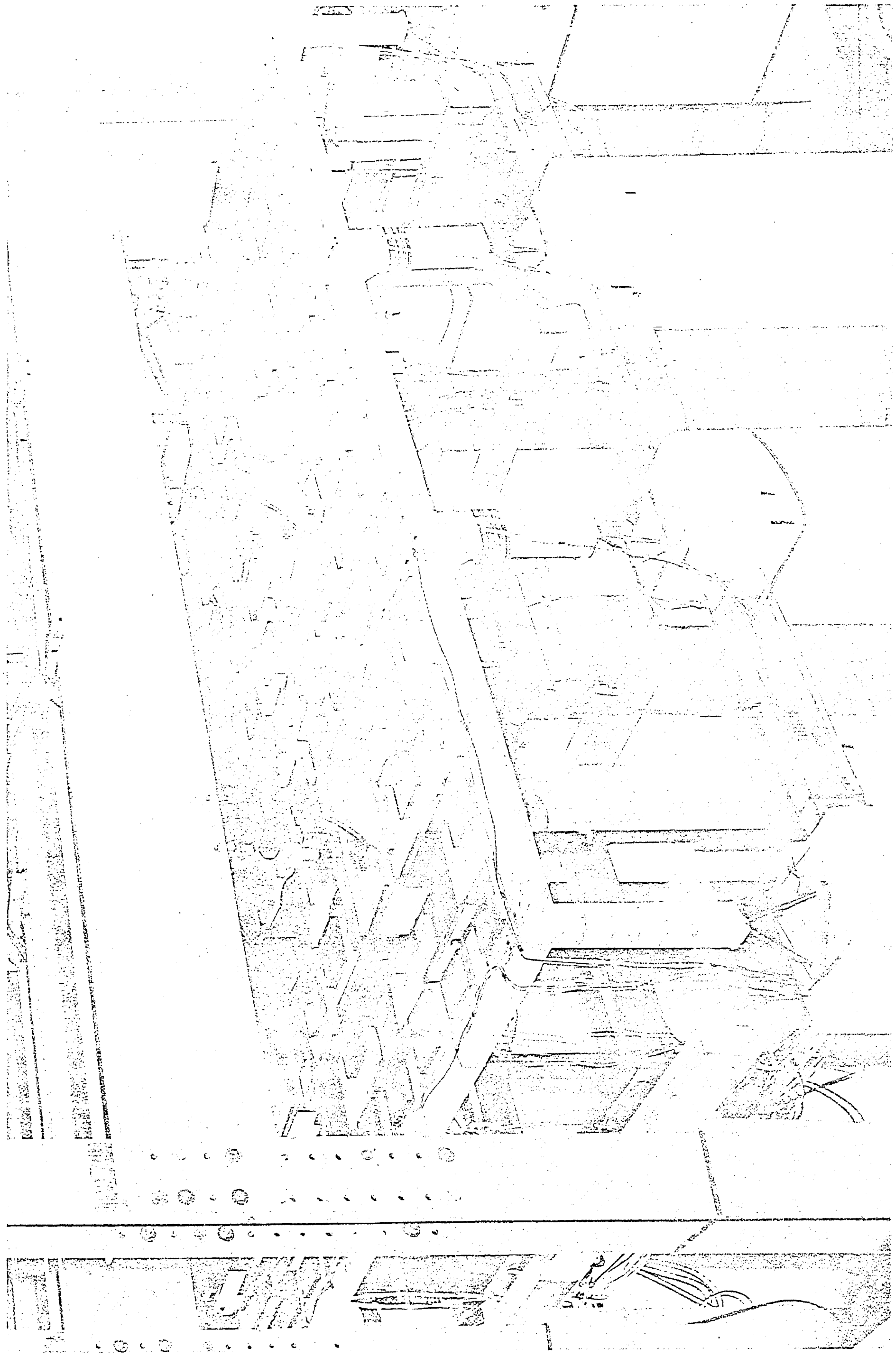

FIG. 2.5 VIEW OF TEST STRUCTURE AND LOADING SYSTEM

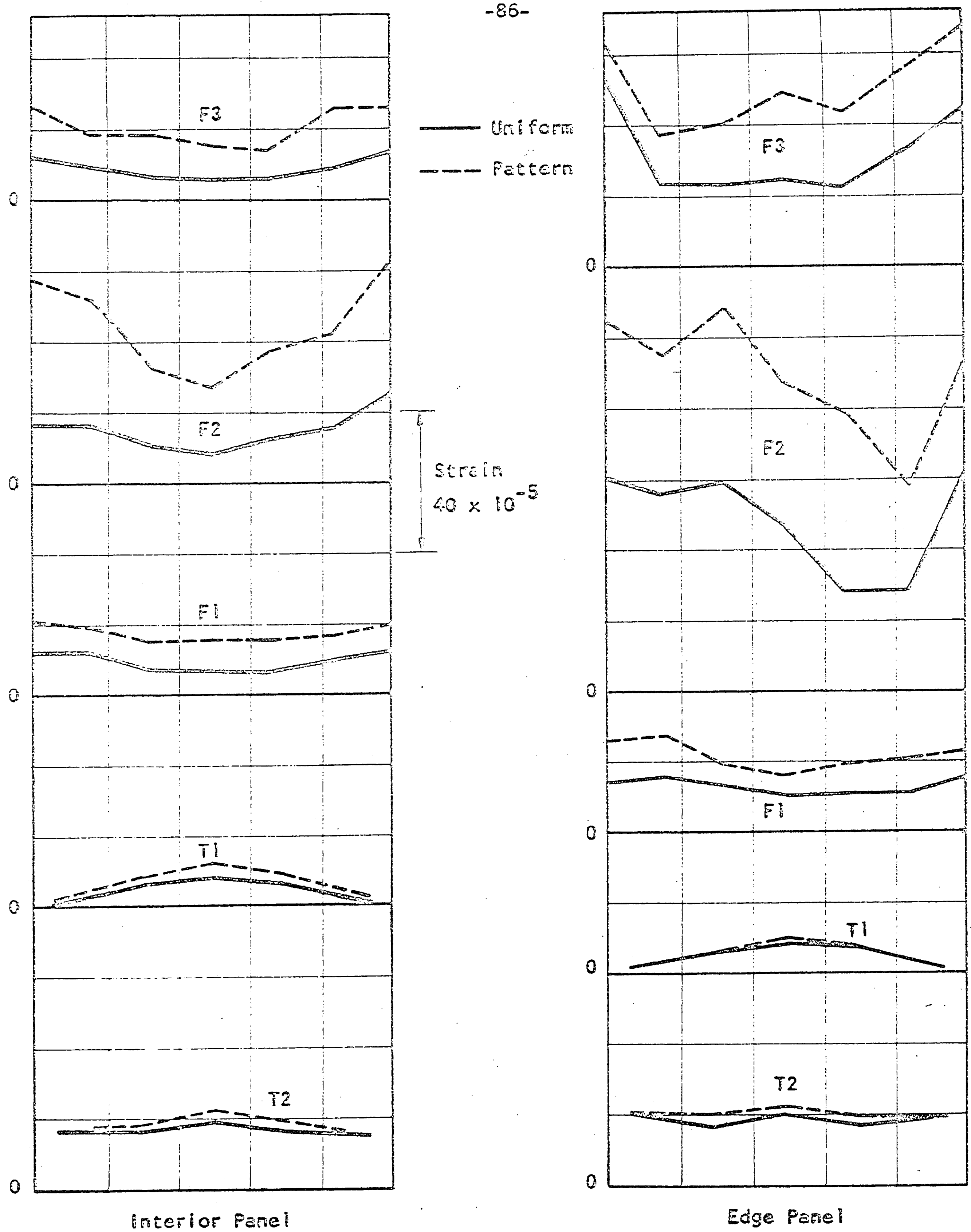

FIG. 2.6 COMPARISON OF PATTERN WITH UNIFORM LOAD STRAINS ACROSS POSITIVE MOMENT SECTIONS

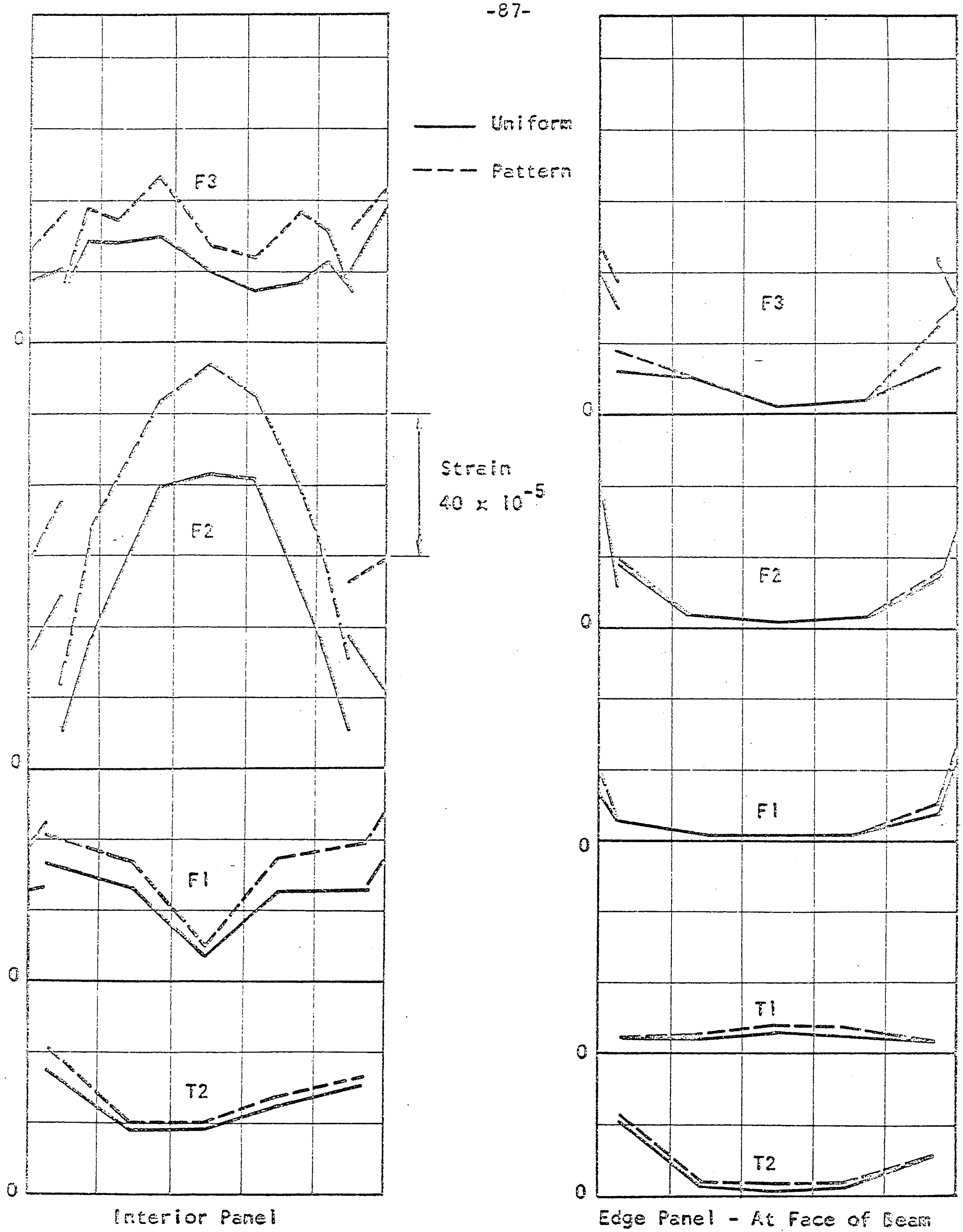

FIG. 2.7 COMPARISON OF PATTERN WITH UNIFORM LOAD STRAINS ACROSS NEGATIVE MOMENT SECTIONS

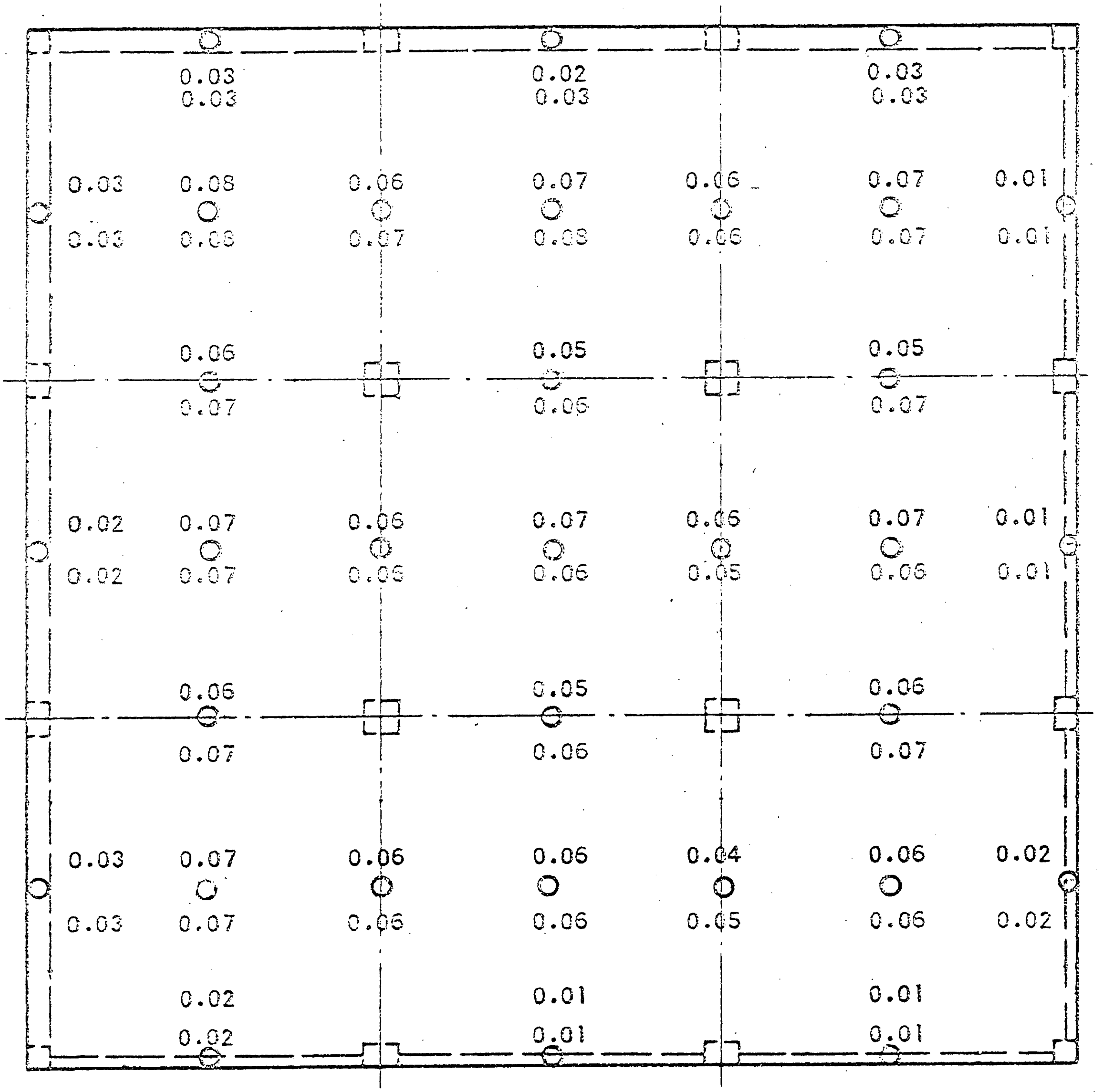

Deflections in inches

Note: Uniform Load Deflections
Strip Load Deflections

FIG. 2.8 STRIP AND UNIFORM LOAD DEFLECTIONS IN STRUCTURE F1

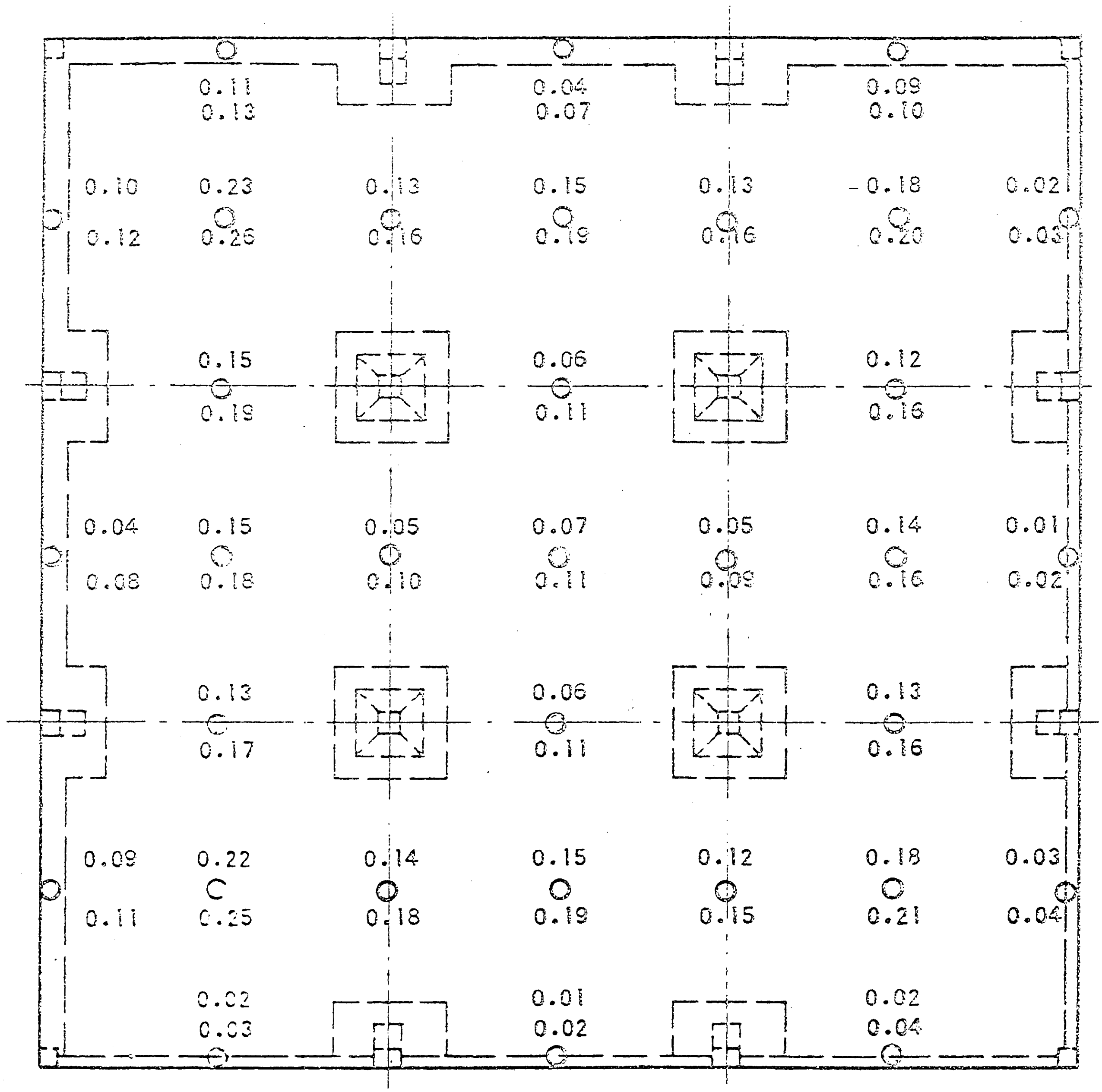

Deflections in inches

Note: Uniform Load Deflections
Strip Load Deflections

FIG. 2.9 STRIP AND UNIFORM LOAD DEFLECTIONS IN STRUCTURE F2

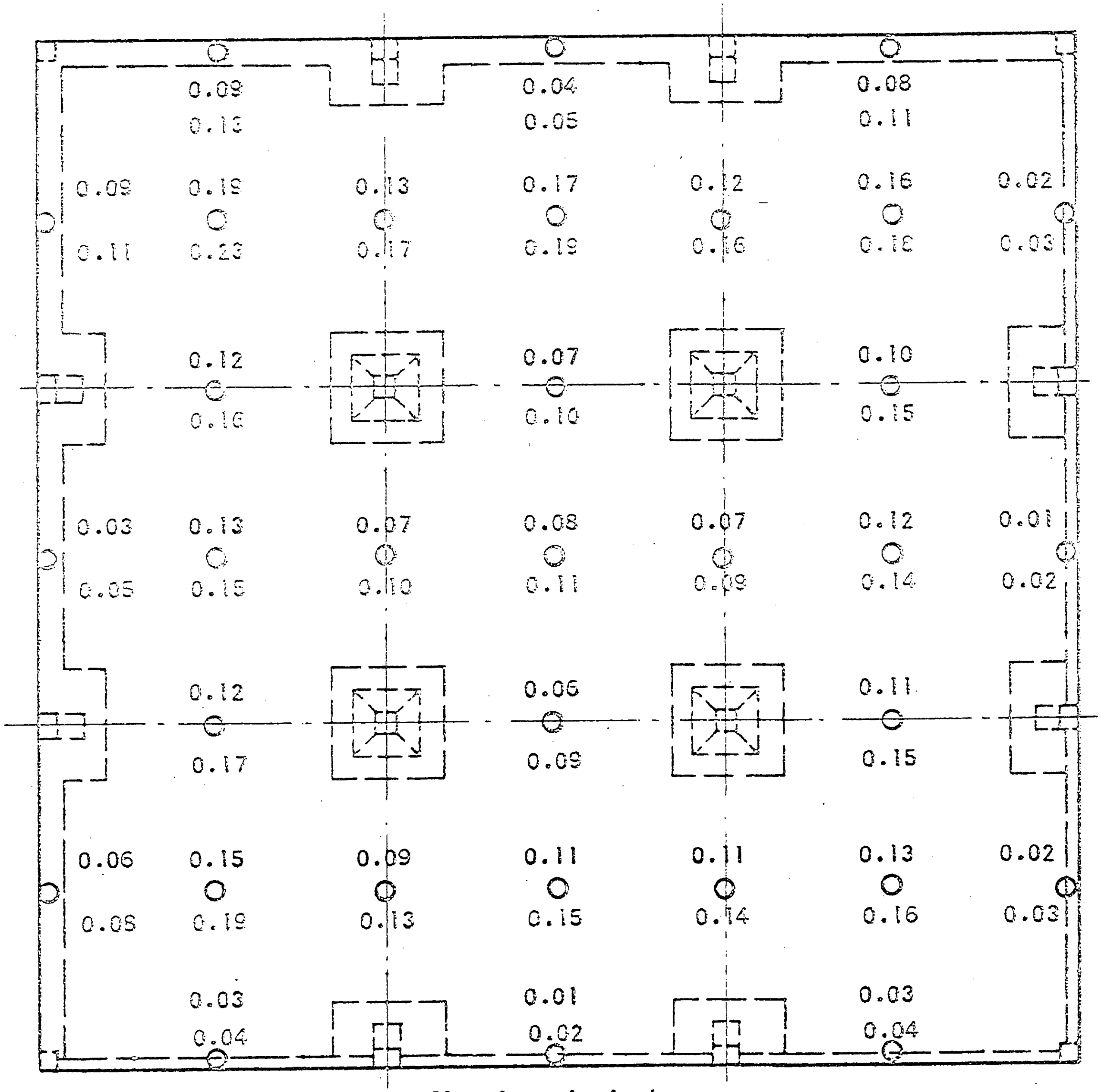

Deflections in inches

Note: Uniform Load Deflections
Strip Load Deflections

FIG. 2.10 STRIP AND UNIFORM LOAD DEFLECTIONS IN STRUCTURE F3

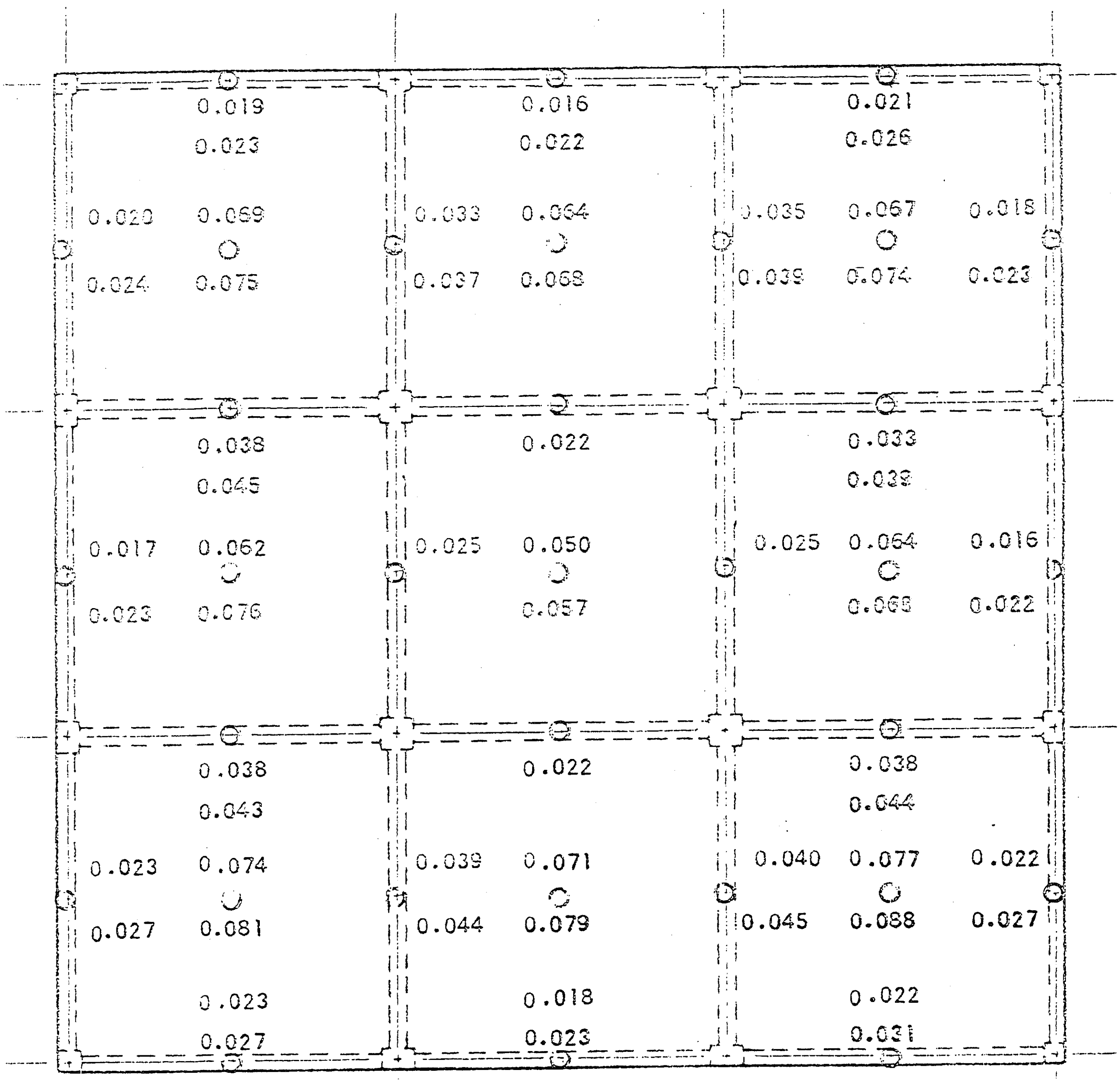

Deflection in inches

Note: Uniform Load Deflections
Checkerboard Load Deflections

FIG. 2.11 CHECKERBOARD AND UNIFORM LOAD DEFLECTIONS IN STRUCTURE T1

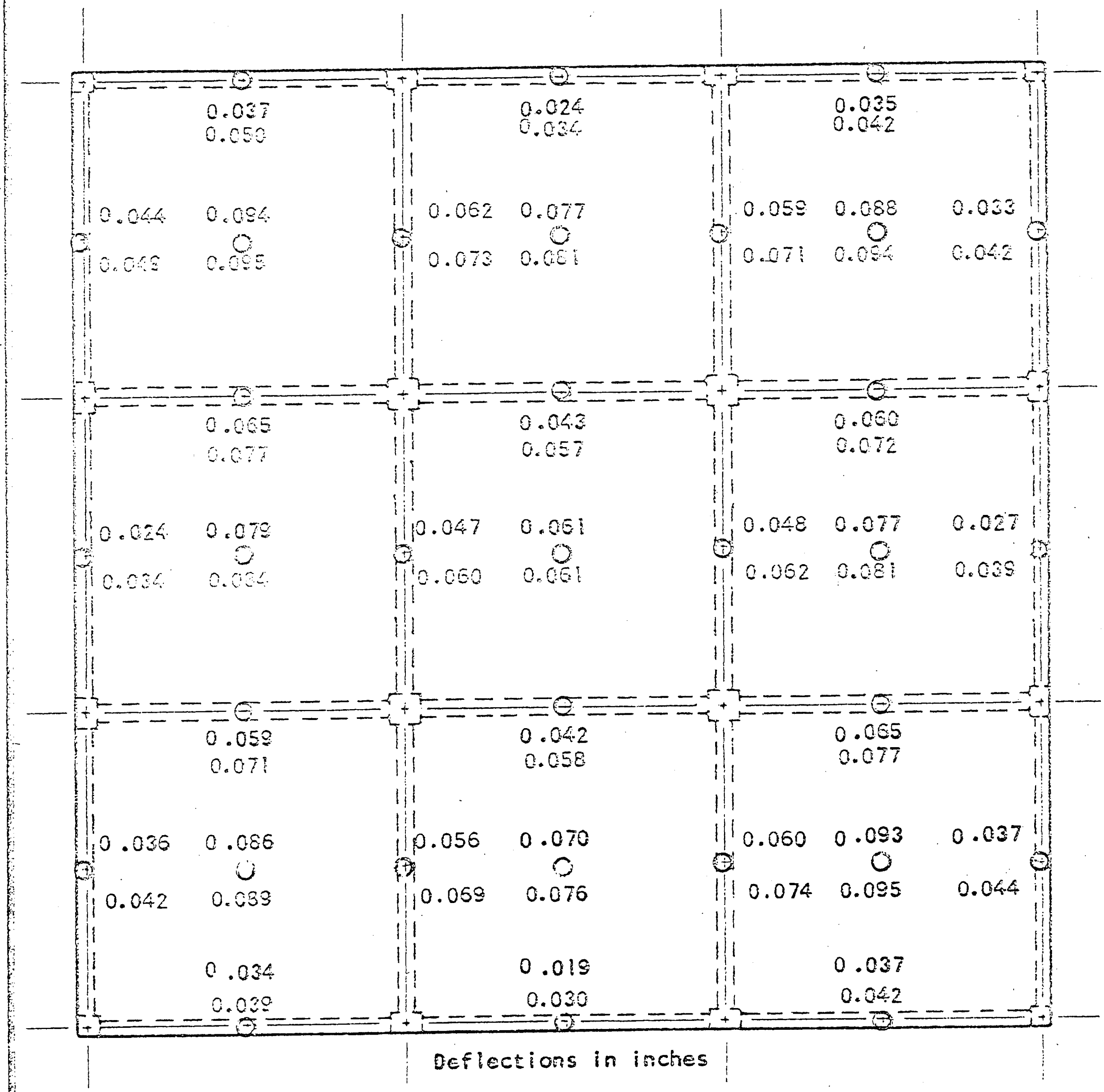

Note: Uniform Load Deflections
Checkerboard Load Deflections

FIG. 2.12 CHECKERBOARD AND UNIFORM LOAD DEFLECTIONS IN STRUCTURE T2

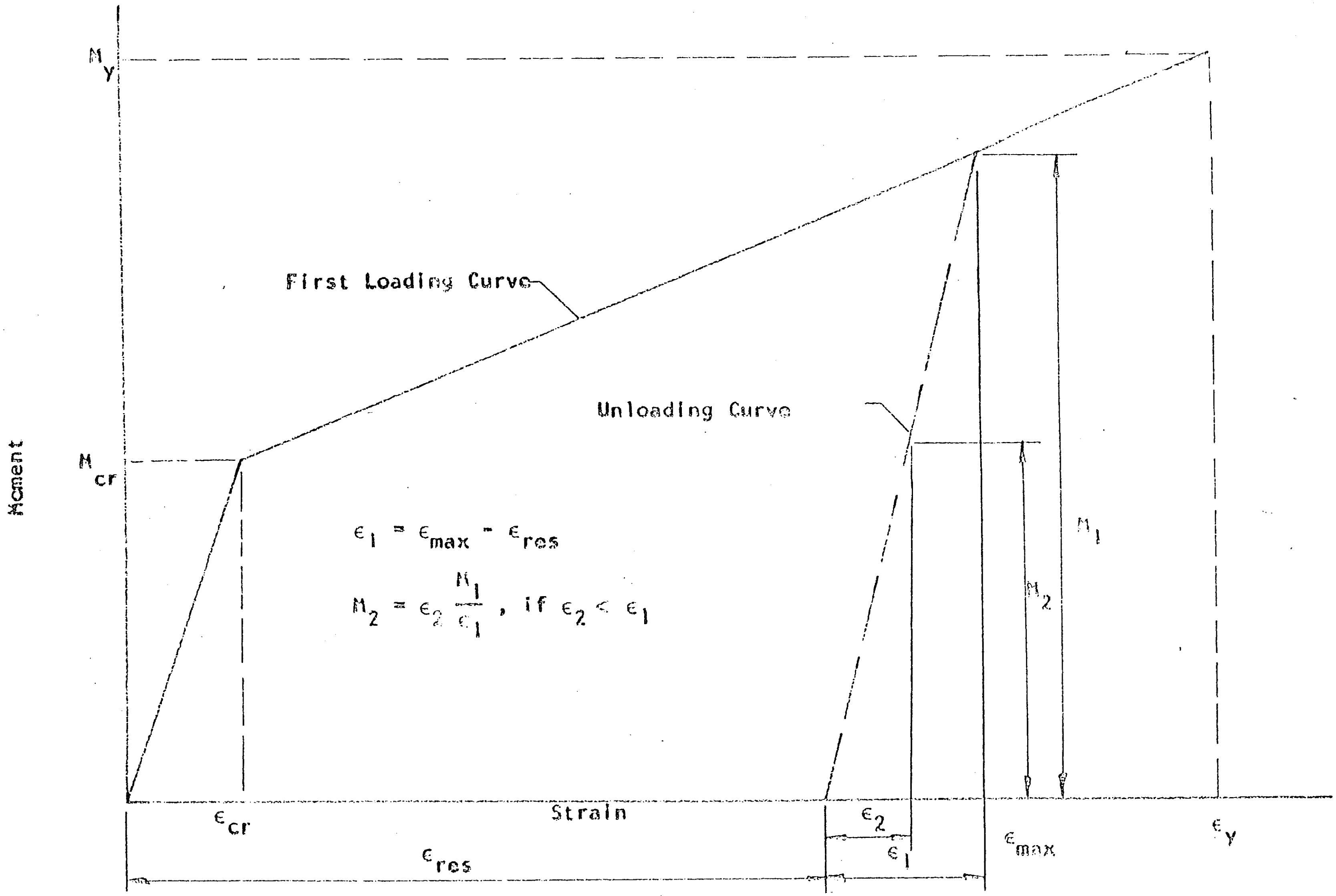

FIG. 3.1 TYPICAL MOMENT-STRAIN RELATIONSHIP FOR A REINFORCED CONCRETE SECTION

Direction of moments

Wall Strip	Middle Strip	Column Strip	Middle Strip	Column Strip	Middle Strip	Wall Strip
0.015 0.016	0.006 0.004	0.019 0.018	0.008 0.003	0.019 0.018	0.008 0.003	-
0.019 0.023	0.024 0.023	0.026 0.028	0.023 0.024	0.026 0.027	0.020 0.024	0.014 0.021
0.027 0.036	0.020	0.042 0.040	0.023	0.042 0.044	0.018	0.019 0.031
0.025 0.034	0.018	0.041 0.038	0.026	0.041 0.044	0.020	0.016 0.026
0.015 0.019	0.022 0.022	0.023 0.022	0.016 0.021	0.025 0.023	0.016 0.018	0.008 0.016
0.025 0.026	0.020	0.039 0.038	0.020	0.037 0.038	0.018	0.016 0.018
0.025 0.027	0.018	0.039 0.037	0.025	0.037 0.039	0.020	0.019 0.030
0.016 0.020	0.020 0.021	0.024 0.026	0.023 0.022	0.024 0.025	0.018 0.022	0.012 0.021
0.011 0.011	0.012 0.005	0.026 0.021	0.009 0.005	0.024 0.021	0.009 0.006	-

Note: Moments in terms of M/qa^3
Uniform Load Moments
Strip Load Moments

FIG. 3.2 STRIP AND UNIFORM LOAD MOMENTS IN STRUCTURE F1

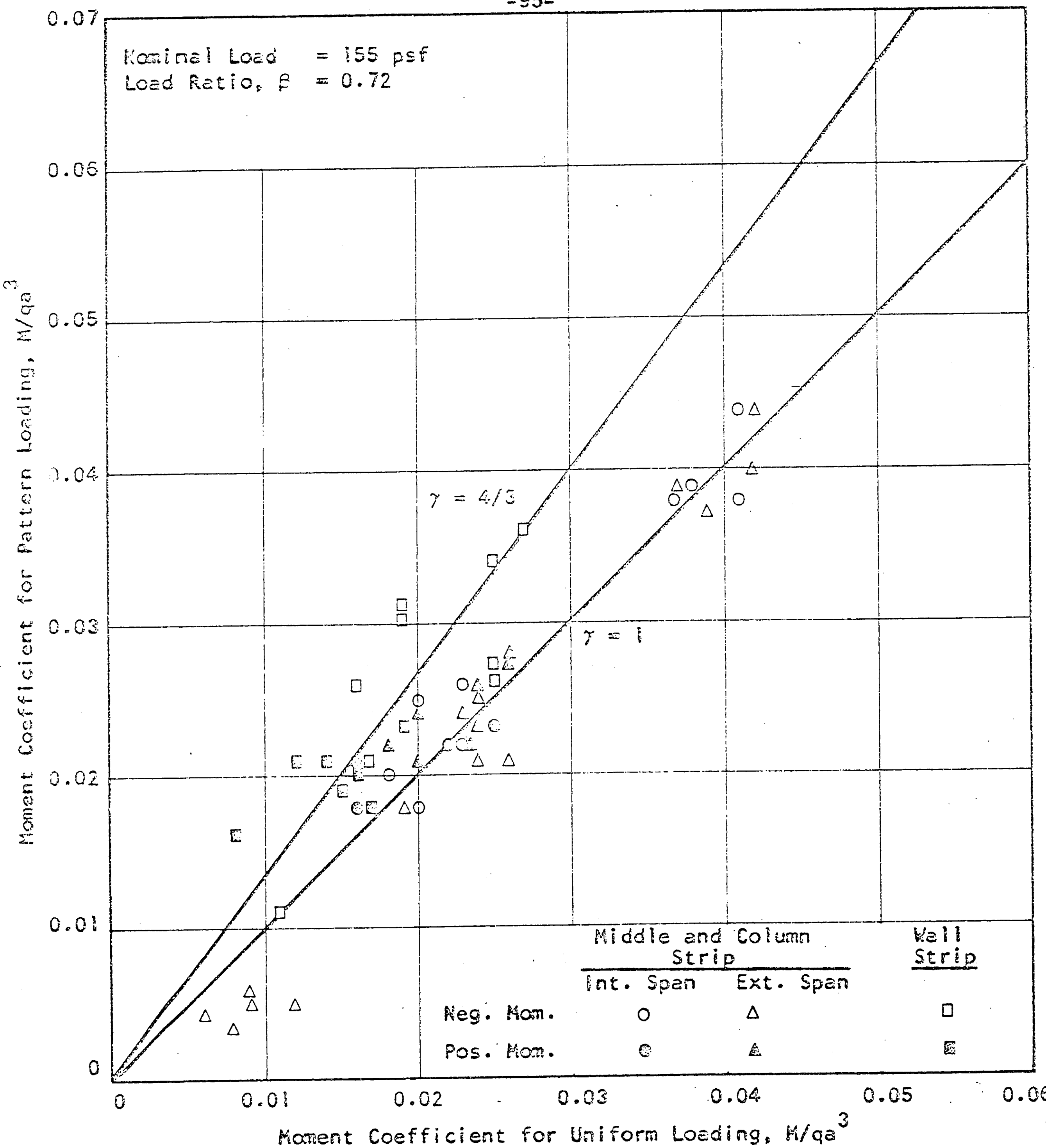

FIG. 3.3 COMPARISON OF STRIP AND UNIFORM LOAD MOMENTS IN STRUCTURE F1

Direction of moments

Wall Strip	Middle Strip	Column Strip	Middle Strip	Column Strip	Middle Strip	Wall Strip
0.018 0.020	0.003 0.003	0.022 0.023	0.003 0.004	0.022 0.022	0.003 0.003	0.030 0.026
0.026 0.029	0.020 0.022	0.023 0.026	0.020 0.023	0.021 0.023	0.016 0.018	0.026 0.033
0.042 0.047 0.040 0.044	0.019 0.018	0.045 0.051 0.039 0.044	0.023 0.026	0.045 0.053 0.039 0.049	0.021 0.023	0.051 0.062 0.049 0.060
0.014 0.019	0.016 0.018	0.016 0.017	0.013 0.015	0.016 0.019	0.015 0.016	0.013 0.026
0.033 0.035 0.039 0.039	0.019 0.021	0.038 0.045 0.042 0.048	0.023 0.023	0.033 0.044 0.042 0.048	0.018 0.020	0.048 0.054 0.061 0.063
0.021 0.021	0.018 0.020	0.020 0.021	0.017 0.019	0.022 0.024	0.018 0.019	0.030 0.035
0.014 0.012	0.006 0.007	0.021 0.020	0.005 0.004	0.020 0.022	0.007 0.006	0.029 0.027

Note: Moments in terms of M/qa^3
Uniform Load Moments
Strip Load Moments

FIG. 3.4 STRIP AND UNIFORM LOAD MOMENTS IN STRUCTURE F2

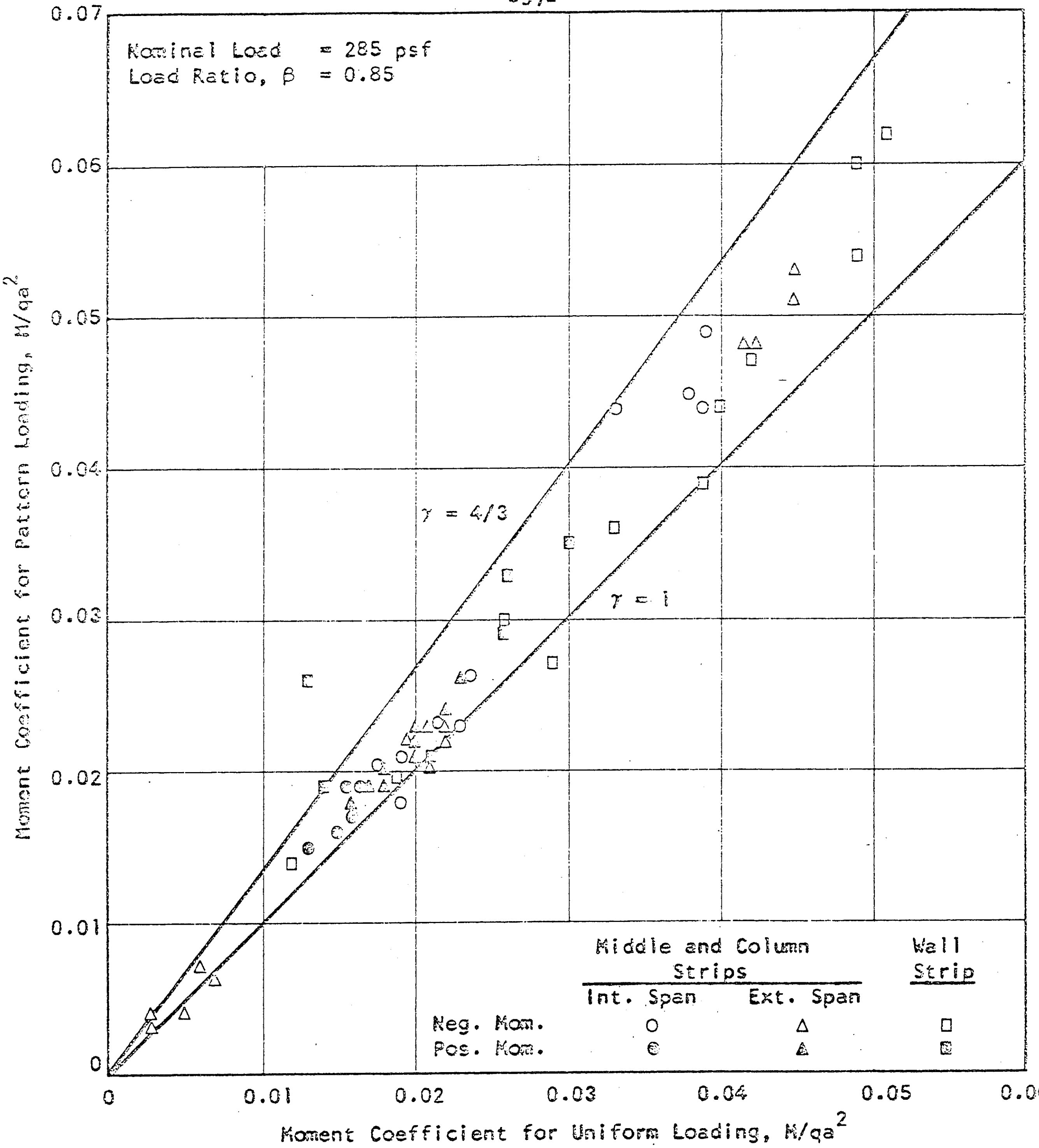

FIG. 3.5 COMPARISON OF STRIP AND UNIFORM LOAD MOMENTS IN STRUCTURE F2

Direction of moments

Wall Strip	Middle Strip	Column Strip	Middle Strip	Column Strip	Middle Strip	Wall Strip
0.022 0.023	0.007 0.007	0.027 0.027	0.006 0.008	0.020 0.025	0.005 0.006	0.022 0.021
0.020 0.020	0.019 0.020	0.020 0.022	0.018 0.020	0.019 0.022	0.014 0.015	0.032 0.035
0.036 0.04 0.032 0.035	0.017 0.018	0.039 0.041 0.035 0.035	0.018 0.019	0.039 0.041 0.038 0.040	0.014 0.016	0.059 0.062 0.051 0.041
0.011 0.015	0.010 0.018	0.013 0.019	0.009 0.018	0.014 0.019	0.009 0.015	0.016 0.031
0.031 0.035 0.030 0.041	0.015 0.018	0.040 0.042 0.041 0.041	0.018 0.018	0.040 0.043 0.042 0.044	0.013 0.014	0.055 0.054 0.060 0.062
0.019 0.023	0.015 0.018	0.015 0.020	0.017 0.019	0.018 0.020	0.015 0.019	0.031 0.033
0.020 0.022	0.008 0.008	0.017 0.017	0.004 0.005	0.022 0.027	0.007 0.005	0.015 0.019

Note: Moments in terms of M/qa^3
Uniform Load Moments
Strip Load Moments

FIG. 3.6 STRIP AND UNIFORM LOAD MOMENTS IN STRUCTURE F3

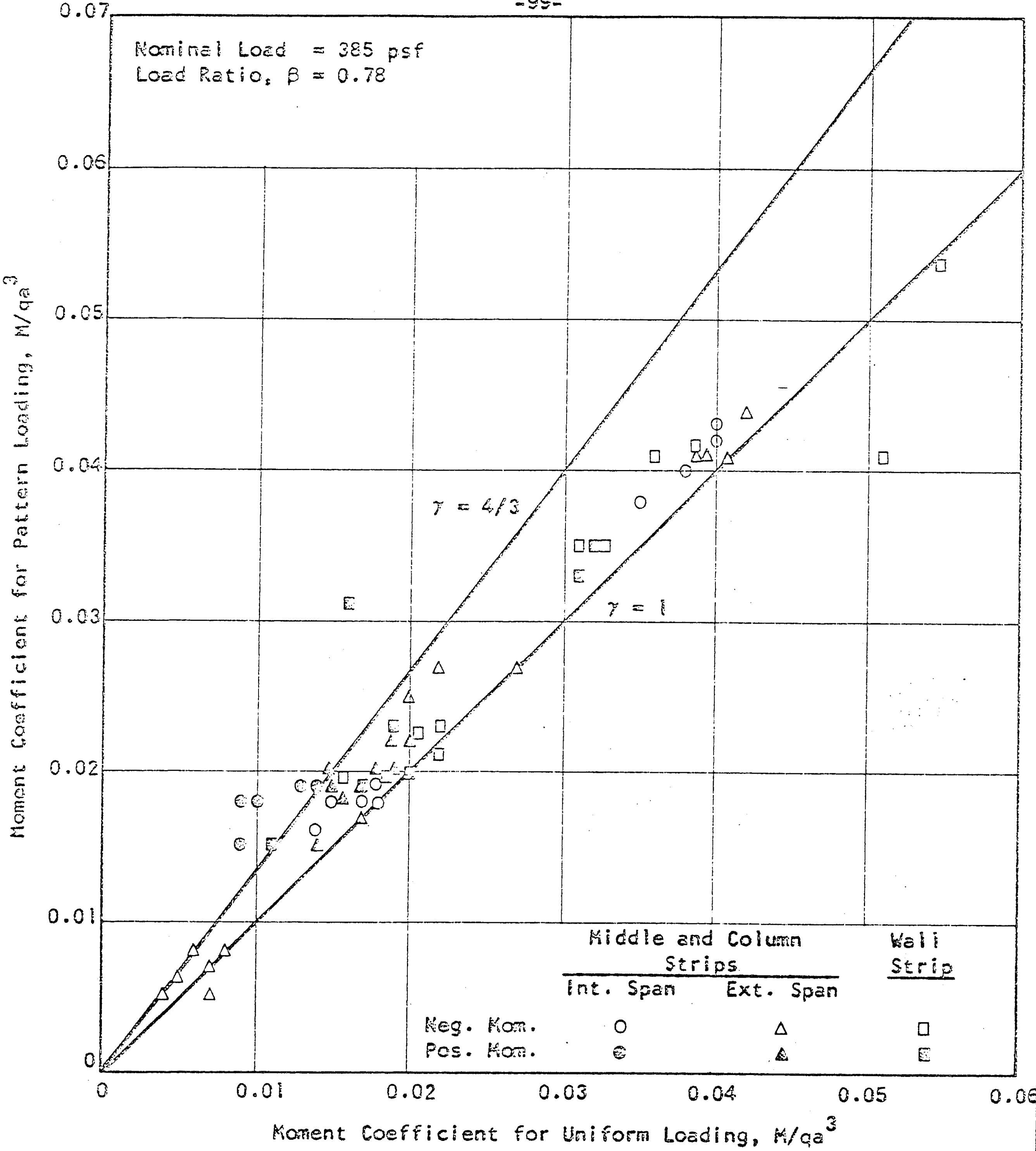

FIG. 3.7 COMPARISON OF STRIP AND UNIFORM LOAD MOMENTS IN STRUCTURE F3

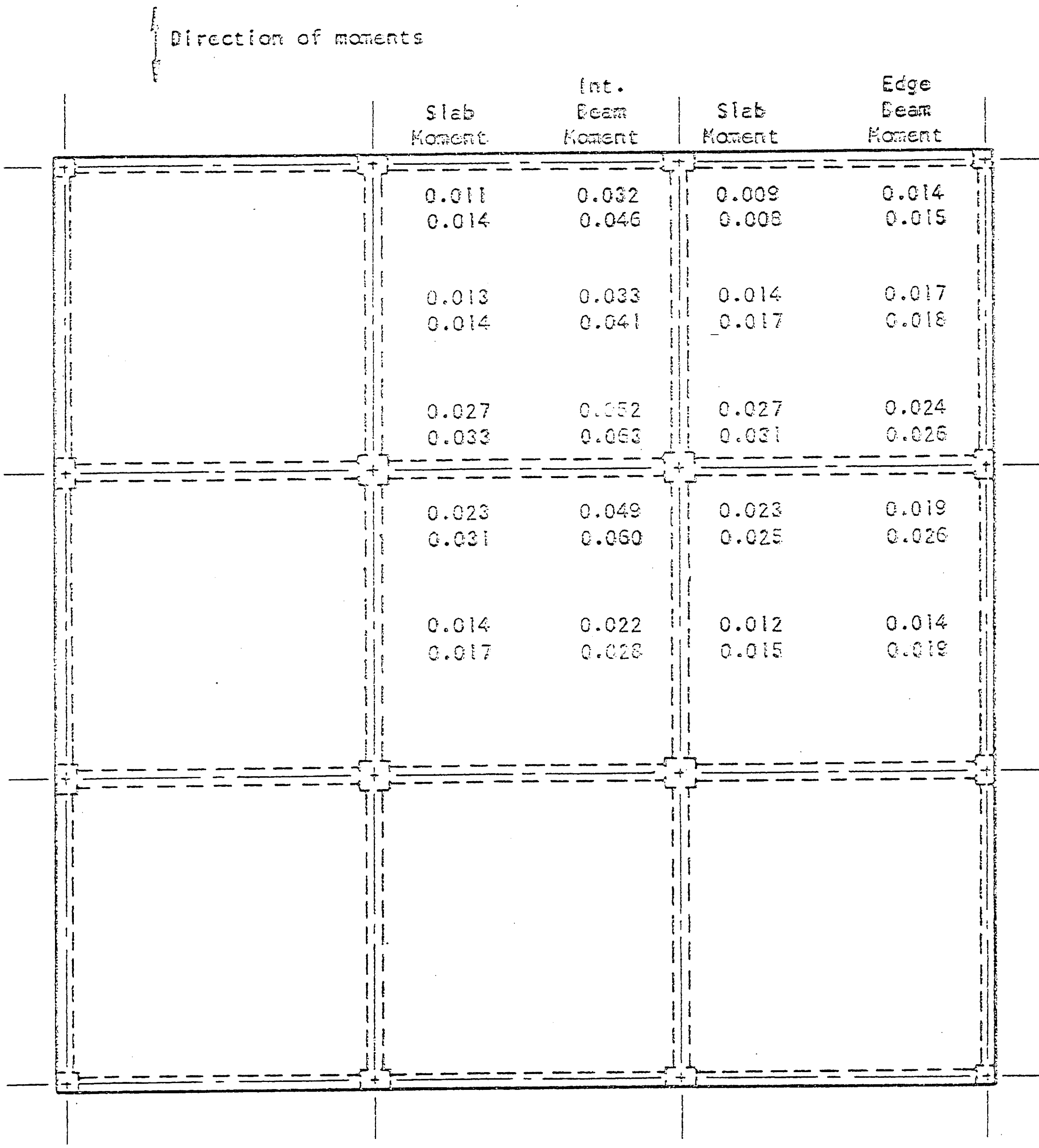

Note: Moments in terms of M/qa^3
Uniform Load Moments
Checkerboard Load Moments

FIG. 3.8 CHECKERBOARD AND UNIFORM LOAD MOMENTS IN STRUCTURE TI

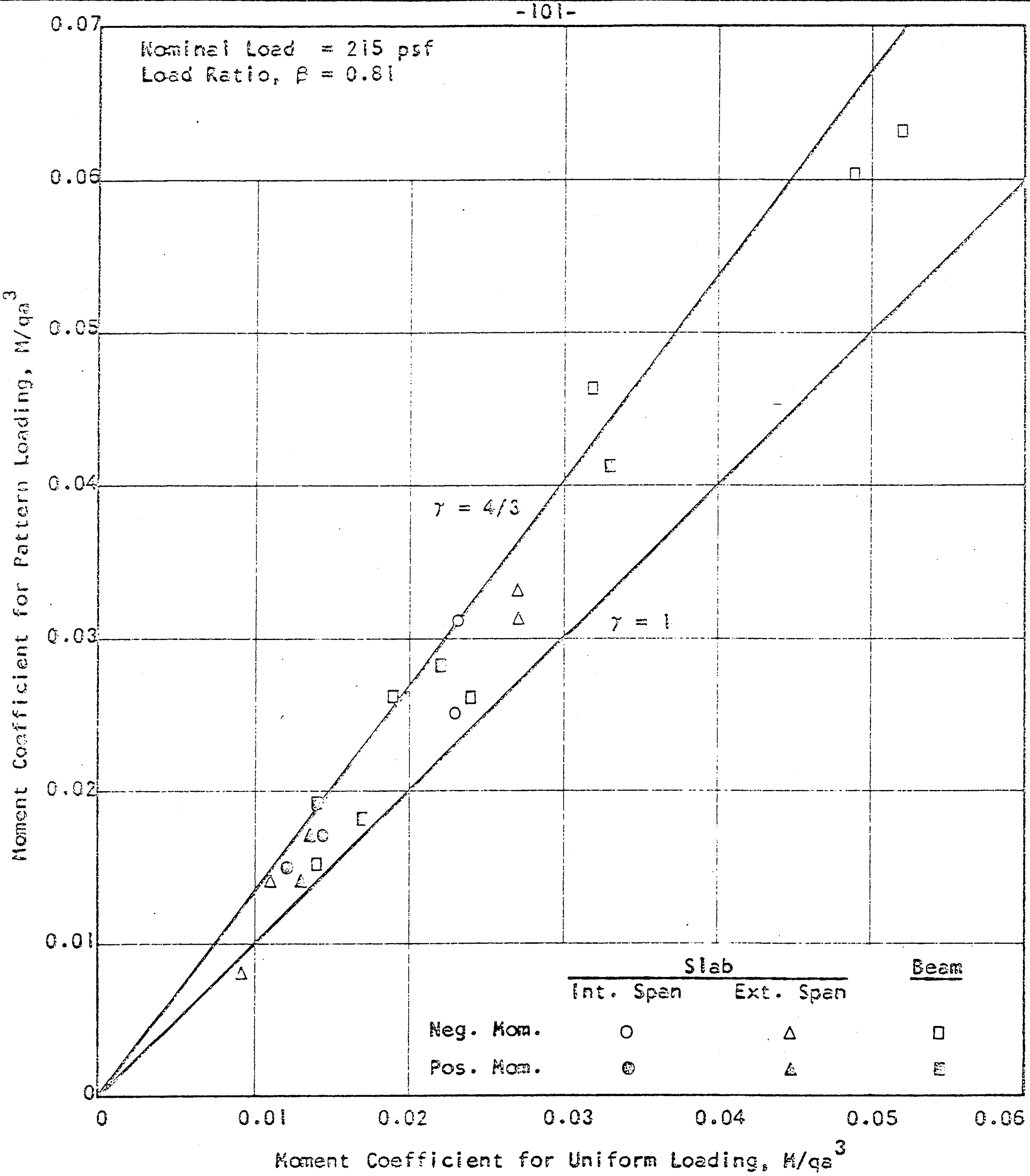

FIG. 3.9 COMPARISON OF CHECKERBOARD AND UNIFORM LOAD MOMENTS IN STRUCTURE T1

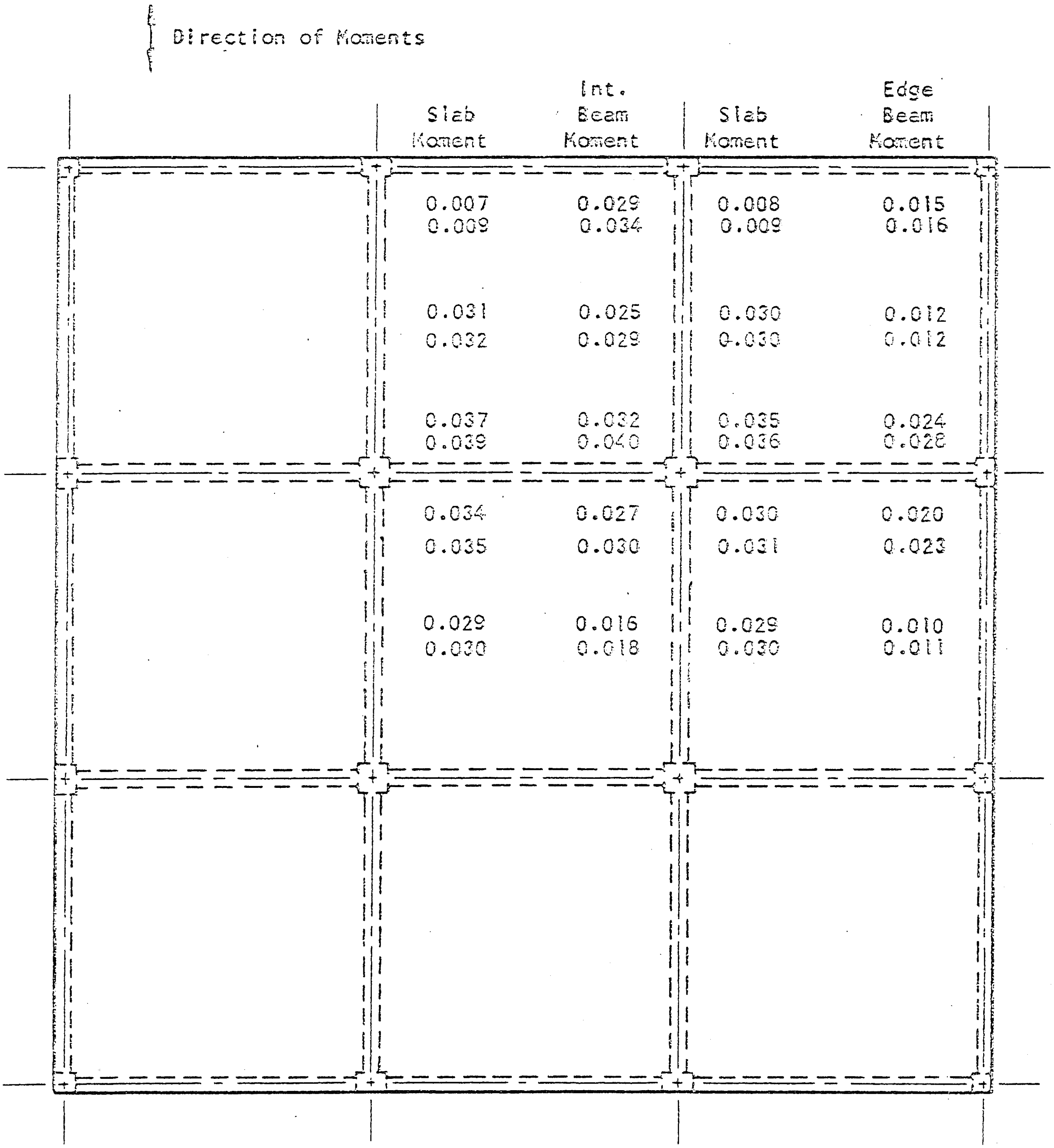

Note: Moments in terms of M/qa^3
Uniform Load Moments
Checkerboard Load Moments

FIG. 3.10 CHECKERBOARD AND UNIFORM LOAD MOMENTS IN STRUCTURE T2

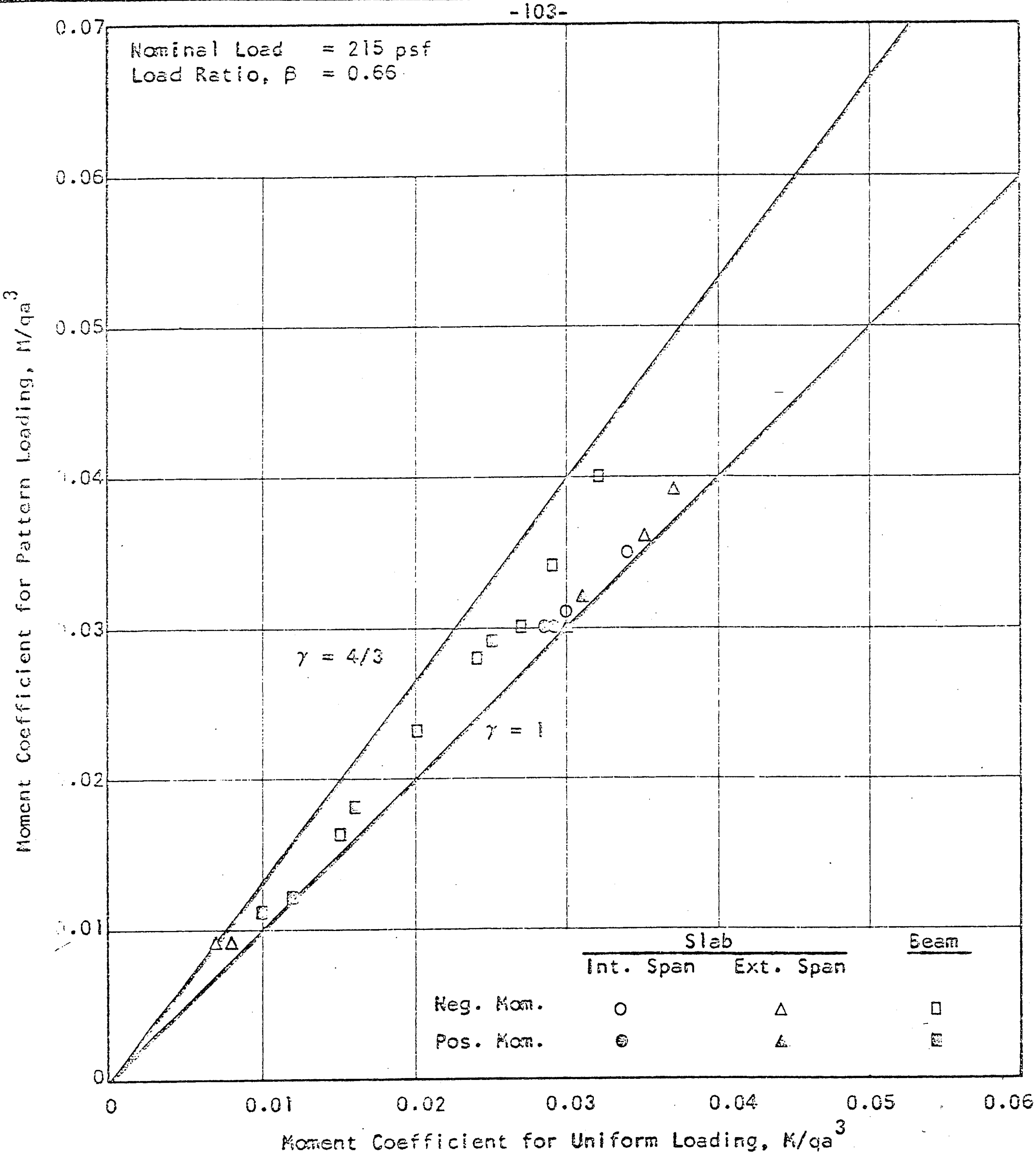

FIG. 3.11 COMPARISON OF CHECKERBOARD AND UNIFORM LOAD MOMENTS IN STRUCTURE T2

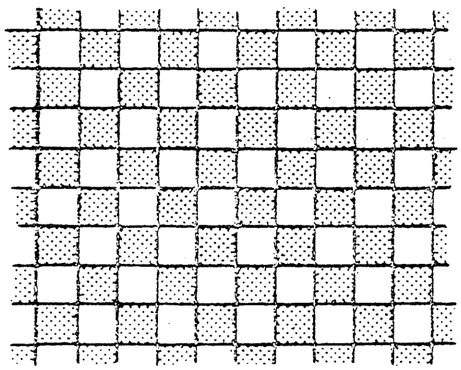

(a) Checkerboard Loading for Maximum Positive Moments

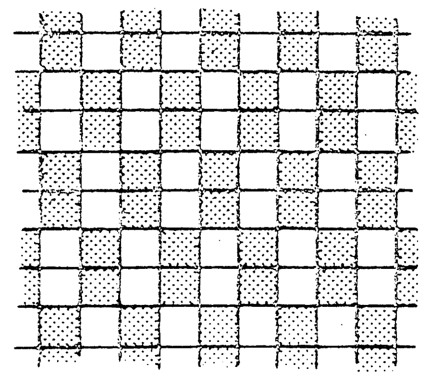

(b) Checkerboard Loading Considered for Maximum Negative Moments

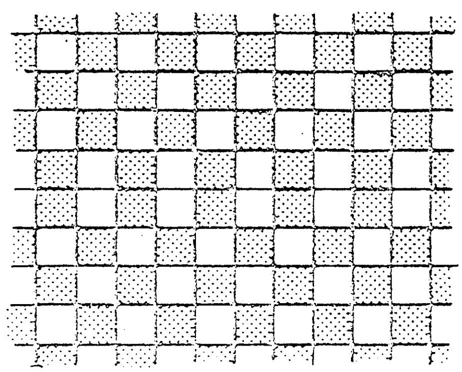

(c) Checkerboard Loading for Theoretical Maximum Negative Moments

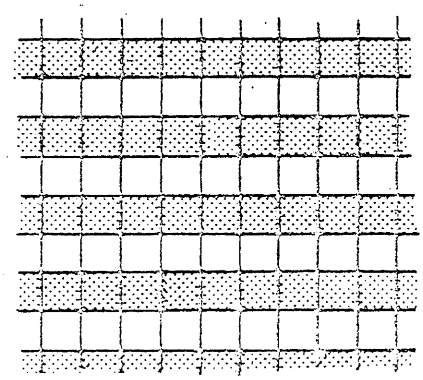

(d) Strip Loading Pattern for Maximum Positive Moments

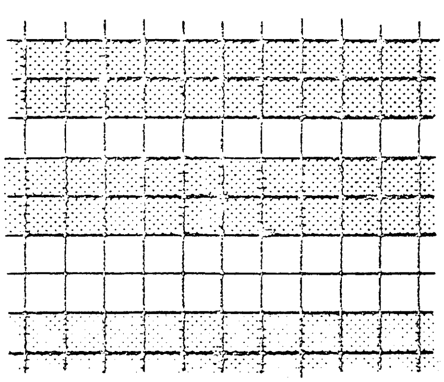

(e) Strip Loading Pattern Considered for Maximum Negative Moments

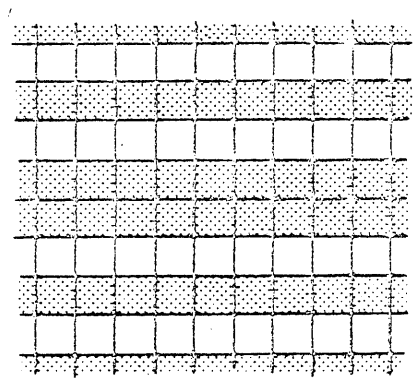

(f) Strip Loading Pattern for Theoretical Maximum Negative Moments

FIG. 4.1 PARTIAL LOADING PATTERNS FOR MAXIMUM POSITIVE AND NEGATIVE MOMENTS

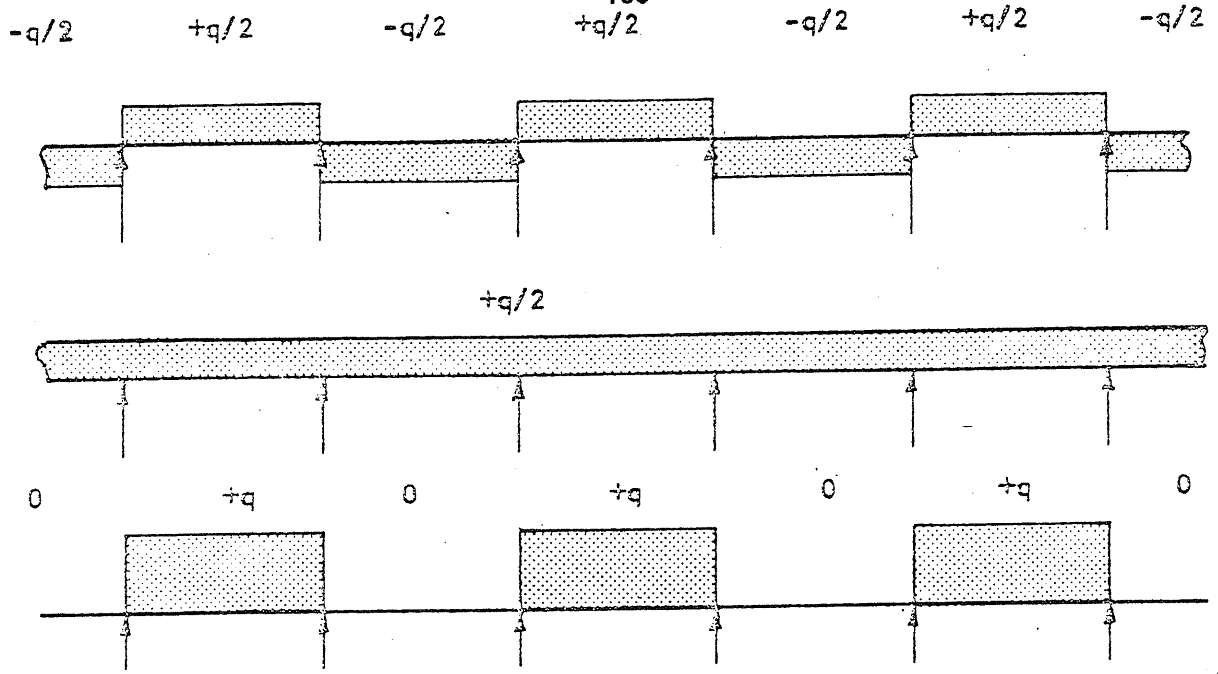

(a) Superposition of Loading Conditions to Obtain Maximum Positive Moments

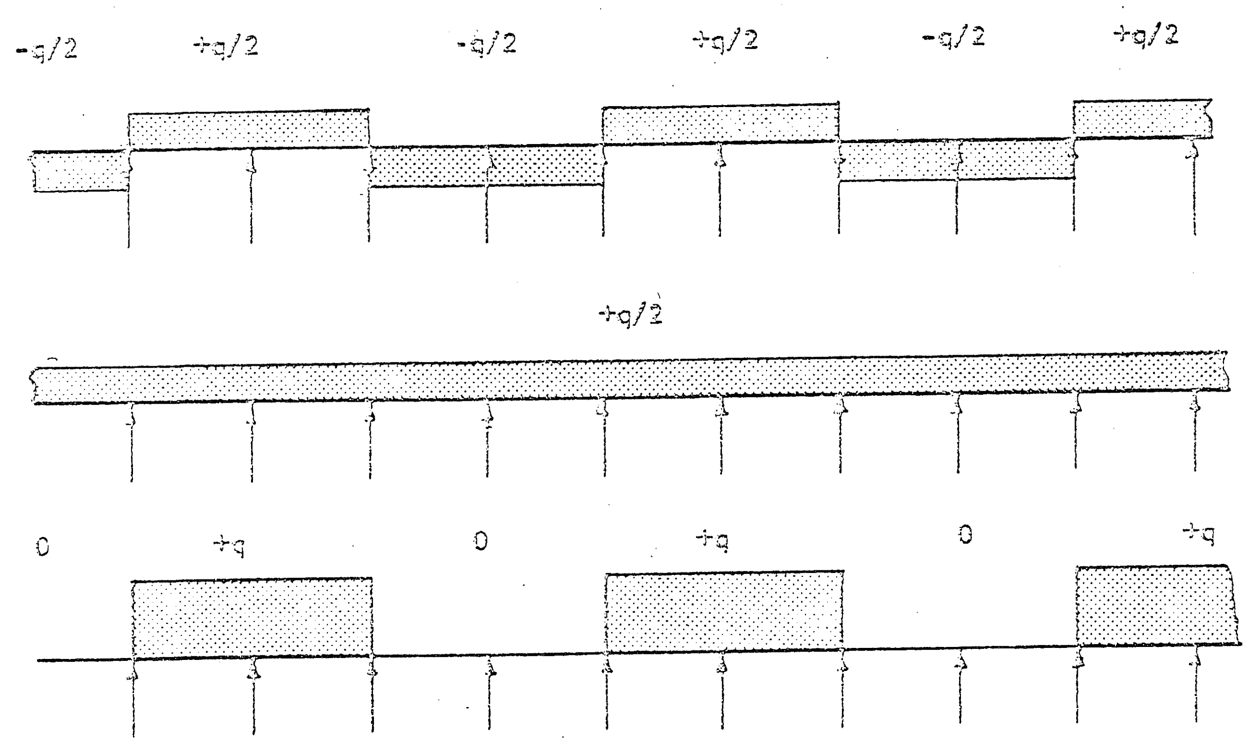

(b) Superposition of Loading Conditions to Obtain Maximum Negative Moments

FIG. 4.2 SUPERPOSITION OF LOADING CONDITIONS TO OBTAIN MAXIMUM MOMENT LOADINGS

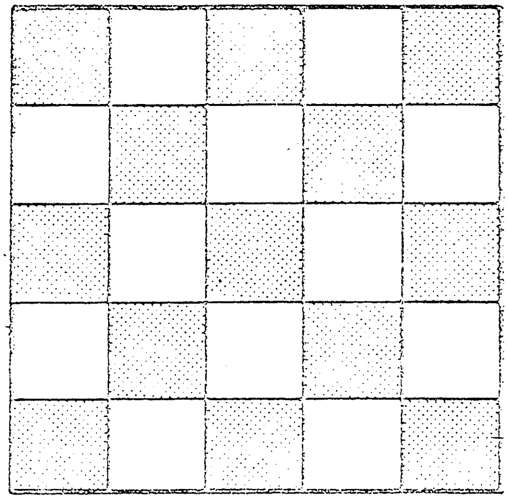

(a) Checkerboard Loading Pattern for Maximum Positive Moments

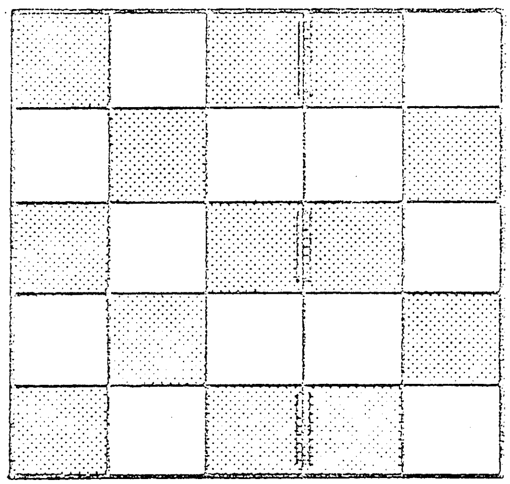

(b) Checkerboard Loading Pattern for Maximum Negative Moments

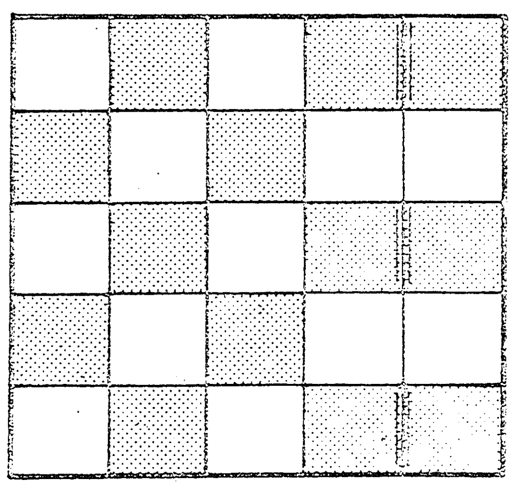

(c) Checkerboard Loading Pattern for Maximum Negative Moments

FIG. 4.3 CHECKERBOARD LOADING PATTERNS FOR SLABS WITH H = ∞

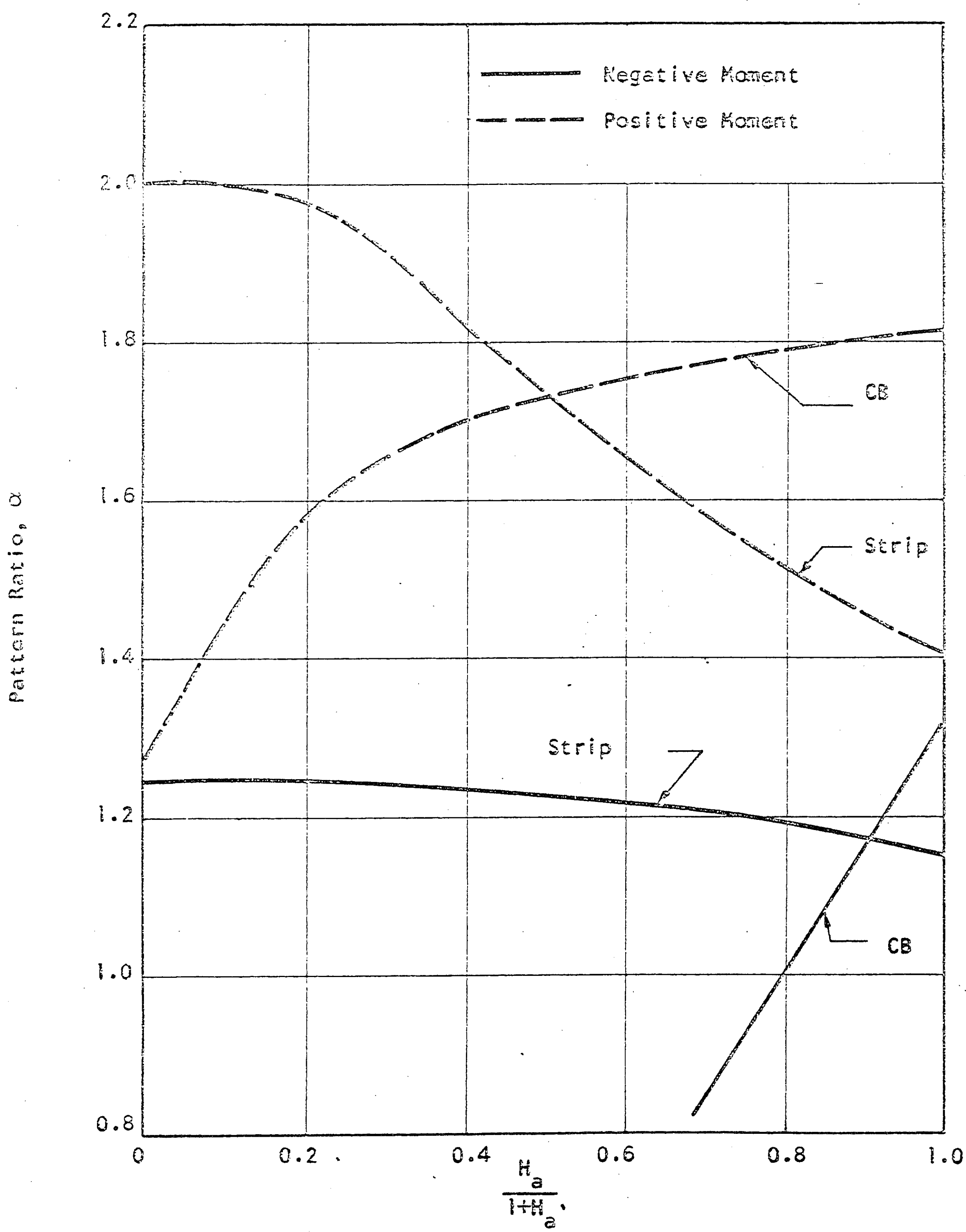

FIG. 4.4 PATTERN RATIO VS. BEAM FLEXURAL STIFFNESS, a/b = 0.5, J = K = 0

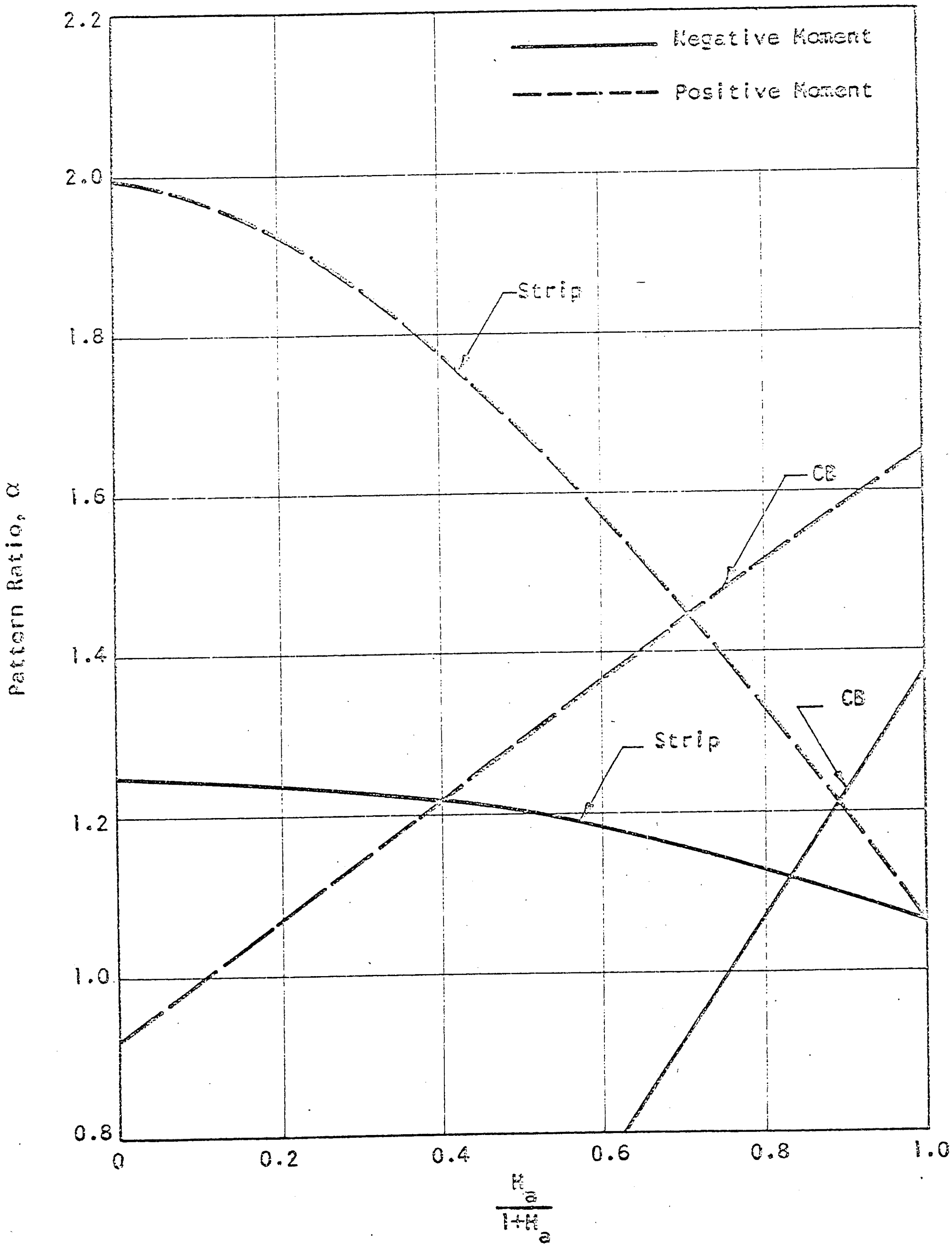

FIG. 4.5 PATTERN RATIO VS. BEAM FLEXURAL STIFFNESS, a/b = 0.8, J = K = 0

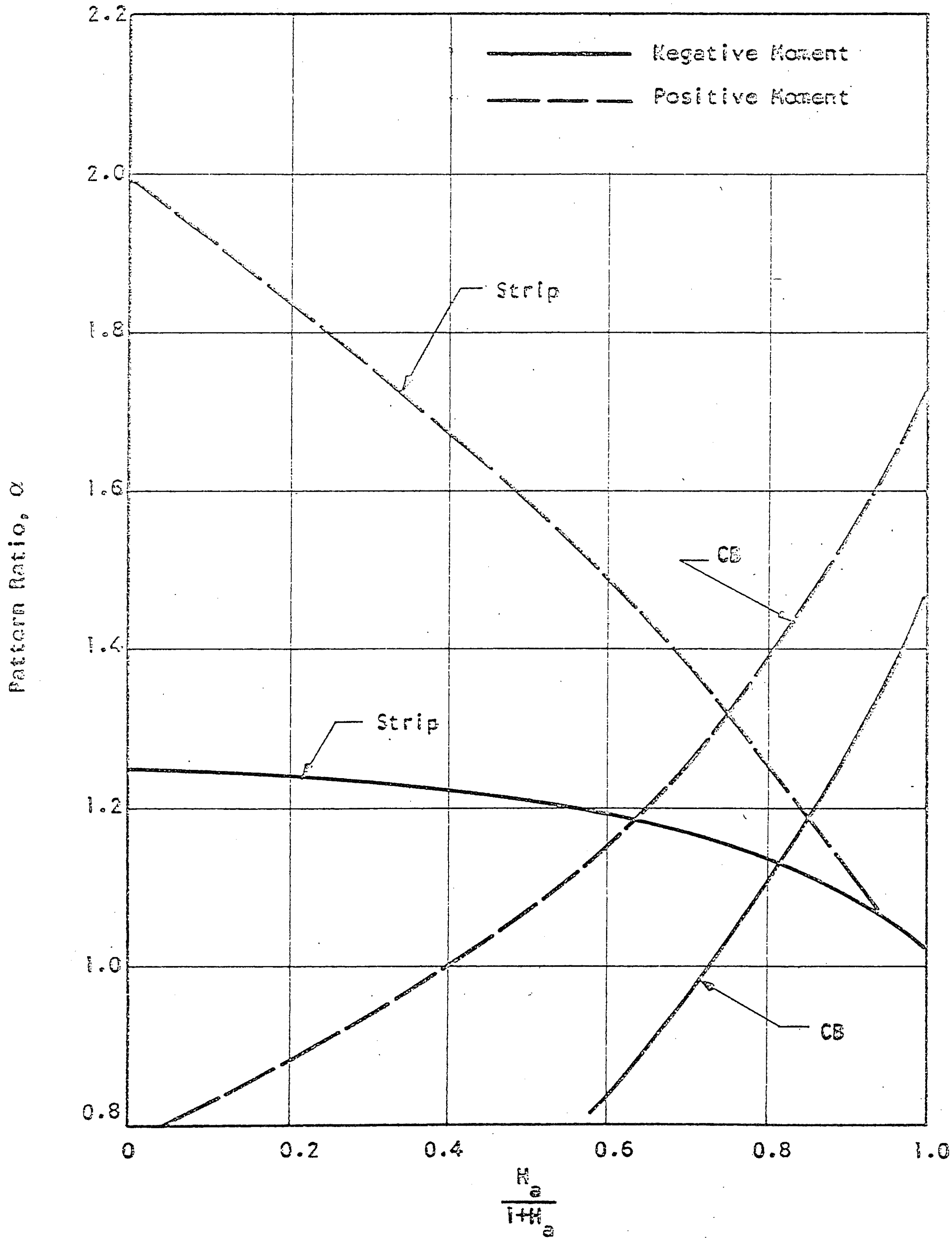

FIG. 4.6 PATTERN RATIO VS. BEAM FLEXURAL STIFFNESS, a/b = 1.0, J = K = 0

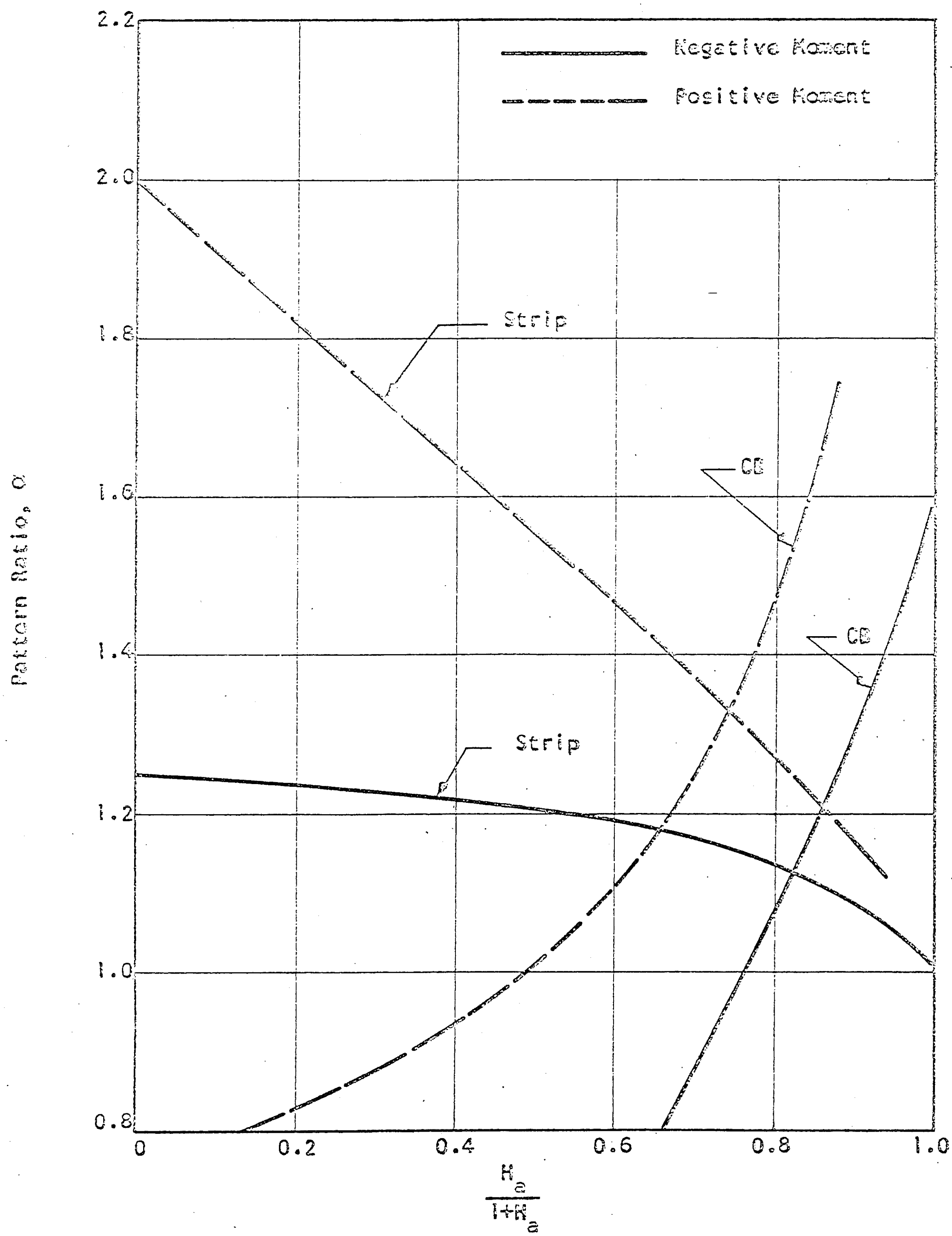

FIG. 4.7 PATTERN RATIO VS. BEAM FLEXURAL STIFFNESS, a/b = 1.25, J = K = 0

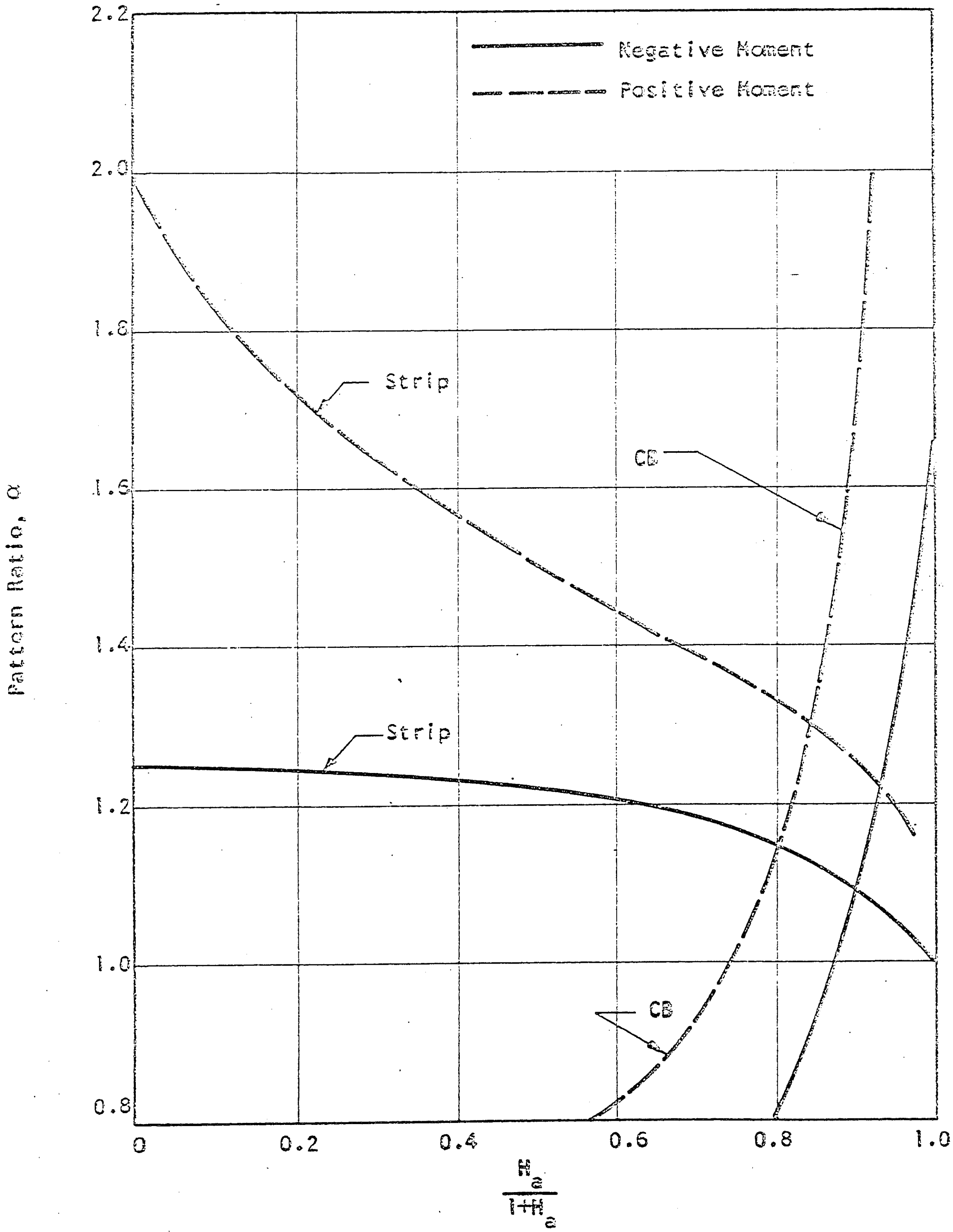

FIG. 4.8 PATTERN RATIO VS. BEAM FLEXURAL STIFFNESS, a/b = 2.0, J = K = 0

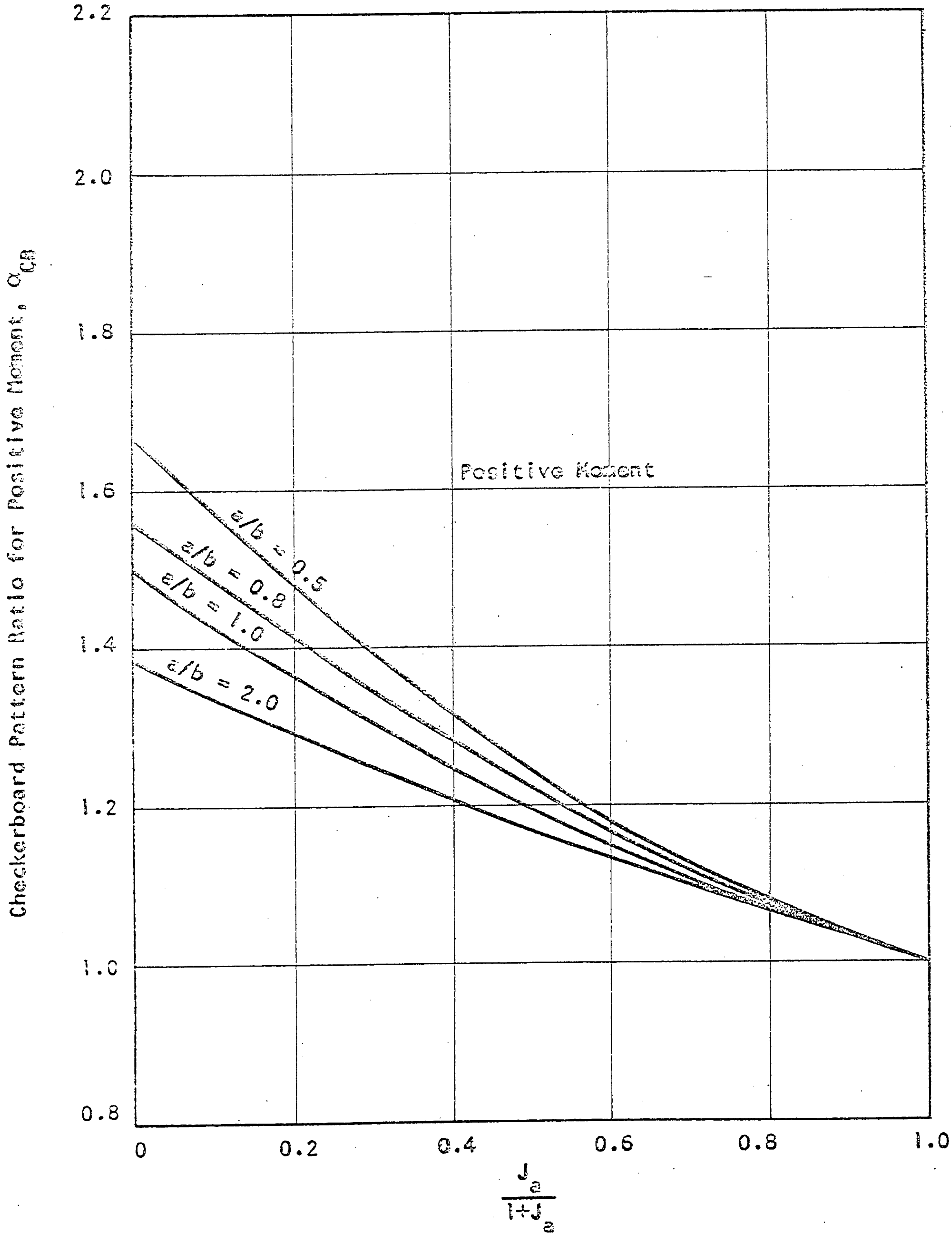

FIG. 4.9 CHECKERBOARD PATTERN RATIO FOR POSITIVE MOMENT VS. BEAM TORSIONAL STIFFNESS, K = 0, H = ∞

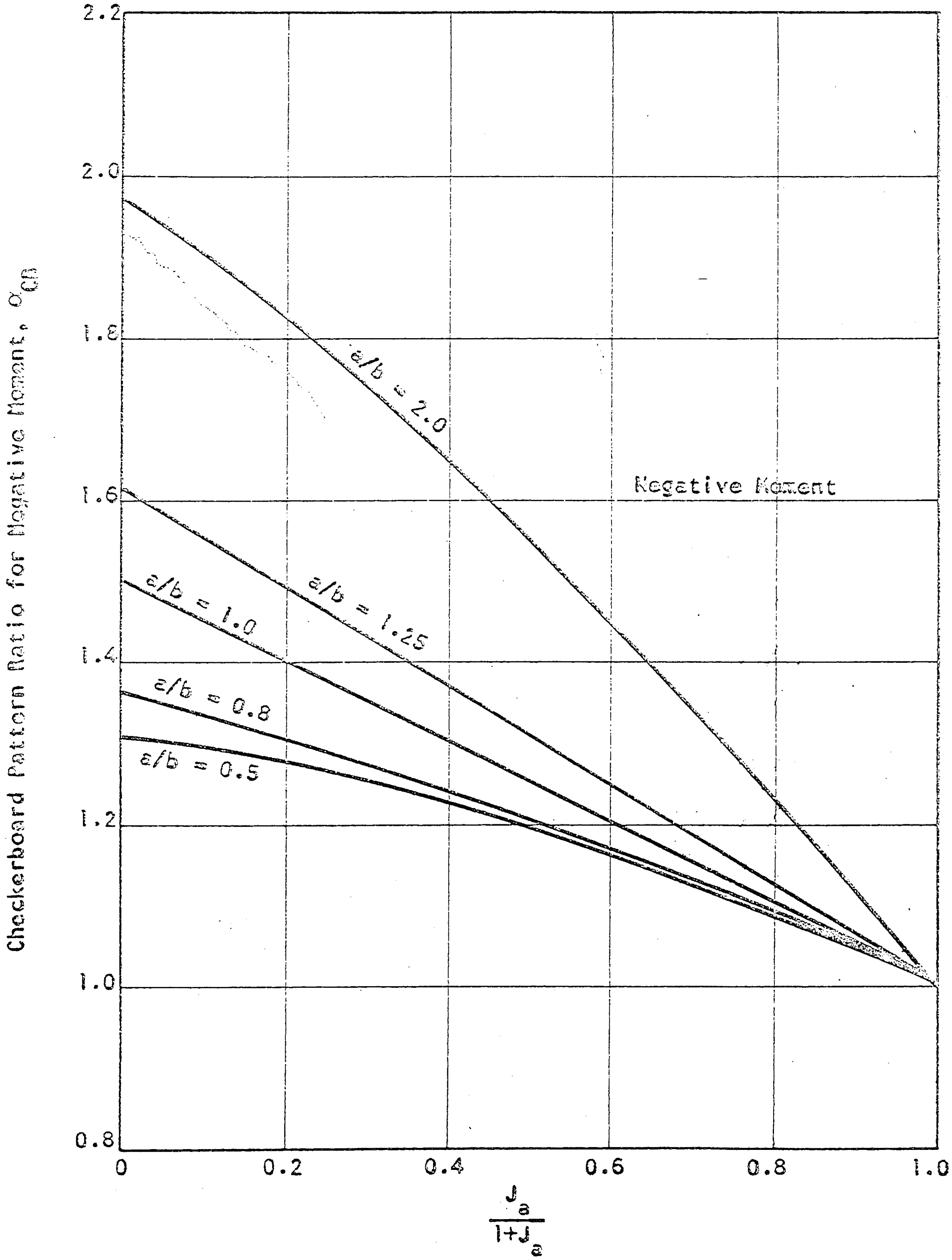

FIG. 4.10 CHECKERBOARD PATTERN RATIO FOR NEGATIVE MOMENT VS. BEAM TORSIONAL STIFFNESS, K = 0, H = ∞

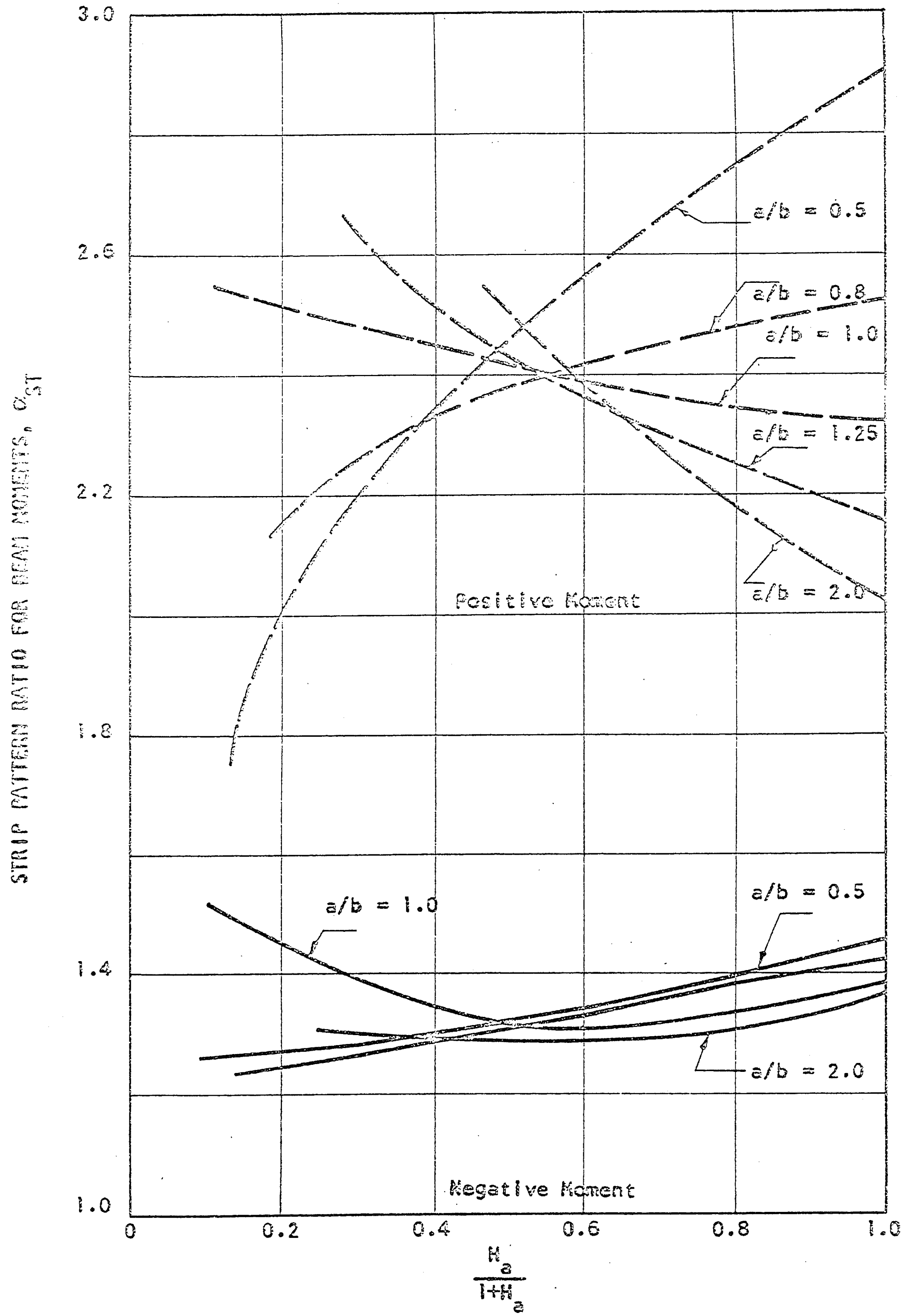

FIG. 4.11 STRIP PATTERN RATIO FOR BEAM MOMENTS VS. BEAM FLEXURAL STIFFNESS, J = K = 0

Direction of Moments

Wall Strip	Middle Strip	Column Strip	Middle Strip	Column Strip	Middle Strip
0.026	0.008	0.033	0.008	0.033	0.008
0.024	0.017	0.026	0.017	0.026	0.017
0.037		0.042		0.042	
	0.015		0.015		0.015
0.037		0.038		0.038	
0.012	0.013	0.018	0.013	0.018	0.013
0.037		0.038		0.038	
	0.015		0.015		0.015
0.037		0.042		0.042	
0.024	0.017	0.026	0.017	0.026	0.017
0.023	0.017	0.027	0.017	0.027	0.017

Note: Moments in terms of M/qa^3

FIG. 5.1 DESIGN MOMENTS FOR STRUCTURE F1

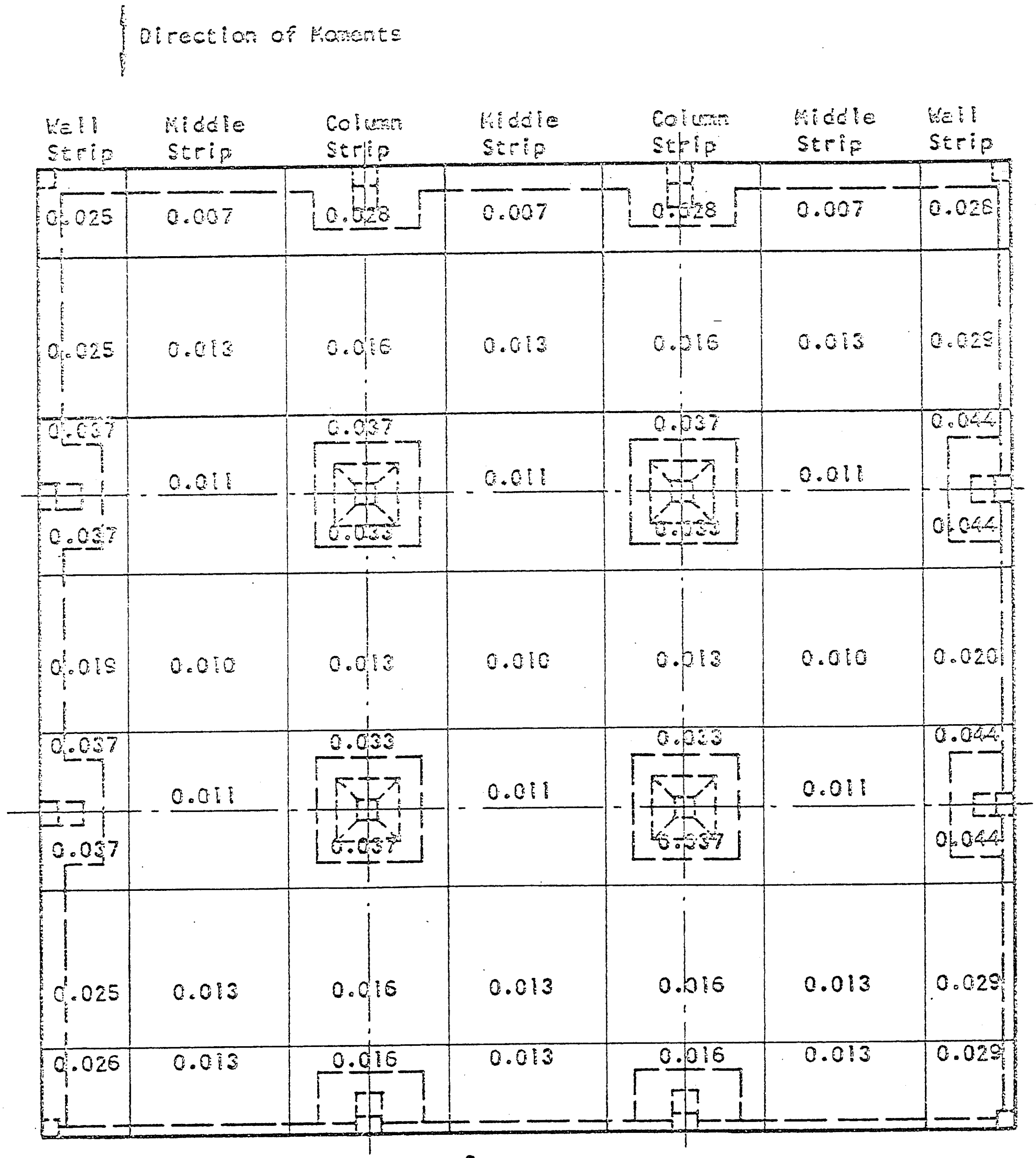

Note: Moments in terms of M/qa^3

FIG. 5.2 DESIGN MOMENTS FOR STRUCTURES F2 AND F3

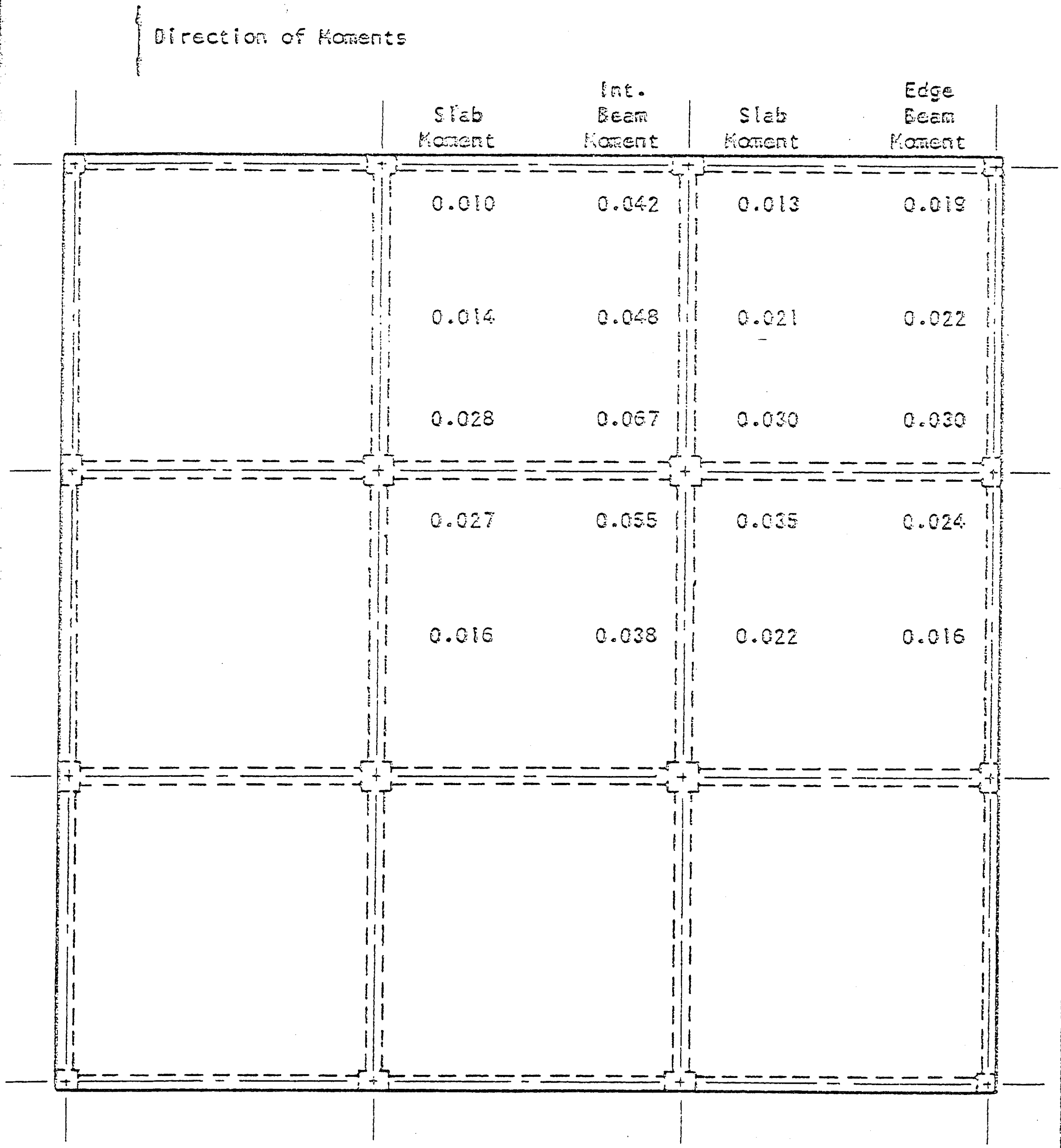

Note: Moments in terms of M/qa^3

FIG. 5.3 DESIGN MOMENTS FOR STRUCTURE T1

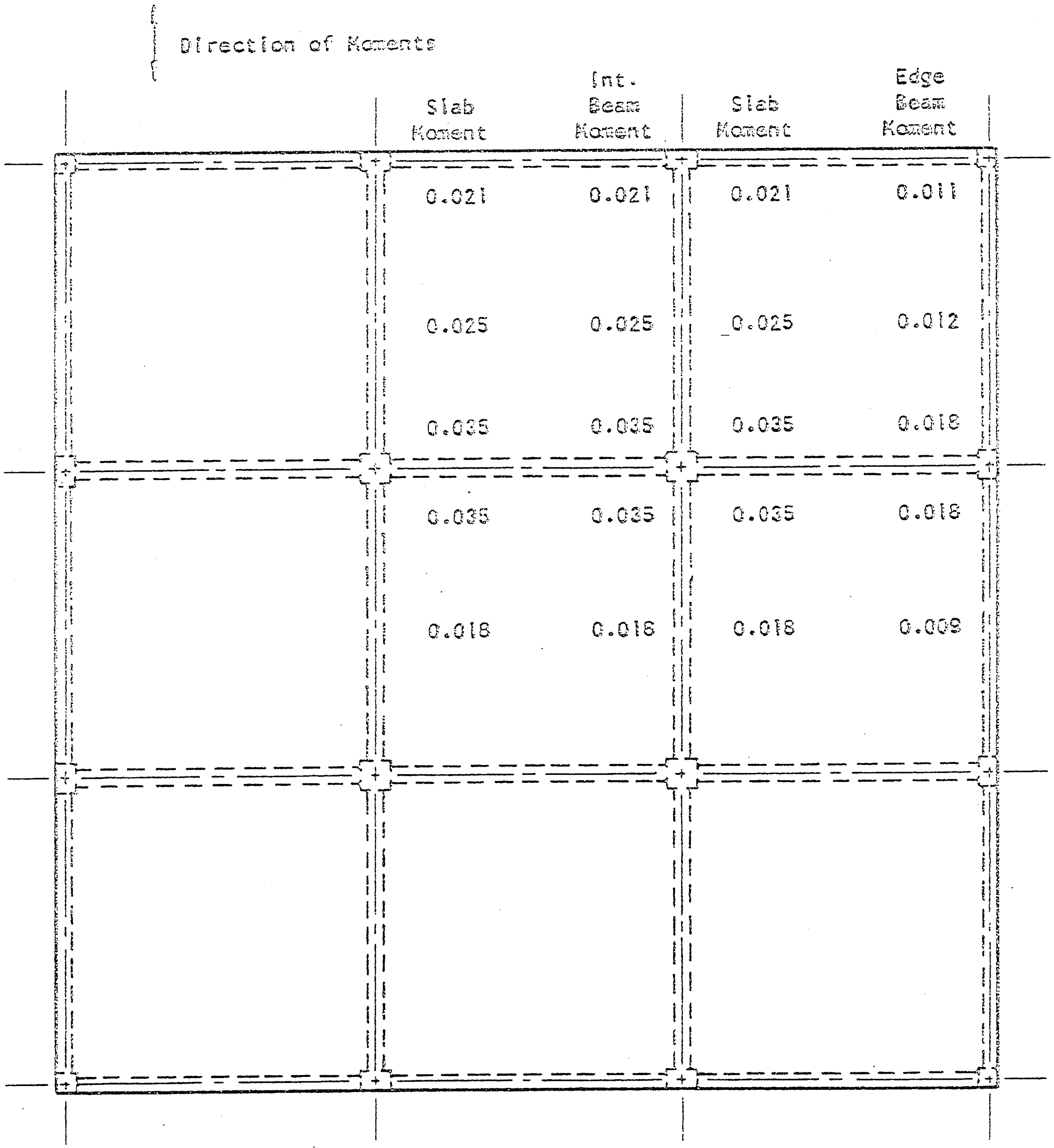

Note: Moments in terms of M/qa^3

FIG. 5.4 DESIGN MOMENTS FOR STRUCTURE T2

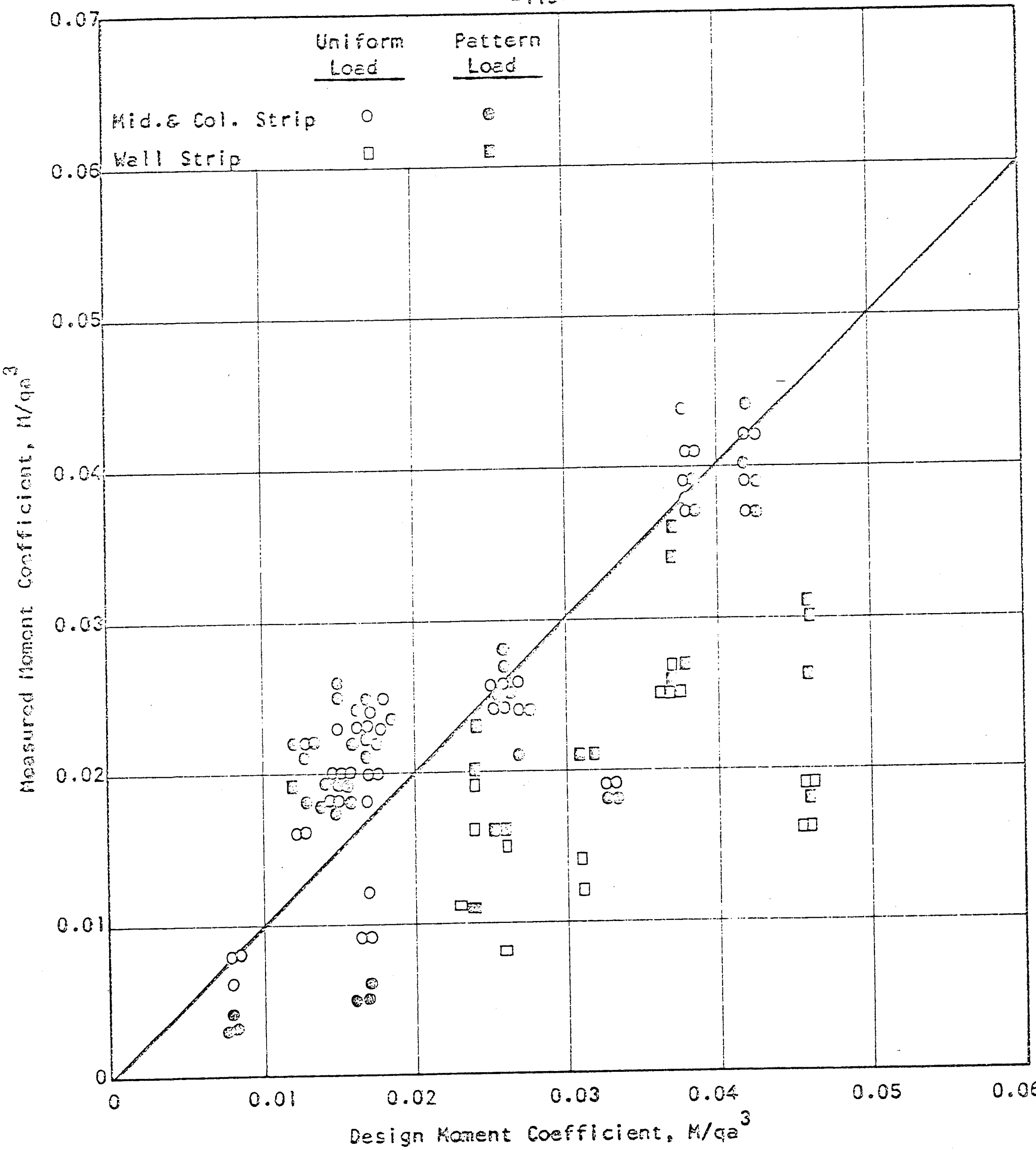

FIG. 5.5 COMPARISON OF DESIGN AND MEASURED MOMENTS IN STRUCTURE F1

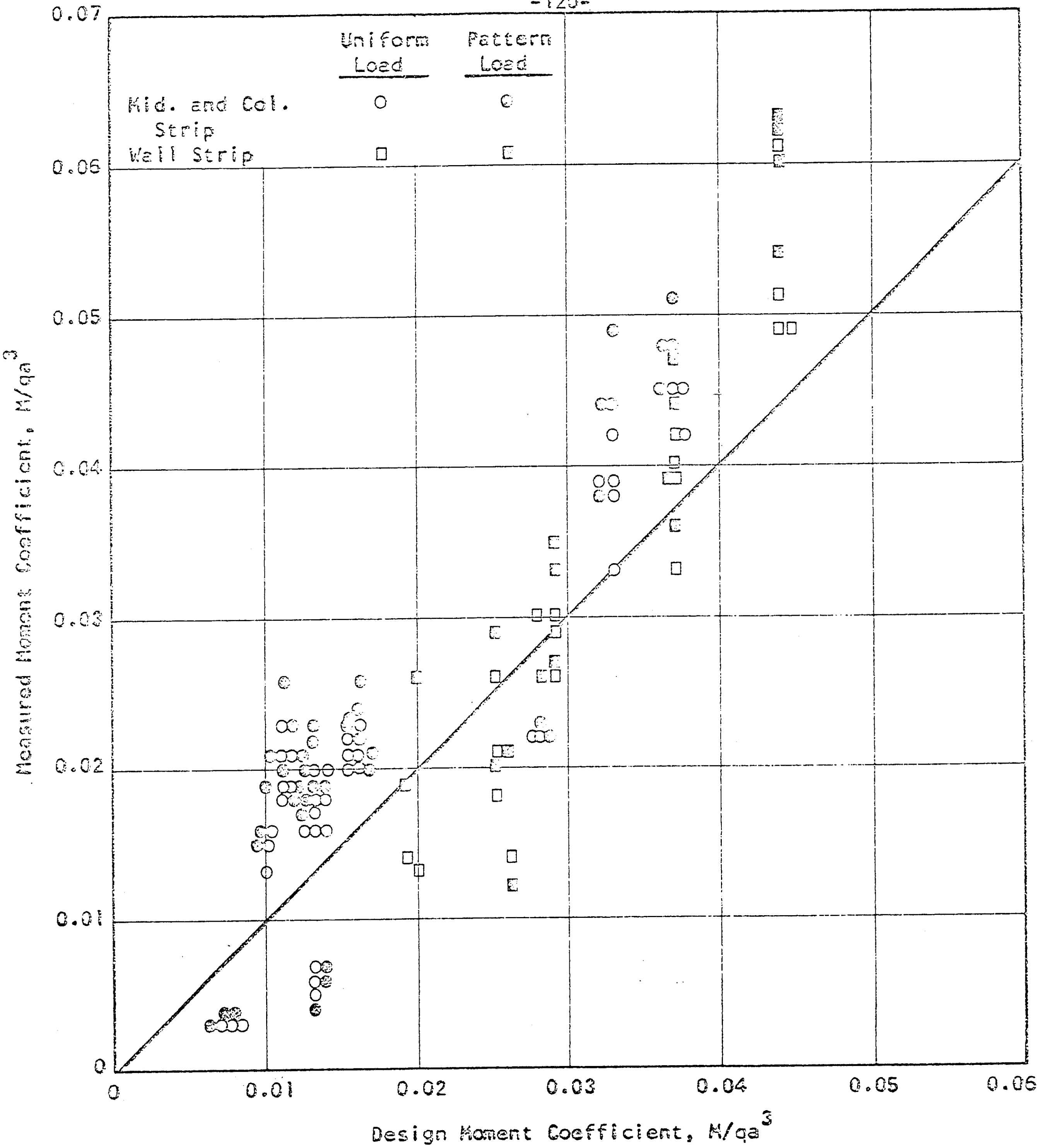

FIG. 5.6 COMPARISON OF DESIGN AND MEASURED MOMENTS IN STRUCTURE F2

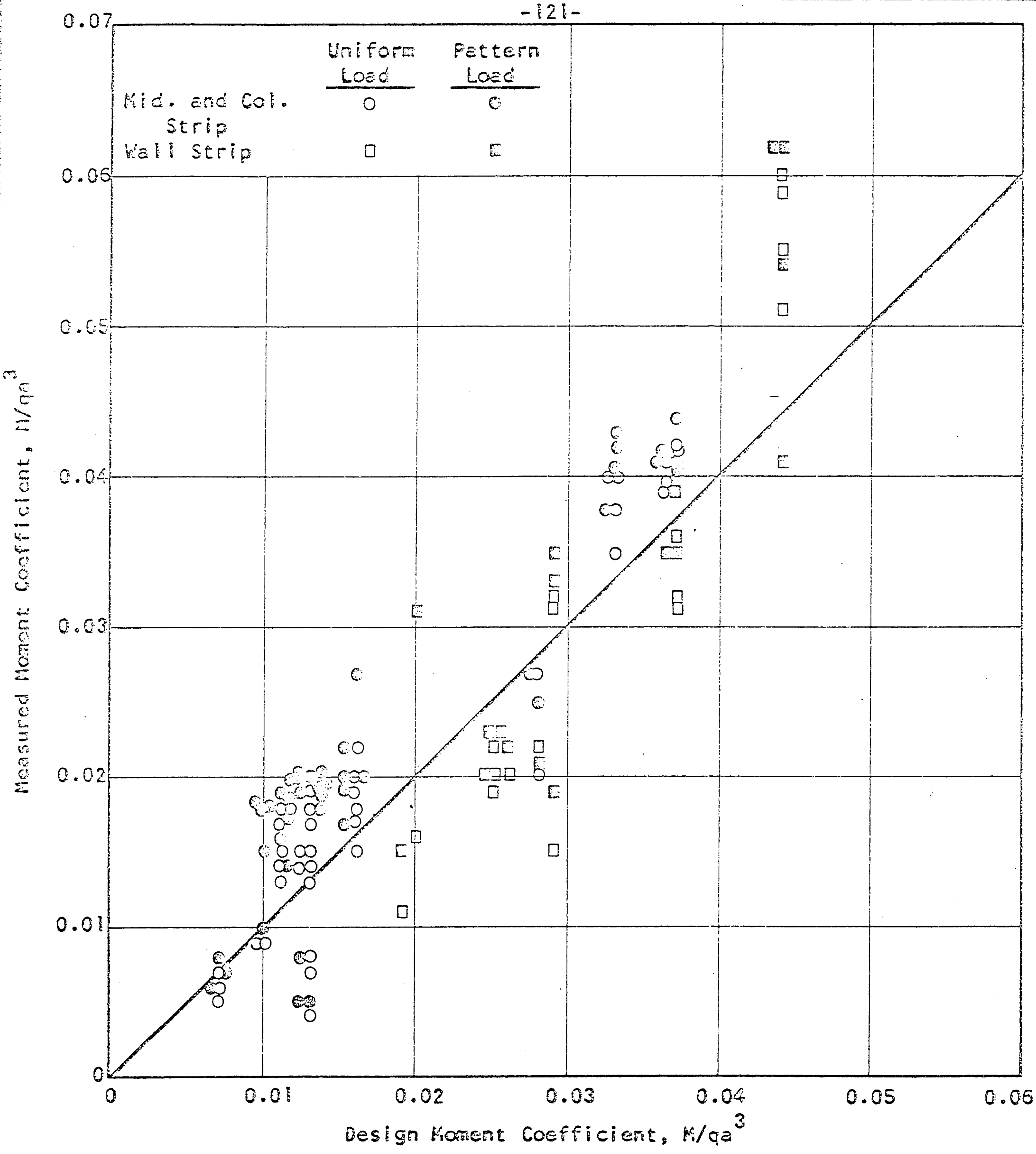

FIG. 5.7 COMPARISON OF DESIGN AND MEASURED MOMENTS IN STRUCTURE F3

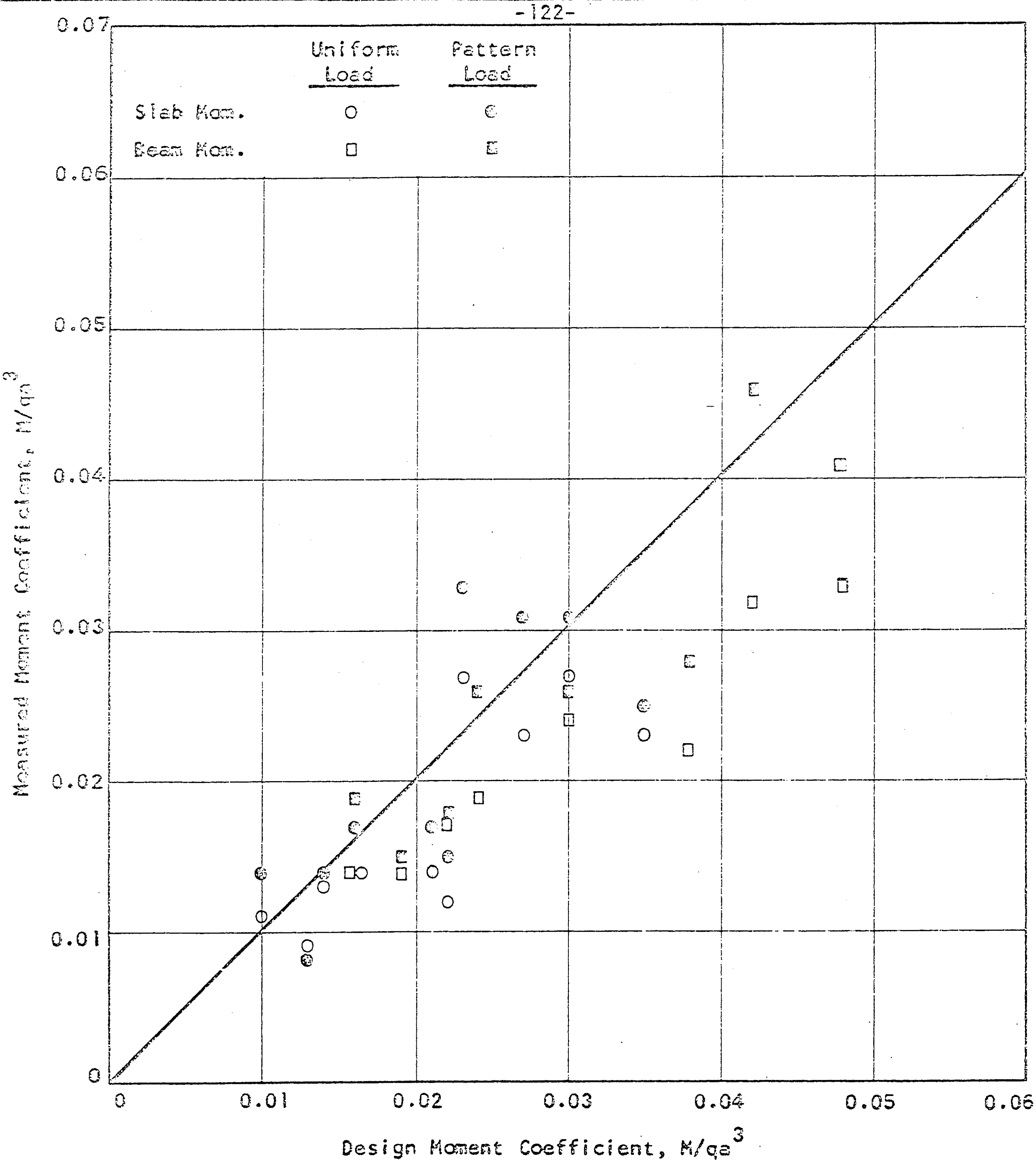

FIG. 5.8 COMPARISON OF DESIGN AND MEASURED MOMENTS IN STRUCTURE T1

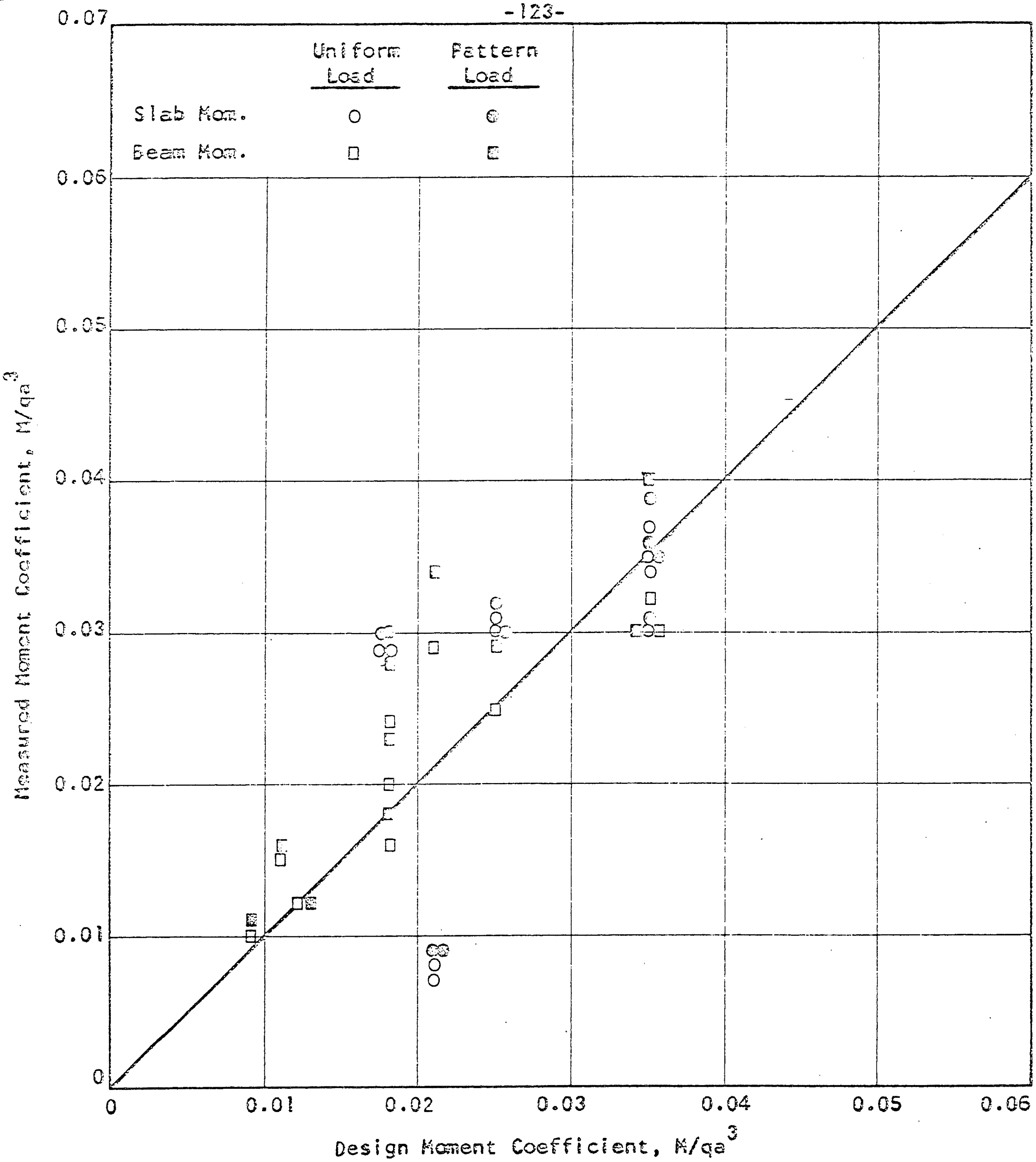

FIG. 5.9 COMPARISON OF DESIGN AND MEASURED MOMENTS IN STRUCTURE T2

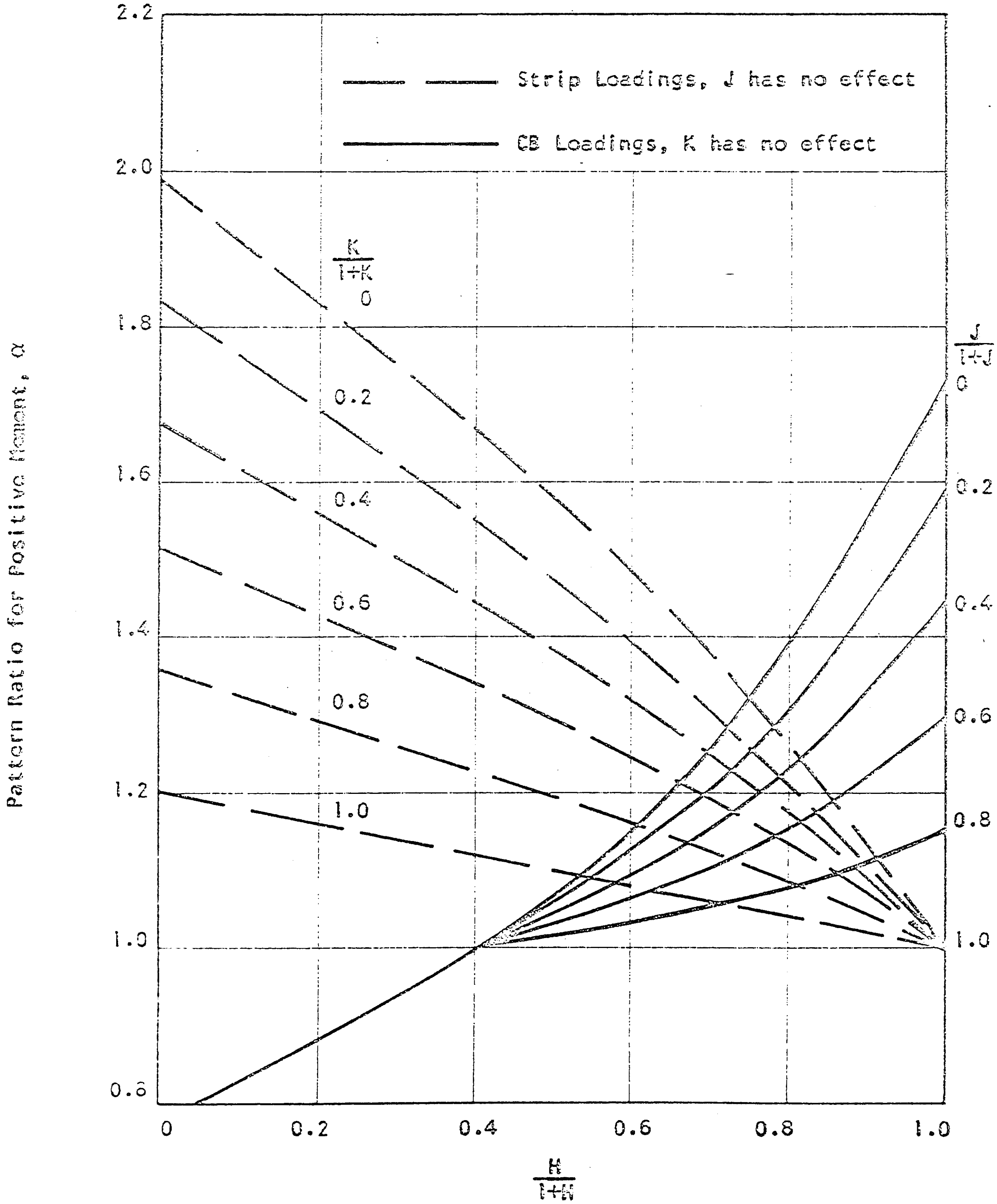

FIG. 6.1 VARIATION OF PATTERN RATIO FOR POSITIVE MOMENT WITH H, J, and K

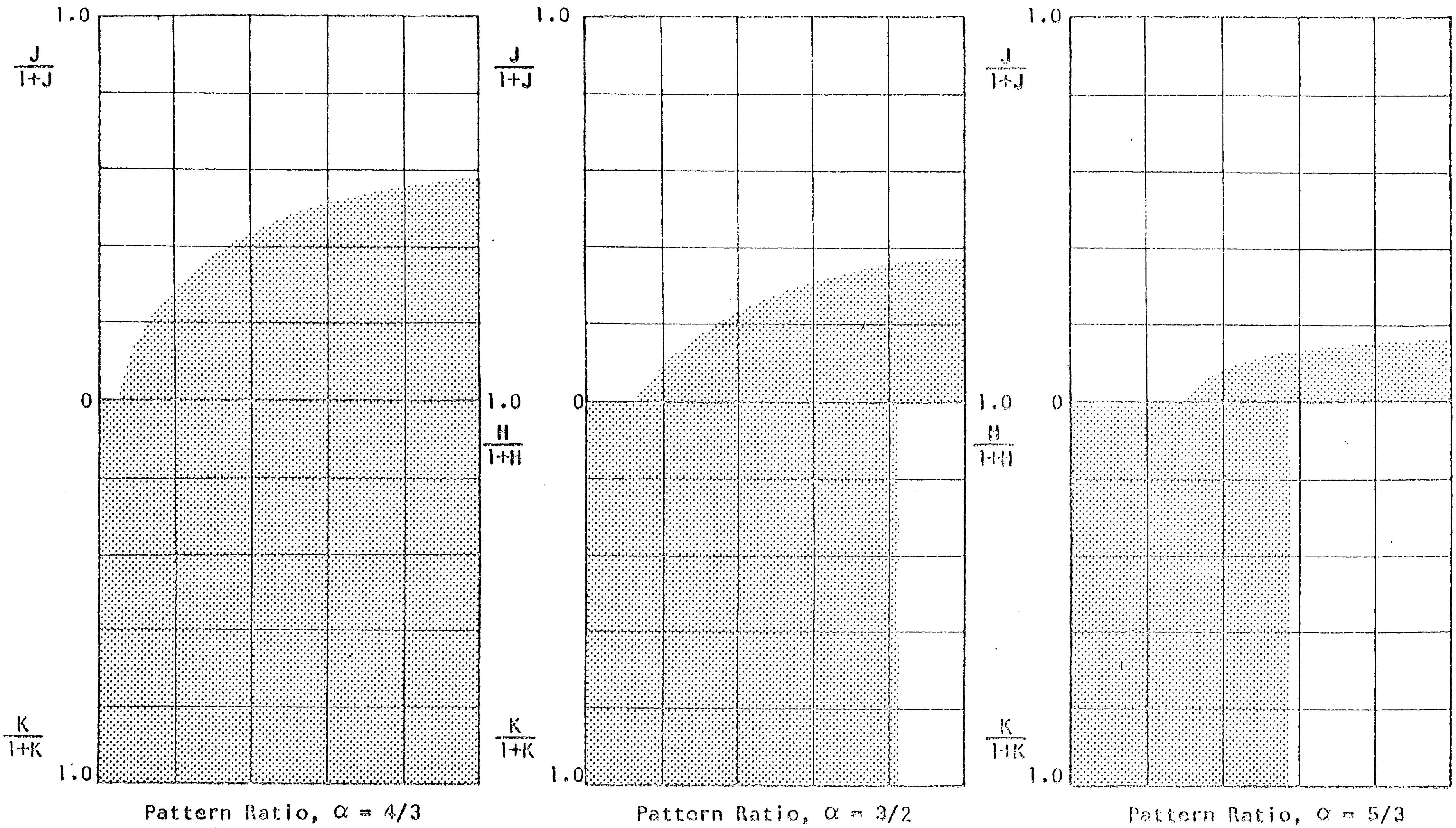

FIG. 6.2 COMBINATIONS OF STIFFNESS PARAMETERS SATISFYING SELECTED PATTERN RATIOS, a/b = 0.5

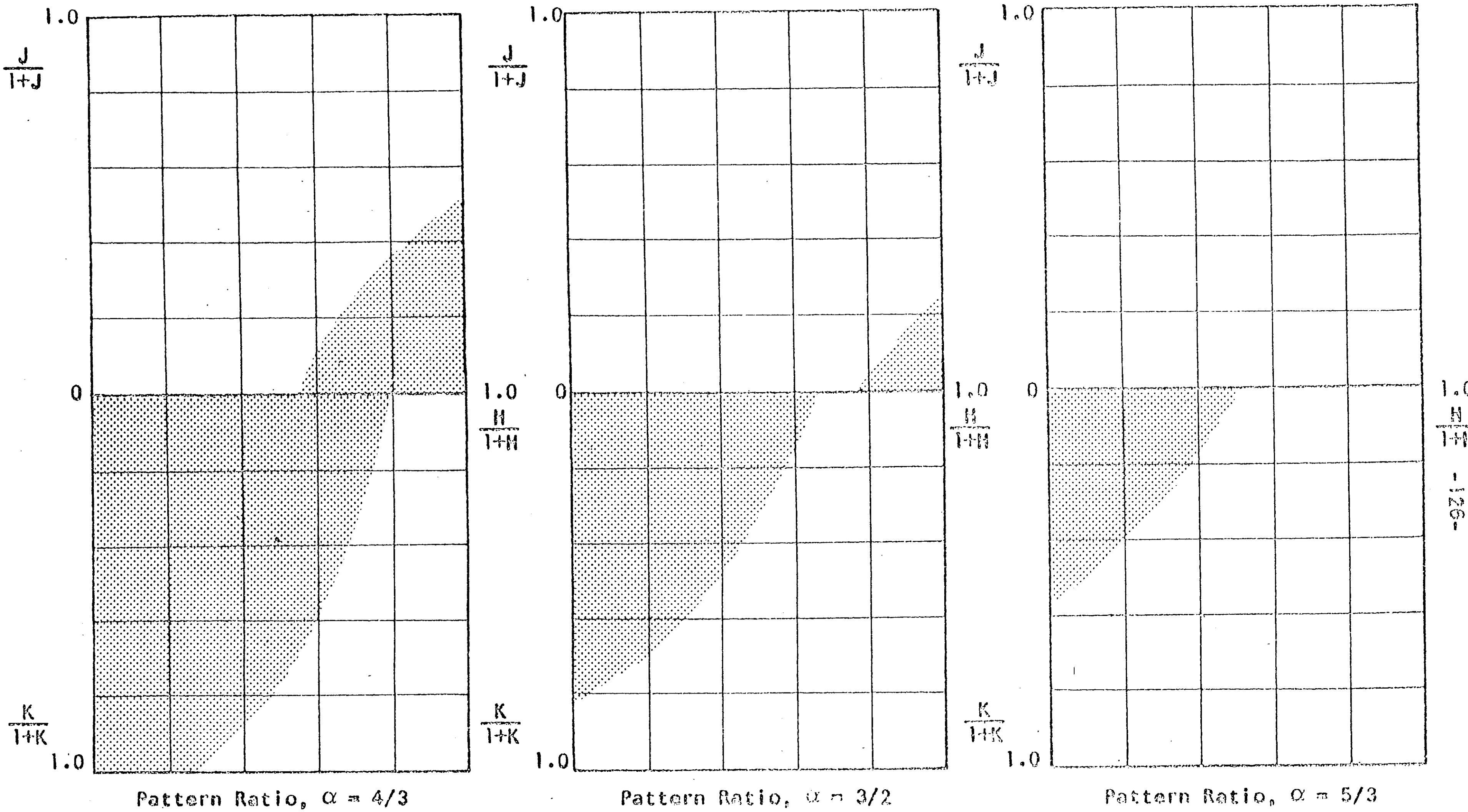

FIG. 6.3 COMBINATIONS OF STIFFNESS PARAMETERS SATISFYING SELECTED PATTERN RATIOS, a/b = 0.8

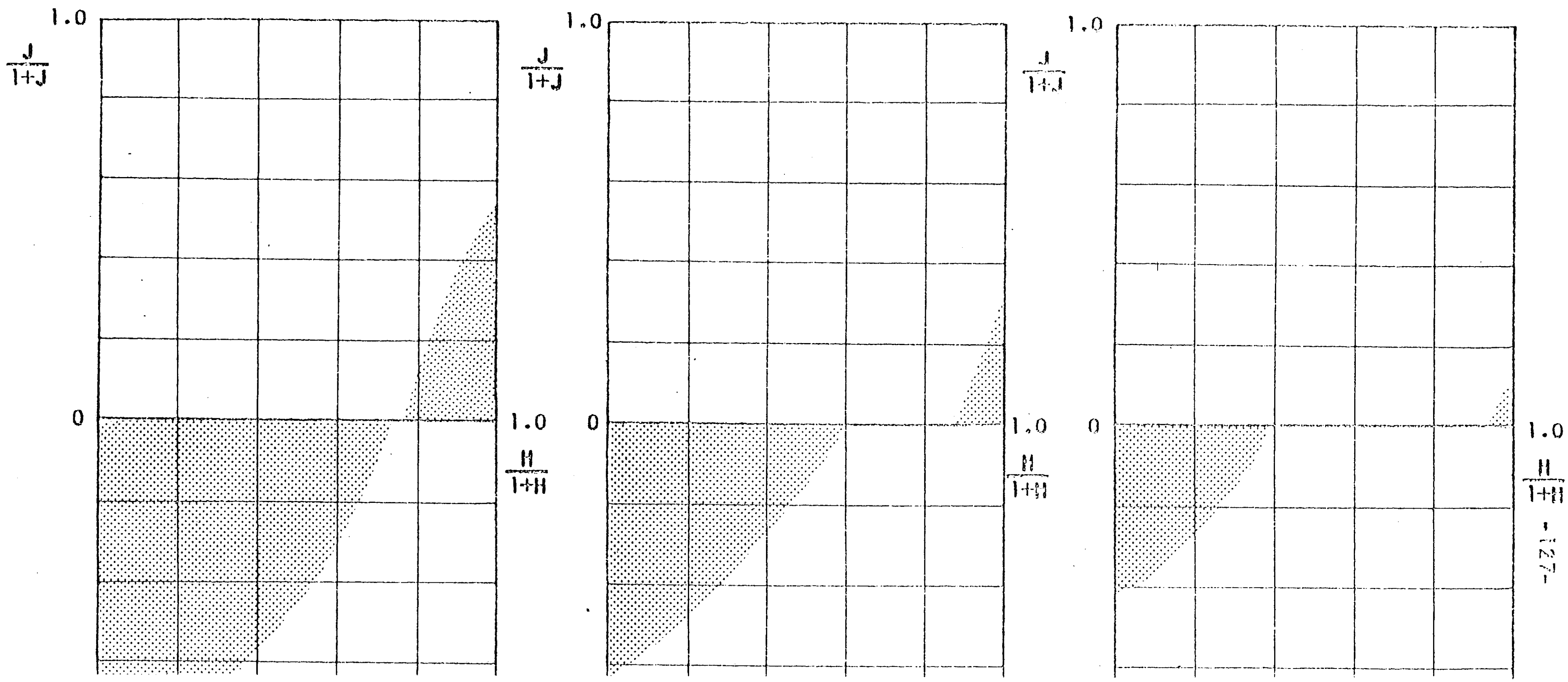
1.0
J/(1+J)
0
1.0
H/(1+H)
1.0
J/(1+J)
0
1.0
H/(1+H)
1.0
J/(1+J)
0
1.0
H/(1+H)

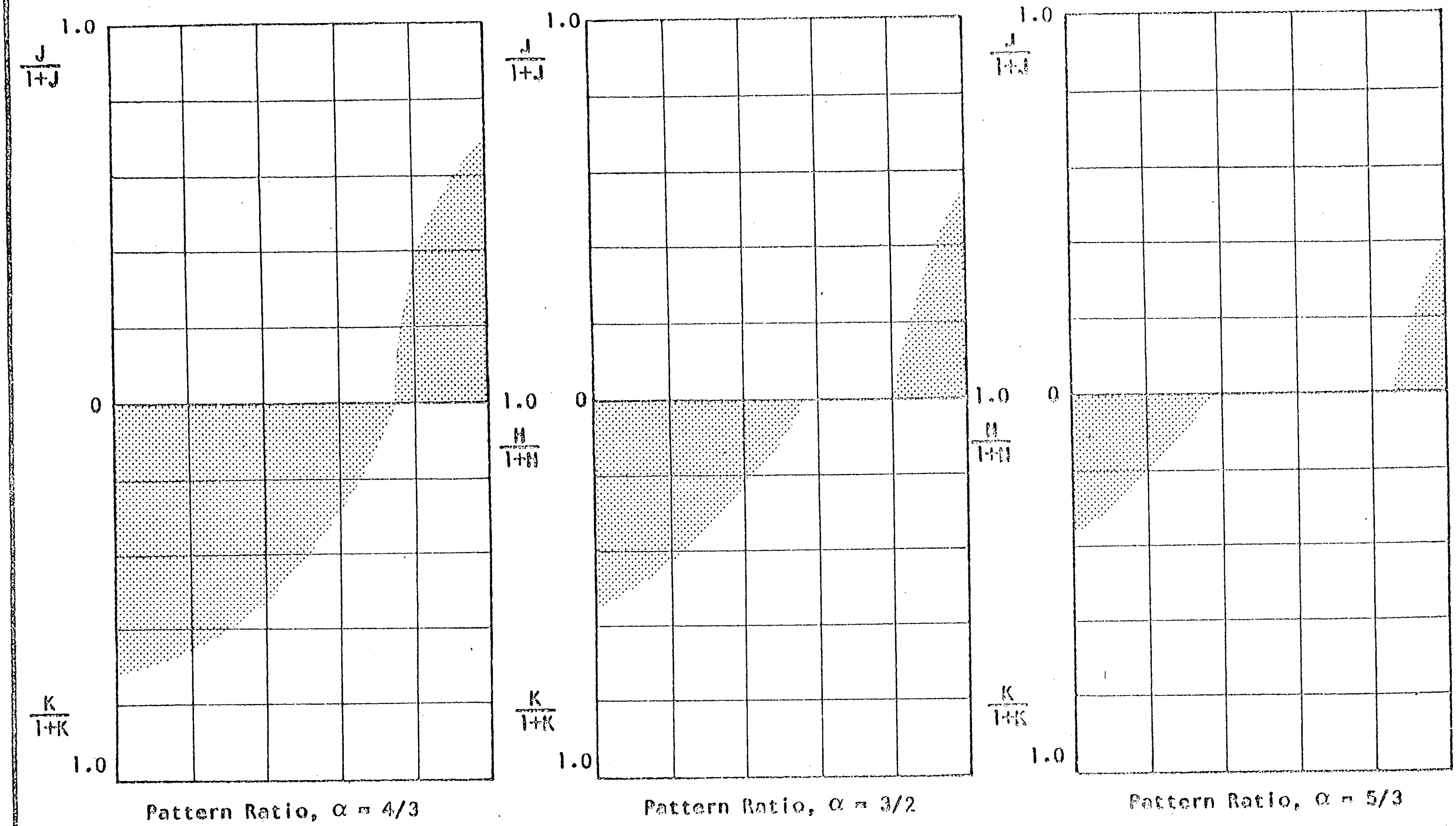

FIG. 6.5 COMBINATIONS OF STIFFNESS PARAMETERS SATISFYING SELECTED PATTERN RATIOS, a/b = 1.25

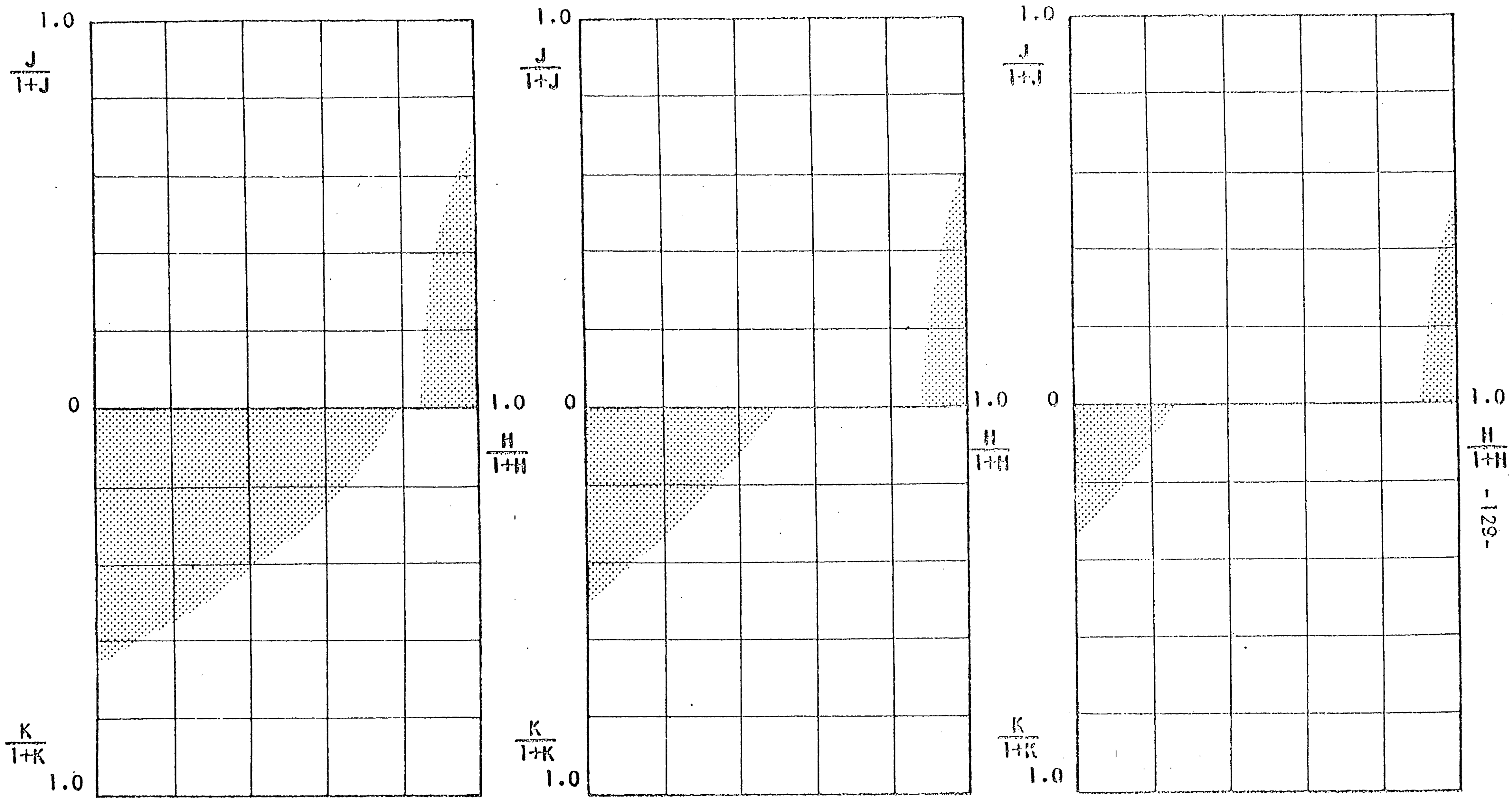

Pattern Ratio, $\alpha = 4/3$ Pattern Ratio, $\alpha = 3/2$ Pattern Ratio, $\alpha = 5/3$

FIG. 6.6 COMBINATIONS OF STIFFNESS PARAMETERS SATISFYING SELECTED PATTERN RATIOS, a/b = 2.0

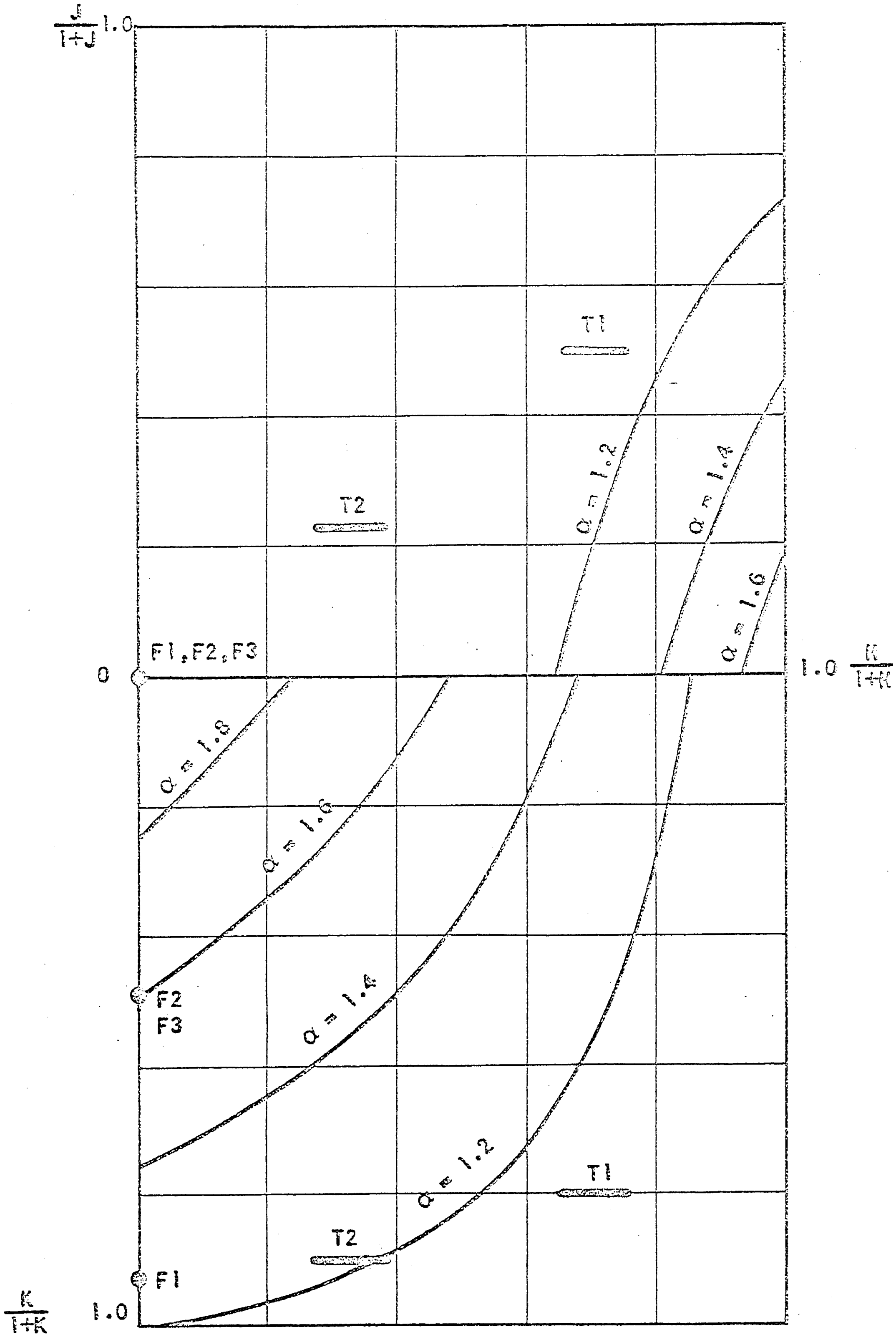

FIG. 6.7 ESTIMATED EFFECTS OF PATTERN LOADS ON THE TEST STRUCTURES

APPENDIX A

FRAME ANALYSIS

A.1 Background

The simplification of a three-dimensional slab to a two-dimensional frame has been used for some time. The frame analysis appeared in the 1941 ACI Code as the "Elastic Analysis" but had been used prior to that time in analyzing and designing floor slabs.

The frame analysis as given in the ACI Code has several drawbacks. By assuming an infinite moment of inertia at the joints between the columns and slabs, the sections are given too great a stiffness. In reducing the negative moments to a critical section some distance from the column center-line, the advantage of a solution based on statics is lost and the moments revert to those used in the Empirical Method.

Corley (27) proposed a frame analysis which alleviated some of the problems in the ACI Code Elastic Analysis. However, the method proposed was not used to determine the effects of pattern loads and in that respect it had certain shortcomings.

The method proposed here is basically a modification of the analysis proposed by Corley. Several changes have been made in order to enable use for strip loadings and coverage of slabs supported on beams. The analysis was used to compute the moments in the five test structures and the results of this study are given in Tables A1, A2 and A3 where comparisons with the measured moments are included.

A.2 Procedure

The procedure is discussed in this section in general terms. It may be applied to flat slabs or flat plates, with or without drop panels and to two-way slabs. The figures are given for a flat slab which is the most complex case. Modifications to be made for various elements of other types of slabs are included in the pertinent discussion.

The first step in any frame analysis involves removing a section one panel wide from the slab structure as shown in Fig. A.1. The cross section of an interior bay of this frame is shown in Fig. A.1. The areas for the moments of inertia of the various sections along the frame are shown. The I/EI diagram for the slab may be used to determine moment distribution constants and fixed-end moments by normal procedures. For a two-way slab where a beam spans between columns the moment of inertia I_{AA} is computed on the basis of an assumed T-beam section. The flange dimensions are determined by a 45 degree line drawn from the bottom edge of the beam.

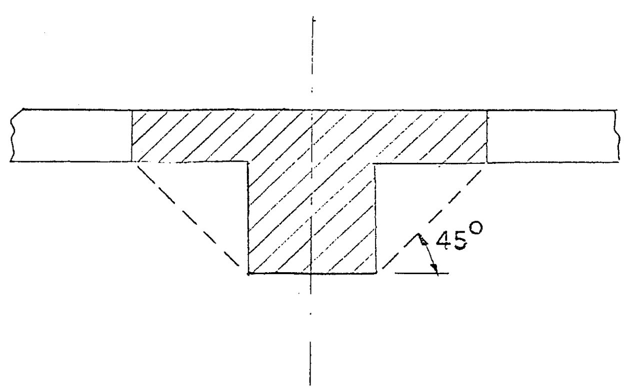

Assumed T-beam Section

Sketch A

It should be noted that the moment of inertia at the column (from the face of the column to the column center line) is based on the moment of inertia of the slab immediately surrounding the column. The moment of inertia at the column is given as $I_{CC} = I_{BB}/(1 - c_2/L_2)^2$. This relationship was established for two reasons. It increases the moment of inertia at the column while maintaining it at a level considerably less than assumed in the ACI Code. The equation also covers the condition of a slab monolithic with very wide columns. The maximum condition of a wall $c_2/L_2 = 1.0$ is covered since $I_{CC} = \infty$ in that case.

The computation of stiffnesses for the columns is considerably more involved. It was shown in Chapter 4 that the positive moment in a slab increases under strip loads even if rigid columns are used. In a frame with infinite column stiffness, no change would be computed. Therefore, it was necessary to consider the section at the columns as a beam-column combination in which the beam across the column could rotate even though the column was infinitely stiff. The resulting section may be likened to a "hammerhead."

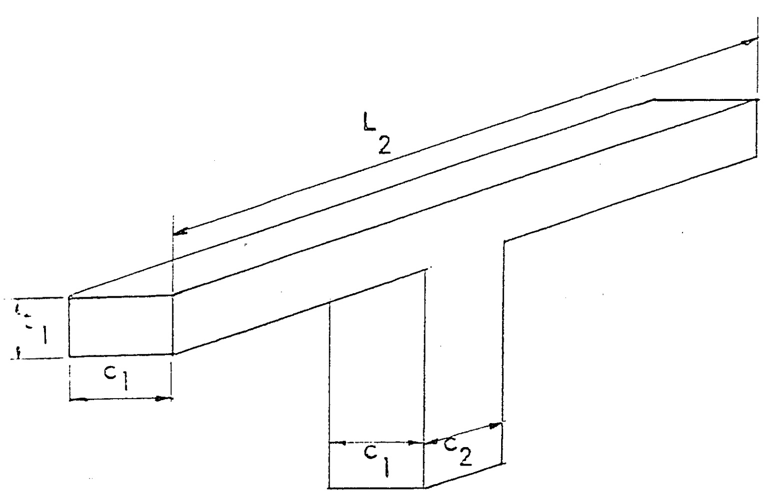

Sketch B

In the case of an edge beam, such a section is quite obvious. Some of the moment is transferred from the slab directly to the column and the remainder is transferred first to the beam and then to the columns. It can be seen that a rigid column does not preclude the rotation of the beam with respect to the columns.

In order to determine the stiffness of this beam-column combination, according to the Cross distribution procedure the following equation is used.

$$K_{bc} = \frac{m_1}{\theta_f + \theta_t} \tag{A.1}$$

where K_{bc} = stiffness of the beam-column combination

m_1 = a distributed torque applied along the axis of the beam

θ_f = total rotation of the end of the column due to bending in the column

θ_t = average rotation, due to twisting, of the beam with respect to the column.

The stiffness of the column can be determined by Eq. A.1 if m_1, θ_f and θ_t are known.

The value of θ_f is independent of the distribution of torque along the beam or the beam torsional stiffness since the total applied torque ultimately is resisted by the column. The moment of inertia of the column is computed on the basis of gross cross section below the capital (if one exists) and then varies linearly from the base of the capital to the base of the slab where it is infinity. It is infinitely stiff from the base of the slab to the center of slab ($t_1/2$ or $t_2/2$ if a drop panel is used).

The computation of θ_t requires several simplifying assumptions. The twisting moment (applied by the slab) is assumed to be triangularly distributed along the beam. If no beam frames into the column, a portion of the slab equal to the width of the column is assumed to offer the torsional resistance. If a beam frames into the column, T-beam action is assumed as shown in Sketch A. The portion of the beam directly above the column or capital is assumed to undergo no rotation.

The method of determining the value of θ_t is illustrated in Fig. A.2. The beam-column combination is shown in Fig. A.2a. The length L_2 is the distance between column center lines. The unit twisting moment is applied according to a triangular distribution along the column center-line. A triangular distribution is used since the moment in the slab tends to be attracted toward the stiffest section which is the column. The twisting moment diagram is parabolic as shown in Fig. A.2c. Once the twisting moment is known at each section the unit rotation diagram can be expressed by the equation $\Phi = T/CG$. and for the beam in this case the expression is

$$\Phi = \frac{(1 - c_2/L_2)^2}{2\,\Sigma\,\lambda b_1 h_1^3}\,\frac{T}{G}$$

where Φ = angle of twist per unit of length

T = twisting moment

λ = a constant which is a function of the cross section

b_1 = the length (the larger dimension) of each rectangular section of the beam

h_1 = the height (the smaller dimension) of each rectangular section of the beam

Σ = summation of all rectangular sections

G = shearing modulus of elasticity, $G = \frac{E}{2(1+\mu)}$, $\mu = 0$ for concrete.

For the beam-column combination shown in Fig. A.2a the average effective angle of rotation is taken as one-third the area of one of the parabolas shown in Fig. A.2d. This yields the following expression for θ_t.

$$\theta_t = \frac{L(1 - c_2/L_2)^3}{36\ G\Sigma\ \lambda\ b_1 h_1^{\ 3}}$$

The section constant $C = \Sigma\ \lambda\ b_1 h_1^{\ 3}$ may be evaluated by dividing the T-beam section into rectangular parts which can then be considered separately. This may result in a small error but is sufficiently accurate for this procedure. A chart has been given in Fig. A.3 for determining λ as a function b_1/h_1. (Taken from Reference 28).

After the values of θ_f and θ_t have been computed the stiffness K_{bc} can be determined and the distribution constants and fixed-end moments are now known for the frame. The moments at the column center lines on the line frame can be determined.

Since the columns have finite dimensions, it is necessary to reduce the negative moments to the critical or design sections. To do this, an assumption must be made concerning the shear distribution. Satisfactory results are obtained if the shear is assumed to be distributed uniformly about the perimeter of the supports. In the case of a flat slab the shear is uniformly distributed around the periphery of the capital and in a two-way slab it is uniformly distributed along the face of the beam and column. The center of reaction is taken as the critical section and the moments are corrected to the center of reaction from the column center line.

It should be pointed out that this method was developed primarily for an interior strip of panels. However, the necessary assumptions have been given which may be extended for analysis of a wall strip having a width of one-half panel. Due to the lack of symmetry and the additional torsional and flexural deformations of an edge beam, the results may be less satisfactory.

A.3 Comparison of Measured Moments With Frame Analysis

The procedure outlined in the preceding section was applied to an interior strip (one-panel width) of each of the five test structures. The results of the procedure were compared with the measured moments in these strips to determine whether the increase in moment due to strip loads and the absolute moment at the critical sections could be estimated.

The measured uniform and strip load moments are given for each slab. The moment ratio γ is computed for both measured and computed moments. The value of β was taken into consideration in computing the moments. The values of measured moment in F1, F2 and F3 were obtained by combining middle and column strip moments. In the case of the two-way slabs, T1 and T2 the measured moments given for the interior strip were composed of the interior beam moments and the interior slab moments. Since no slab moments were obtained under strip loads in the two-way slabs, it was necessary to use the measured maximum beam moments in conjunction with the uniform load slab moments. It was felt that the strip load slab moments would have been approximately equal to the uniform load moments.

In making comparisons between absolute moments at a section, it must be remembered that the frame analysis is based on statics and the full static moment (the sum of positive and average negative moments) is always present in any given bay. The measured moments tended to be slightly less than the static moment in most bays. This is especially true in end bays where the exterior negative slab moment is difficult to analyze accurately. Therefore, the basic criterion for judgment is whether the frame analysis provides sufficient moment capacity at a section to deal with uniform or strip loads without excessive over-designing.

The moments in the interior strip of structure F1 are given in Table A1. A comparison of the moment ratios for measured and computed moments indicate that the frame analysis was quite accurate for pattern load effects. The computed absolute values of positive moments were nearly equal to the measured values. Negative moments were higher by the frame analysis than measured. However, it would appear that the total measured values may have been less than the static moment. Only at the exterior negative sections is there a serious discrepancy and it may be explained partially by a general reduction of stiffness due to cracking in the beam-column connection at the exterior column.

The moments in structures F2 and F3 are given in Table A2. It can be seen that the moment ratios compare favorably. The only large deviation in moment ratios is that at the interior positive section in F2. The absolute moments at that section are small and a small absolute moment change results in a significant change in relative moments. The actual value of γ is probably between 1.18 and 1.60.

Absolute moment comparisons between F2 and F3 show that the measured moments are less in F3 than in F2. It can be seen that the absolute values of measured and computed moments compare favorably in structure F2. However, measured moments are less than computed in F3 and it is likely that the measured moments are low in F3. The largest deviation between measured and computed moments is at the deep beam edge exterior negative section where the computed values are in excess of measured moments. In making the adjustment of moment to the critical section, it was assumed that the shear was distributed uniformly along the supports and in the case of the deep beam, the center of reaction is very near the column center line so little correction was necessary. In view of the measured moments, it appears that the actual center of reaction is a greater distance from the column center line than assumed.

The moments in structures T1 and T2 are listed in Table A3. The computed moment ratios for both structures compare favorably with the measured values. The most serious difference occurs at the exterior negative section of T1. However, the trends indicated by Fig. 3.9 show that the measured beam moment was excessively high at that location. The comparisons of absolute moment vary 10-20 percent at some sections. It should be remembered that the total moment is provided for in each bay and no serious difficulties would arise if these moments were used for design moments. The design of structure T2 indicated that although the distribution of moment was not as favorable as might be desired the structure behaved satisfactorily. (See Sec. 5.6).

In summary, the computed moments given in this section for the test structures compared well with the measured moments. It is felt that the proposed frame analysis is adequate in determining the moments under uniform or pattern loads and that it is sufficiently broad to enable analysis of a range of panel sizes and supports.

TABLE A1 COMPARISON OF MEASURED WITH COMPUTED MOMENTS IN STRUCTURE F1, $\beta = 0.72$

Interior Strip, One-Panel Wide

Section	Ext. M^- (Shallow Beam)	Ext. M^+	Int. M^-		Int. M^+	Int. M^-		Ext. M^+	Ext. M^- (Deep Beam)
	Moment Coefficients of qa^3								
Measured Uniform Load Moments	0.027	0.049	0.065	0.064	0.040	0.058	0.058	0.047	0.034
Measured Maximum Moments	0.021	0.052	0.068	0.067	0.044	0.063	0.063	0.048	0.026
Moment Ratio, γ	-	1.06	1.04	1.05	1.10	1.09	1.09	1.02	-
Computed Uniform Load Moments	0.043	0.049	0.074	0.068	0.038	0.069	0.075	0.049	0.056
Computed Maximum Moments	0.049	0.054	0.078	0.075	0.049	0.075	0.078	0.055	0.063
Moment Ratio, γ	1.14	1.10	1.05	1.10	1.29	1.09	1.04	1.12	1.13

TABLE A2 COMPARISON OF MEASURED WITH COMPUTED MOMENTS IN STRUCTURES F2 AND F3

Interior Strip, One-Panel Wide

Moment Coefficients of qa^3

Section	Ext.M^- (Shallow Beam)	Ext.M^+	Int.M^-		Int.M^+	Int.M^-		Ext.M^+	Ext.M^+ (Deep Beam)
Structure F2, $\beta = 0.85$									
Measured Uniform Load Moments	0.025	0.042	0.068	0.062	0.029	0.061	0.065	0.038	0.025
Measured Maximum Moments	0.027	0.049	0.079	0.072	0.033	0.067	0.071	0.042	0.025
Moment Ratio, γ	1.08	1.17	1.16	1.16	1.18	1.10	1.09	1.11	1.00
Computed Uniform Load Moments	0.024	0.045	0.072	0.062	0.025	0.062	0.071	0.044	0.040
Computed Maximum Moments	0.030	0.053	0.078	0.073	0.041	0.072	0.077	0.052	0.048
Moment Ratio, γ	1.25	1.18	1.08	1.18	1.64	1.16	1.08	1.18	1.20
Structure F3, $\beta = 0.78$									
Measured Uniform Load Moments	0.029	0.038	0.057	0.055	0.023	0.058	0.060	0.034	0.024
Measured Maximum Moments	0.034	0.042	0.060	0.058	0.037	0.060	0.061	0.039	0.027
Moment Ratio, γ	1.17	1.11	1.05	1.05	1.60	1.03	1.02	1.15	1.12
Computed Uniform Load Moments	0.024	0.045	0.072	0.062	0.025	0.062	0.071	0.044	0.040
Computed Maximum Moments	0.031	0.054	0.077	0.073	0.043	0.073	0.077	0.053	0.049
Moment Ratio, γ	1.29	1.20	1.08	1.18	1.72	1.18	1.08	1.20	1.23

TABLE A3 COMPARISON OF MEASURED WITH COMPUTED MOMENTS IN STRUCTURES T1 AND T2

Interior Strip, One-Panel Wide

Section	Ext. M^-	Ext. M^+	Int. M^-		Int. M^+
	Moment Coefficients of qa^3				
Structure T1, β = 0.81					
Measured Uniform Load Moments	0.043	0.046	0.079	0.071	0.036
Measured Maximum Moments	0.057	0.054	0.090	0.083	0.042
Moment Ratio, γ	1.33	1.17	1.14	1.17	1.17
Computed Uniform Load Moments	0.029	0.054	0.081	0.070	0.036
Computed Maximum Moments	0.033	0.061	0.083	0.078	0.050
Moment Ratio, γ	1.14	1.13	1.03	1.11	1.39
Structure T2, β = 0.66					
Measured Uniform Load Moments	0.036	0.056	0.069	0.061	0.045
Measured Maximum Moments	0.041	0.060	0.077	0.064	0.047
Moment Ratio, γ	1.14	1.07	1.12	1.05	1.05
Computed Uniform Load Moments	0.044	0.049	0.076	0.068	0.038
Computed Maximum Moments	0.051	0.052	0.078	0.073	0.046
Moment Ratio, γ	1.16	1.06	1.03	1.07	1.21

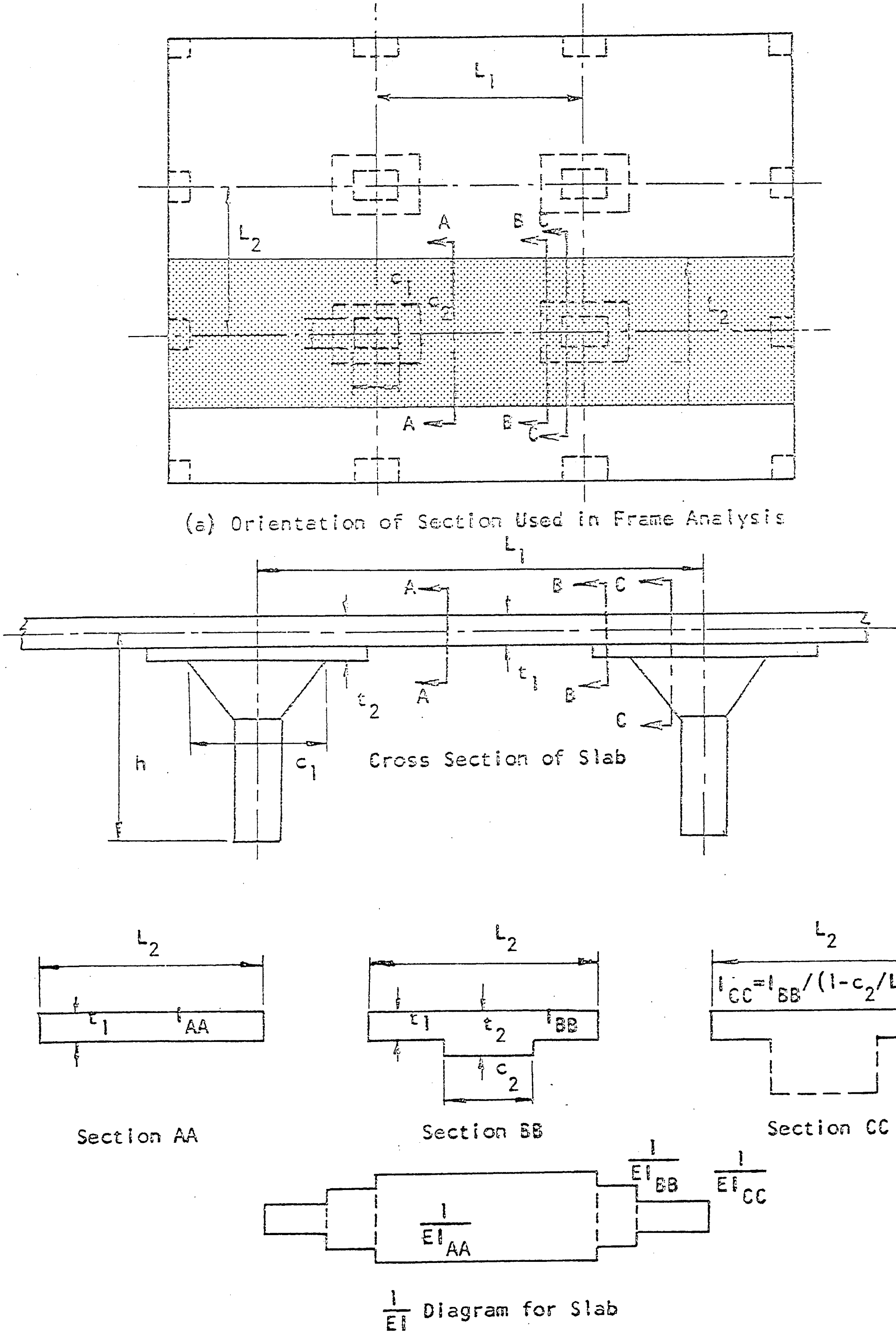

FIG. A.1 LOCATION AND CROSS SECTIONS OF ASSUMED FRAME

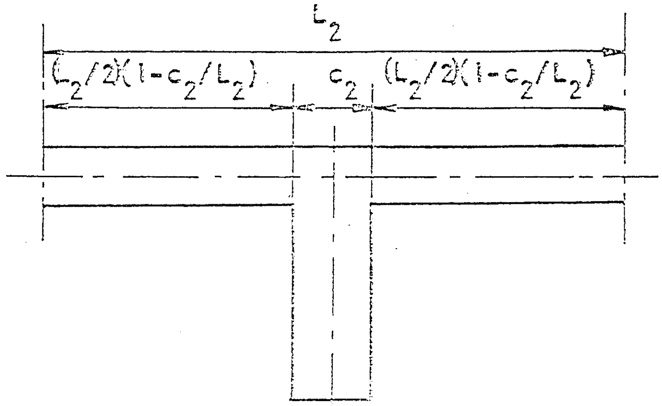

(a) Beam-Column Combination

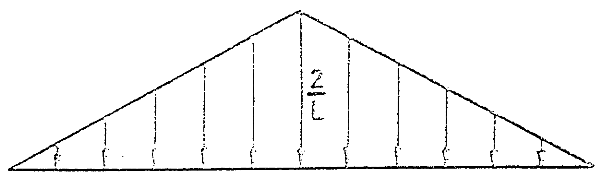

(b) Distribution of Unit Twisting Moment Along Column Center Line

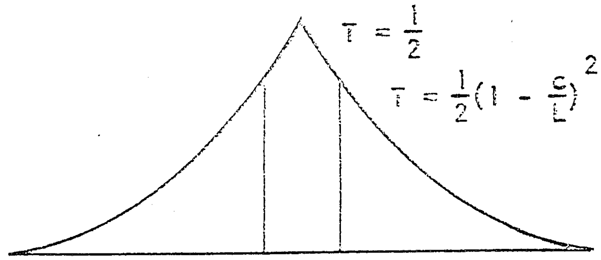

(c) Twisting Moment Diagram

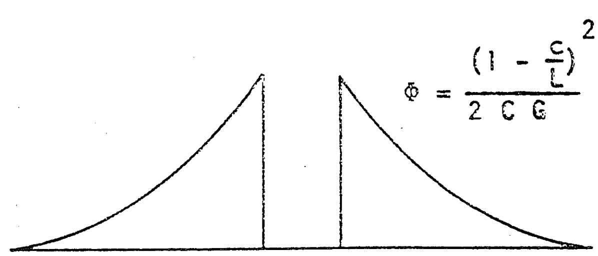

(d) Unit Rotation Diagram

FIG. A.2 ROTATION OF BEAM UNDER APPLIED UNIT TWISTING MOMENT

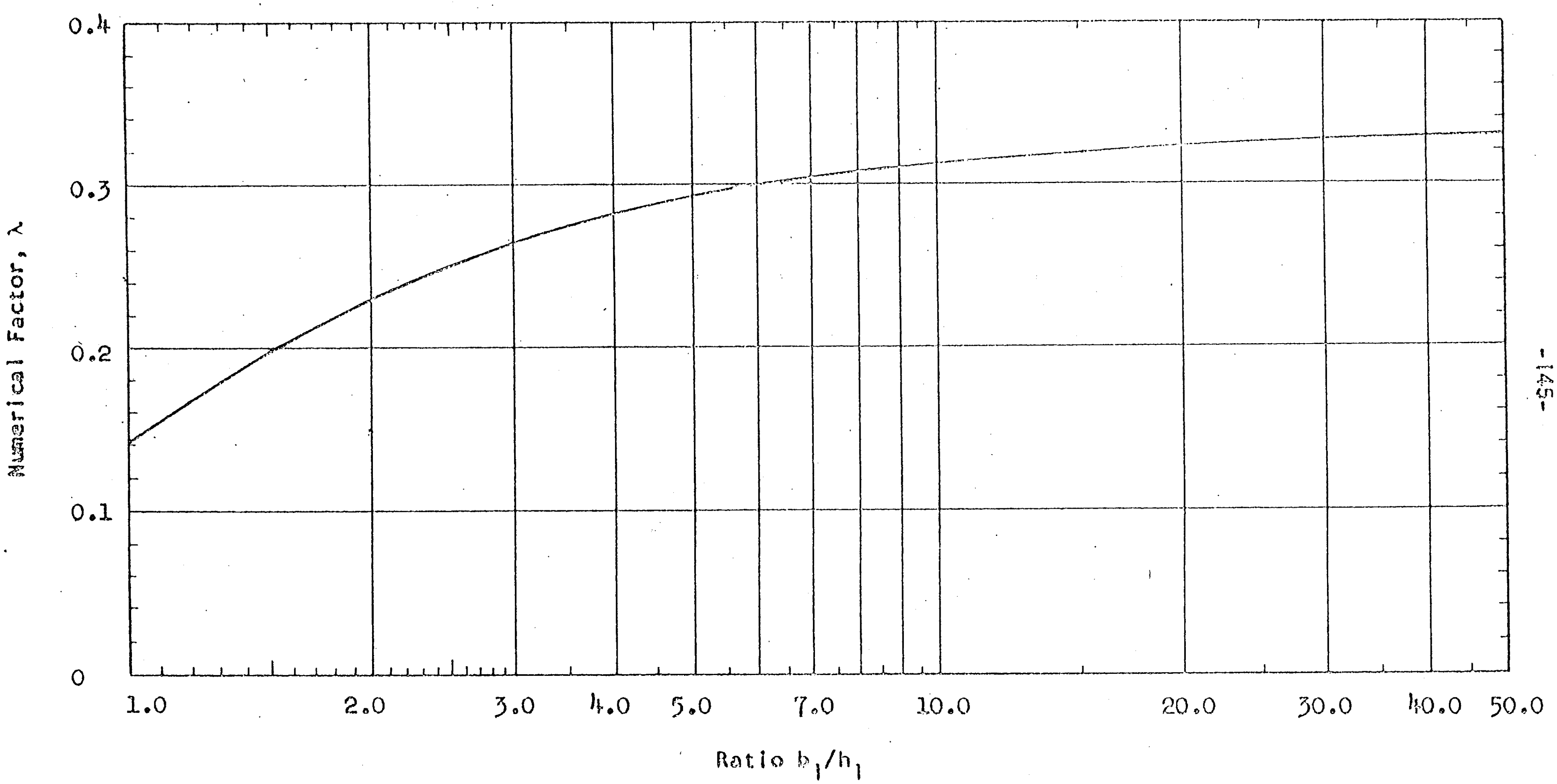

FIG. A.3 CONSTANT FOR TORSIONAL ROTATION OF A RECTANGULAR CROSS SECTION